Application of New Planar Falling Film Reactors for Degradation and Mineralization of Few Pharmaceuticals and Organic Pollutants in Aqueous Solutions by Means of Ozonation, Photocatalysis and Non-thermal plasma

A dissertation
Submitted to the Council of
the College of Science at the University of
Sulaimani in Partial Fulfillment of the Requirements
for the Degree of Doctor of Philosophy in Chemistry
(Environmental Chemistry)

By

Kosar Hikmat Hama Aziz

M.Sc. Analytical Chemistry (2011), University of sulaimani

Supervised by

Dr. Ibrahim Khorshid
Professor

Dr. Detliv Möller
Professor

Dr. Mohammad Amin M. Rashid
Assistant Professor

March, 2018 Nawroz, 2718

بِسْمِ اللّهِ الرَّحمنِ الرَّحيم

يَرْفَعِ اللَّهُ الَّذِينَ آمَنُوا مِنْكُمْ

وَالَّذِينَ أُوتُوا الْعِلْمَ دَرَجَاتٍ

وَاللَّهُ بِمَا تَعْمَلُونَ خَبِيرٌ

المجادلة / آية 11

Supervisor Certification

I certify that the preparation of dissertation entitled **"Application of new planar falling film reactors for degradation and mineralization of few pharmaceuticals and organic pollutants in aqueous solutions by means of ozonation, photocatalysis and non-thermal plasma"** accomplished by **(Kosar Hikmat Hama Aziz)**, was prepared under our supervision in the college of Science, at the University of Sulaimani, as partial fulfillment of the requirements for the degree of Doctor of Philosophy in (Chemistry).

Signature:
Supervisor: **Dr. Ibrahim Khorshid**
Scientific Title: Professor
Date: 6/ 2/ 2018

Signature:
Supervisor: **Dr. Detliv Möller**
Scientific Title: Professor
Date: 6/ 2/ 2018

Signature:
Supervisor: **Dr. Mohammad Amin M. Rashid**
Scientific Title: Assistant Professor
Date: 6/ 2 / 2018

In view of the available recommendation, I forward this thesis for debate by the examining committee.

Signature:
Name: **Dr. Bakhtyar Kamal Aziz**
Title: Assistant Professor
Head of the Department
Date: / / 2018

Linguistic Evaluation Certification

I hereby certify that this thesis entitled **"Application of new planar falling film reactors for degradation and mineralization of few pharmaceuticals and organic pollutants in aqueous solutions by means of ozonation, photocatalysis and non-thermal plasma"** prepared by (**Kosar Hikmat Hama Aziz**), has been read and checked and after indicating all the grammatical and spelling mistakes; the thesis was given again to the candidate to make the adequate corrections. After the second reading, I found that the candidate corrected the indicated mistakes. Therefore, I certify that this thesis is free from mistakes.

Signature:

Name: **Dr. Azad Hasan Fatah**

Position: English Department, School of Languages, University of Sulaimani

Date: 21/2/ 2018

Examining Committee Certification

We certify that we have read this dissertation entitled **"Application of new planar falling film reactors for degradation and mineralization of few pharmaceuticals and organic pollutants in aqueous solution by means of ozonation, photocatalysis and non-thermal plasma"** prepared by (**Kosar Hikmat Hama Aziz**), and as Examining Committee, examined the student in its content and in what is connected with it, and in our opinion it meets the basic requirements toward the degree of doctor of philosophy in chemistry **"Environmental Chemistry"**.

Signature:
Name: **Dr. Salah Aldin Naman**
Title: Professor
Date: 29/3/ 2018
(Chairman)

Signature:
Name: **Dr. Abdul Salam Rahim**
Title: Professor
Date: 29/3/ 2018
(Member)

Signature:
Name: **Dr. Azad Tofiq Faizullah**
Title: Professor
Date: 29/3/ 2018
(Member)

Signature:
Name: **Dr. Kafia Mawlood Shareef**
Title: Professor
Date: 29/3/ 2018
(Member)

Signature:
Name: **Dr. Bakhtyar Kamal Aziz**
Title: Assistant Professor
Date: 29/3/ 2018
(Member)

Signature:
Name: **Dr. Ibrahim Khorshid Ahmad**
Title: Professor
Date: 29/3/ 2018
(Supervisor-Member)

Signature:

Name: **Dr. Detliv Möller**

Title: Professor

Date: / / 2018

(Supervisor-Member)

Signature:

Name: **Dr. Mohammad Amin M. Rashid**

Title: Assistant Professor

Date: / / 2018

(Supervisor-Member)

Approved by the Dean of the College of Science.

Signature:

Name: Dr. Soran Mohammed Mamand

Title: Assistant Professor

Date: / / 2018

Dedication

This Thesis is Dedicated to:

My deceased uncle Dlawar Ali Mirza

My Family

All My Friends

With my love and respect

Kosar Hikmat Hama Aziz

Acknowledgements

Firstly, I would like to express my sincere gratitude and appreciation to my supervisors, Professor Dr. Ibrahim Khorshid, Professor Dr. Detliv Möller and Assist Professor Dr. Mohammad Amin, for their continuous support, precious guidance and encouragement throughout the course of this work. I would also like to extend my deepest gratitude to Dr. Hans Miessner and Dr. Siegfried Muller at Brandenburg University of Technology (*BTU-Cottbus-Senftenberg*) for their invaluable cooperation, thoughtful insights, inspiring suggestions, guidance and expertise throughout the project.

Special thanks and a profound appreciation is extended to Dr. Ali Mahyar for his kind assistance. I wish gratefully acknowledge and thank the technical staff Mr. Dieter Kalass and Mr. jurgen Hofmeister for their assistance with the prompt and excellent technical support.

I would like to express my gratitude to the University of Sulaimani and ministry of higher education for supporting and funding the Split-Site Ph.D project. I would also like to express my gratitude to the Council of the department of Chemistry, for helping and offering all the necessary requirements throughout this work. I deeply appreciate the encouragement, support and patience of my family during this work.

This work was a part of Split-site Ph.D program between University of Sulaimani-Kurdistan Region, Iraq and Brandenburg University of Technology (*BTU-Cottbus-Senftenberg*), Germany.

Finally, I would like to express on my great thanks for the administration of *Laboratory of Atmospheric Chemistry and Air Pollution Control, Brandenburg University of Technology (BTU Cottbus-Senftenberg), D-12489 Berlin, Germany.* For their full cooperation during the course of this work.

Abstract

The effectivity and efficiencies of ozonation and various advanced oxidation processes (AOPs) based on photocatalysis and non-thermal plasma generated by a dielectric barrier discharge (DBD), in different gas atmospheres in the degradation and mineralization of aqueous solutions of organic pollutants including non-steroidal anti-inflammatory drugs (NSAIDs) diclofenac (DCF) and ibuprofen (IBP), chlorophenoxy herbicide 2,4-dichlorophenoxyacetic acid (2,4-D), 2,4-dichlorophenol, and methylene blue (MB) were investigated and compared. The removal of MB has also followed by Fenton, photo-Fenton, and photocalaytic oxidation in the presence of hydrogen peroxide. To enable a direct comparison of the efficiencies of the mentioned methods, a planar falling film reactor with comparable design has been used. The results obtained in the present work show that the degradation of all the studied organic pollutants by photocatalytic oxidation (P.C. Oxidation) and DBD plasma in air atmosphere were only moderate, while the degradation by ozone in darkness (direct ozonation) was very effective and possessed the highest energy yield at 50% conversion (G_{50}) of all pollutants. However, it should be noted that the mineralization of the studied organics, was poor. The reason was due to the formation of stable towards ozone by-products, especially low chain carboxylic acids. The fate of these by-products during the degradation with different treatment methods has been followed and discussed.

Combination of ozonation with the photocatalysis showed a synergistic effect on the degradation of IBP and 2,4-D and the mineralization rates of all pollutants were enhanced. However, the energy yields at G_{50} were diminished, due to the additional power demands of UVA light. A significant enhancement in the decolorization of MB by the addition of H_2O_2 into the P.C. Oxidation system was observed and the complete decolorization was achieved after one-hour treatment. The degradation efficiency and the production of reactive species like ozone and H_2O_2 by the DBD plasma significantly depends on the

composition of gas atmosphere and amount of the applied electrical power. The effects of various gas atmospheres and the input energy power on the generation of H_2O_2 and ozone as well as on the degradation efficiency of the examined methods were investigated. The addition of Fe^{2+} into the solution improves the removal of pollutants by the DBD plasma under the argon atmosphere due to the occurrence of Fenton reaction.

The mineralization efficiency of examined methods were followed by the total organic carbon (TOC) removal. The highest TOC removal was obtained by the photocatalytic ozonation and DBD plasma either in combination with Fenton oxidation or in an Ar/O_2 atmosphere.

CONTENTS

Abstract ..... *i*

Contents ..... *iii*

List of tables ..... *iv*

List of figures ..... *iiv*

List of abbreviations ..... *xi*

Chapter One

Introduction and Literature review.....1

1. Introduction.....1

1.1 Advanced oxidation processes (AOP) 2

1.2 Titanium dioxide photocatalyst.....3

1.2.1 Superhydrophilicity.....6

1.2.2 Heterogeneous photocatalytic oxidation.....8

1.3 Ozone (O_3) oxidation 8

1.4 Photocatalytic ozonation.....9

1.5 Hydrogen peroxide oxidation 10

1.6 Non-thermal plasma.....11

1.7 Application of non-thermal plasma for water treatment.....12

1.8 Degradation of aqueous organic pollutants.....13

1.8.1 Pharmaceuticals 14

1.8.2 Pesticides.....16

1.8.3 Organic dyes.....18

1.9 Objectives of this study.....22

Chapter Two

2. Experimental 23

2.1 Materials 23

2.2 Reactors and equipment 24

2.2.1 Photocatalytic reactor 24

2.2.2 Dielectric barrier discharge (DBD) reactor 26

2.2.3 Instruments and devices 27

2.3 Experimental conditions 28

2.4 Analytical methods 29

2.4.1 High-performance liquid chromatography (HPLC) 29

2.4.2 Ion chromatography (IC) 32

2.4.3 Total organic carbon (TOC) analysis 36

2.4.4 Spectrophotometry 36

Preparation of reagents and analysis procedure 36

2.4.5 Gas chromatography-mass spectrometry (GC/MS) 39

2.4.6 Real wastewater treatment by DBD plasma 39

2.5 Average thickness of the liquid falling film 40

2.6 Calibration and optimization of ozone generator 41

2.7 The effect of UVA lamp on ozone decomposition 42

2.8 The effect of ozone on the reactor frame made of polyvinylchloride 43

2.9 The effect of H_2O_2 concentration on methylene blue degradation by UVA/TiO_2/H_2O_2 and optimization the amount of Fe^{2+} in Fenton processes 45

Chapter Three

3. Results and discussion 0

3.1 Formation of reactive species in the DBD reactor 47

3.2 Degradation of organic pollutants 53
3.3 Degradation by non-thermal DBD plasma 56
3.4 Degradation based on ozonation and photocatalysis 56
3.5 Degradation of pharmaceutical DCF and IBP 58
3.6 Degradation of 2,4-D and 2,4-DCP 62
3.7 Degradation of methylene blue 67
3.8 Energy yield 74
3.8.1 Energy yield (G_{50}) of pharmaceutical DCF and IBP 75
3.8.2 Energy yield (G_{50}) of 2,4-D and 2,4-DCP 77
3.8.3 Energy yield (G_{50}) of MB 80
3.9 Mineralization and by-products degradation 82
3.9.1 Mineralization and by-products degradation of DCF and IBP 83
3.9.2 Proposed degradation pathways of DCF and IBP by photocatalysis 87
3.9.2.1 Degradation products of DCF 87
3.9.2.2 Degradation products of IBP 90
3.9.3 Mineralization and by-products degradation of 2,4-D 92
3.9.4 Mineralization and by-products degradation of MB 96
3.10 Real wastewater treatment by DBD plasma in argon atmosphere 100
4. Conclusions 102
5. Appendix 103
6. Suggestions for future works 105
References 106

List of Tables

Table No. **Table Title** **Page No.**

1.1 Ozonation and various AOPs reported for MB degradation…….....20

2.1 List of the chemical compounds; MW = molar weight……23

3.1 Rate constants for reactions of ozone and OH radical with pollutants….57

3.2 Degradation products observed for DCF during photocatalysis identified by GC/MS……...88

3.3 Degradation products observed for IBP during photocatalysis identified by GC/MS……90

3.4 Results of real wastewater treatment by DBD plasma (in µg/L); < BG = less than the quantification limit of the method……..…….101

List of Figures

Figure No. **Figure Title** **Page No.**

1.1 A schematic diagram of TiO_2 photocatalytic mechanism.....6
1.2 Mechanism of photo-induced superhydrophilicity of TiO_2.....7
1.3 Molecular structure of diclofenac (DCF).....14
1.4 Molecular structure of ibuprofen (IBP).....15
1.5 Molecular structure of 2,4-D.....17
1.6 Molecular structure of a methylene blue (MB).....21

2.1 A schematic diagram of the photocatalytic reactor.....25
2.2 Spectrum of UVA lamps.....26
2.3 Schematic diagram of the DBD reactor.....27
2. 4 Calibration curve of diclofenac concentration vs. peak area.....30
2. 5 Calibration curve of ibuprofen concentration vs. peak area.....31
2.6 Calibration curve of 2,4-D concentration vs. peak area.....31
2.7 Calibration curve of 2,4-dichlorophenol concentration vs. peak area.....32
2.8 Calibration curve of acetic acid concentration vs. peak area.....33
2. 9 Calibration curve of oxalic acid concentration vs. peak area.....33
2. 10 Calibration curve of glyoxylic acid concentration vs. peak area.....34
2.11 Calibration curve of glycolic acid concentration vs. peak area.....34
2.12 Calibration curve of chloride concentration vs. peak area.....35
2.13 Calibration curve of sulfate concentration vs. peak area.....35
2.14 Calibration curve of methylene blue concentration vs. peak area.....38
2.15 Calibration curve of hydrogen peroxide concentration vs. peak area.....38
2.16 Calibration and optimization of ozone generator.....42
2.17 Effect of UVA light irradiation on decomposition of ozone; 0.5L DI, T = 24˚C, pH = 5.5 and O3 feed gas = 130±5 mg/L.....43

2.18 Effect of UVA light irradiation on decomposition of ozone; 0.5L DI, T = 24˚C, pH = 5.5 and O3 feed gas = 130±5 mg/L.....44
2.19 Effect of H_2O_2 concentration on decolorization of MB (50 mg/L) by UVA/TiO_2/H_2O_2. 45
2.20 Optimization of the concentrations of H_2O_2 and Fe^{2+} on decolorization of 50 mg/L MB in Fenton oxidation. 46

3.1 Formation of H_2O_2 in deionized water and in solutions containing (C_o=100 mg/L 2,4-D or 2,4-DCP) and (C_o=50 mg/L DCF, IBP or MB) by DBD plasma at different input powers, in Ar and Ar/O_2 (80:20) atmosphere (the treatment time includes also the pause intervals without discharge which is explained in experimental part) 49
3.2 Concentration of generated O_3 in deionized water and in solutions containing (C_o=100 mg/L 2,4-D and 2,4-DCP) and (C_o=50 mg/L DCF, IBP and MB) by DBD plasma in Ar/O_2 (80:20) atmosphere (the treatment time includes also the pause intervals without discharge, explained in experimental part). 52
3.3 Variation of generated nitrite and nitrate ion concentrations by DBD in deionized water (P = 200W) in air atmosphere (the treatment time includes also the pause intervals without discharge, explained in experimental part).....53
3.4 Relative concentration profiles of DCF removal (C_0 = 50 mg/L, pH 5.6) by DBD/Ar at 150W and P.C. Oxidation (in DBD the treatment time includes also the pause intervals without discharge).....54
3.5 Relative concentration profiles of 2,4-D removal (C_0 = 100 mg/L, pH 3.35) by DBD/Ar at 150W and P.C. Oxidation (in DBD the treatment time includes also the pause intervals without discharge). 55
3.6 Relative concentration profiles during DCF and IBP degradation (C_o= 50 mg/L each, pH = 5.6) by ozonation and P. C. Ozonation. 59

3.7 Relative concentration profiles during DCF and IBP degradation (C_o= 50 mg/L each, pH = 5.6) by P. C. Oxidation and DBD plasma under air atmosphere.....60
3.8 Relative concentration profiles during DCF and IBP degradation (C_o= 50 mg/L each, pH = 5.6) by DBD plasma under argon atmosphere at 150 and 200W (the treatment time includes also the pause intervals without discharge). 61
3.9 Relative concentration profiles during DCF and IBP degradation (C_o= 50 mg/L each, pH = 5.6) by DBD plasma in Ar/O_2 atmosphere and Ar/Fenton at 150 and 200W (the treatment time includes also the pause intervals without discharge). 62
3.10 Relative concentration profiles of 2,4-D and 2,4-DCP degradation (C_o= 100 mg/L each) by ozonation, P.C. Ozonation, and P.C. Oxidation. 64
3.11 Relative concentration profiles of 2,4-D degradation (C_o= 100 mg/L, pH = 3.35) by the DBD plasma at 150W in Ar, Ar/Fenton, and Ar/O_2 (80:20) atmosphere and (P = 200W in air), (the treatment time includes also the pause intervals without discharge). 66
3.12 Relative concentration profiles of 2,4-DCP degradation (C_o= 100 mg/L, pH = 6.85) by the DBD plasma at 150W in Ar, Ar/Fenton, and Ar/O_2 (80:20) atmosphere and (P = 200W in air), (the treatment time includes also the pause intervals without discharge). 67
3.13 Relative concentration profiles of MB decolorization (C_o=50 mg/L, pH = 5) by (A) H_2O_2-photocatalysis, and P.C. Oxidation (B) Fenton, ozonation, and P.C. Ozonation.....69
3.14 The variation of concentration H_2O_2-decay during the degradation of 50 mg/L MB at different initial concentration. 70
3.15 Relative concentration profiles of MB decolorization (C_o= 50 mg/L, pH = 5) by DBD plasma in Ar, Ar/O_2, and Ar/Fenton atmosphere at 150W (the treatment time includes also the pause intervals without discharge). 72

3.16 Effect of the initial concentration of MB on the energy yield of MB decolorization by the DBD plasma (P = 150W, pH= 5) under the argon atmosphere.....73
3.17 Energy Yields (G50) of the ozonation and other applied AOPs for the degradation of DCF (C_o = 50 mg/L). 76
3.18 Energy Yields (G50) of the ozonation and other applied AOPs for the degradation of IBP (C_o = 50 mg/L).....77
3.19 Energy Yields (G50) of the ozonation and other applied AOPs for the degradation of 2,4-D (C_o= 100 mg/L).....78
3.20 Energy Yields (G50) of the ozonation and other applied AOPs for the degradation of 2,4-DCP (C_o = 100 mg/L).....79
3.21 Energy Yields (G50) of the ozonation and other applied AOPs for the decolorization of MB (C_o= 50 mg/L).....81
3.22 Variation of acetate intermediate by-product concentrations during the degradation of 50 mg/L : (A) DCF, (B) IBP.....84
3.23 Variation of oxalate intermediate by-product concentrations during the degradation of 50 mg/L : (A) DCF, (B) IBP.....85
3.24 TOC removal after 90 min treatment of DCF (C_o= 50 mg/L, initial TOC 26.2 mg/L).....86
3.25 TOC removal after 90 min treatment of IBP (C_o= 50 mg/L, initial TOC 30.7 mg/L).....86
3.26 Proposed degradation pathways of DCF by photocatalysis.....89
3.27 Proposed degradation pathways of IBP by photocatalysis. 91
3.28 Variation of 2,4-DCP intermediate by-product concentrations during the degradation of 100 mg/L 2,4-D.....93
3.29 Variation of oxalate intermediate by-product concentrations during the degradation of 100 mg/L 2,4-D.....93
3.30 Variation of glycolate intermediate by-product concentrations during the degradation of 100 mg/L 2,4-D.....94

3.31 Variation of glyoxylate intermediate by-product concentrations during the degradation of 100 mg/L 2,4-D.....94
3.32 Relative TOC concentration profiles in ozonation and other applied AOPs: (A) 2,4-D (initial TOC = 42.1 mg/L) and (B) 2,4-DCP (initial TOC = 43 mg/L).....95
3.33 Variation of acetate intermediate by-product concentrations during the degradation of 50 mg/L MB.....97
3.34 Variation of oxalate intermediate by-product concentrations during the degradation of 50 mg/L MB.....98
3.35 Variation of sulfate intermediate by-product concentrations during the degradation of 50 mg/L MB.....98
3. 36 TOC removal (%) from a MB solution (C_o= 50 mg/L MB, initial TOC = 27.7 mg/L) by ozonation and other applied AOPs.....100

List of Abbreviations

Abbreviations	Description
AOP	Advanced oxidation process
a.u.	Arbitrary unit (procedure defined unit)
DBD	Dielectric barrier discharge
DCF	Diclofenac
2,4-D	2,4-dichlorophenoxyacetic acid
2,4-DCP	2,4-dichlorophenol
EPR	Electron paramagnetic resonance spectroscopy
eV	Electron volte
G_{50}	Energy yields at 50% conversion
IBP	Ibuprofen
IC	Ion chromatography
HPLC	High performance liquid chromatography
GC/MS	Gas chromatography/Mass spectrometry
MB	Methylene blue
PAG	Pilkington active glass
MTBE	Methyl tert-butyl ether
NTP	Non-thermal plasma
RMS	Root mean square
TOC	Total organic carbon, mg L^{-1}
PTFE	Polytetrafluoroethylene
σ	Liquid film thickness
Q	Liquid flow rate
A	Average surface area

Chapter One

Introduction

&

Literature Review

Chapter One

Introduction and Literature Review

1. Introduction

Water contamination with organic compounds such as pharmaceutical residues, pesticides and organic dyes has been reported as a major environmental concern [1-4]. Contaminants of emerging concern (CECs) include those micro-pollutants that are found in trace amounts in drinking water and in recent time have received public attention owing to potential human health and environment impacts [5]. Widespread consumption and disposal of these pollutants by industries, manufacturing plants, hospitals, frames and institutions considered as a major source of water pollution. Therefore, a significant amount of these pollutants are released into the environment. Since the use of organic compounds cannot be controlled or eliminated, due to the population growth and industrial development, their release into the environment has to be optimized and limited, as it may cause risks to human health, climate and aquatic environments [6-11]. Large number of organic pollutants including pharmaceutical residues, pesticides, herbicides and organic dyes have been recently detected in the surface and ground water at the trace concentration mainly in the range of ng to μg L^{-1} [1, 4, 12-14]. In order to mitigate the risk of these pollutants on environment, wastewater remediation by efficient techniques from these sources is essential before discharging them into water environments. Various treatment methods including physical, chemical and biological as well as a combination of these techniques have been developed and used for the removal of organic pollutants from aqueous solutions. Physical methods are based on a mechanical separation of the pollutants from water by a particular supporting system. Chemical oxidation processes are often used for decomposition of

non-biodegradable organic pollutants by powerful oxidizing agent, such as ozone, chlorine and hypochlorite. However, the use of such oxidant is limited due to the formation of possibly toxic non-degradable by-products, for instance, halogenated organic by-products in case of chlorine treatment. Biological methods are relatively low cost and widely used for municipal and industrial wastewater treatment. However, biological degradation of organic pollutants is significantly slower than other processes. Moreover, most of toxic organic pollutants are non-biodegradable and do not effectively remove by biological treatments. In order to minimize the previously mentioned limitations, new powerful technologies based on the generation of oxidation species have been developed and extensively investigated. These methods are called advanced oxidation processes (AOP). Traditional physicochemical treatment such as adsorption process is effective method and widely used for removal of organic pollutants from wastewater [15-17]. Unlike the principle decontamination of adsorption method, as the pollution is only transferred from the aqueous solution to the adsorbents that cannot avoid the risk of the contaminating the environment. Furthermore, the need of additional treatment processes such as filtration and frequent adsorbent reactivation makes this process inconvenient and costly. Advanced oxidation processes (AOPs) are recognized as a successful and promising methods for the degradation and mineralization of organic pollutants found in water bodies. These methods involve the generation of active, unstable and non-selective oxidizing species like hydroxyl radical that may oxidize most of the persistent organic pollutants present in water [2, 18-20].

1.1 Advanced oxidation processes (AOP)

Nowadays, many scientific studies have focused on improving the design and efficiency of existing methods that are applicable in the field of water and wastewater treatment, aiming to solve new problems with cheaper, simpler,

sustainable, more efficient and environmental friendly methods. The application of advanced oxidation technologies is one of these developments.

AOPs were first proposed for drinking water purification in 1980. Later on, these processes were widely investigated and developed for treatment of various types of wastewater. It is defined as the water treatment process (oxidation process) that involves an input of energy (either chemical, electrical or radiative) into the water environment to produce *in situ* highly reactive chemical oxidizing species, such as the hydroxyl radical (oxidizing potential of 2.80 V), which has recently emerged as an important class of technologies to accelerate the non-selective oxidation and hence the destruction of a wide range of recalcitrant organic and inorganic contaminants in polluted water and air which cannot be eliminated by conventional wastewater treatment methods [21, 22]. This method is unlike the principle of the decontamination methods of adsorption, coagulation-flocculation, sedimentation and membrane separation which very often shift the pollutant problem from water to another medium. The application of AOPs under proper conditions leads to the decomposition and mineralization of a variety of toxic pollutant into CO_2, H_2O and harmless mineral salts.

The advanced oxidation processes basically use ozone, hydrogen peroxide, and oxygen in many combinations. These are either combined with each other or applied with UV-Vis irradiation and/or various types of homogeneous and heterogeneous catalyst to generate *in situ* highly reactive radical species mainly but not exclusively hydroxyl radical, that can destroy a wide range of organic and inorganic pollutants.

1.2 Titanium dioxide photocatalyst

Titanium dioxide is the most common and widely studied semiconductor used as a photocatalyst for environmental purification due to its high photo-activity, inexpensive, low toxicity and good chemical and thermal stability. It

is commercially available under various trademark such as Degussa P-25 and Millennium TiONA PC50 which are commonly used in scientific studies. TiO_2 exists in nature in three different polymorph forms namely, anatase (tetragonal), rutile (tetragonal) and brookite (orthorhombic). Anatase is the most photo-active form that has a band gap of 3.2 eV therefore; UV light irradiation ($\lambda \leq 387nm$) is required to generate electron-hole pairs. All three polymorphs can be prepared in the laboratory. Anatase and brookite will transform to the thermodynamically stable rutile when heated at temperature exceeding to 600 °C [23-25]. Degussa (Evonik) P25 is a titania photocatalyst composed of anatase and rutile crystal structure in the ratio of 70-80 anatase: 30-20 rutile that is used widely in many catalytic and photocatalytic application [26]. The principle of photocatalysis is based on the generation of electron-hole (e^--h^+) pair (R1) when a semiconductor illuminate with light of sufficient energy (greater than the band gap of the semiconductor) to produce highly reactive species like hydroxyl and superoxide radicals (Fig. 1.1) which can cause to the photocatalytic degradation of pollutants. In order to achieve successful and continuous production of reactive oxidizing chemical species as well as preventing the electron-hole recombination, two redox reactions must be occur simultaneously. The first one includes the reduction of adsorbed electrophilic dissolved oxygen molecule on the TiO_2 by photo-generated electrons to form superoxide anion radical (R2) that may further react with H^+ to generate hydroperoxyl radical (R3) followed by H_2O_2 and finally hydroxyl radical (R4,5). The second one involves oxidation of adsorbed water molecule or hydroxyl anion by photo-generated holes to produce hydroxyl radicals (R6). The powerful hydroxyl and superoxide anion radicals can subsequently oxidize and mineralize organic pollutants into CO_2, H_2O and mineral salts (R7-9) [24].

$$TiO_2 + h\nu \rightarrow TiO_2\,(e^- + h^+) \quad (R1)$$

$$O_2 + e^- \rightarrow O_2\bullet^- \quad (R2)$$

$$O_2\bullet^- + H^+ \rightarrow \bullet OOH \quad (R3)$$

$$2 \bullet OOH \rightarrow H_2O_2 + O_2 \quad (R4)$$

$$H_2O_2 + h\nu \rightarrow \bullet OH + \bullet OH \quad (R5)$$

$$H_2O + h^+ \rightarrow \bullet OH + H^+ \quad (R6)$$

$$\bullet OH + Pollutants \rightarrow\rightarrow\rightarrow\rightarrow H_2O + CO_2 \quad (R7)$$

$$O_2\bullet^- + Pollutants \rightarrow\rightarrow\rightarrow\rightarrow H_2O + CO_2 \quad (R8)$$

$$\bullet OOH + Pollutants \rightarrow\rightarrow\rightarrow\rightarrow H_2O + CO_2 \quad (R9)$$

Degussa P25 which consist of a mixture of anatase and rutile is considered to be more photo-reactive than the pure crystalline anatase or rutile [27]. Recombination of photo-generated electron-holes is the significant limitation as it decreades the over all photo-active efficiency. The TiO_2 crystalities of Evonic (Degussa) P25 compose of a mixture of anatase and rutile, the photoexicited electron at conduction band from the anatase part jump to conductive band of the rutile phase which may act as an electron sink, because the conductive band potential of rutile is more possitive than that of anatase [24, 27]. This phenomenon, leading to increase the seperation of photo-generated electron-holes, resulting in reduced recombination, and consequently, an increase in photoactivity.

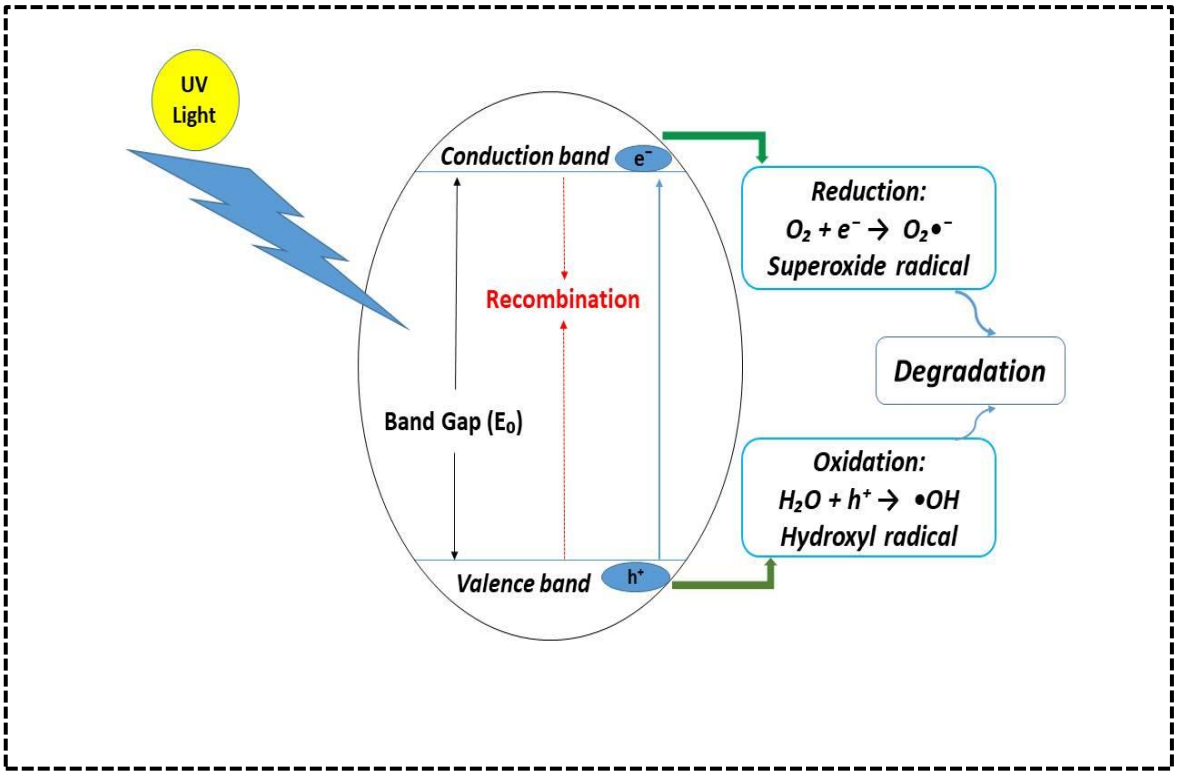

Figure 1.1 Schematic diagram of TiO_2 photocatalytic mechanism

Many studies in the literature have been reported for improving the photocatalytic efficiency of TiO_2 either via morphological modification such as increasing surface area and porosity, or via chemical and physical modification, by incorporation of other materials (doping) into the TiO_2 structure such as carbon atoms [28], transition metal ions, noble metals and non-metals [24, 29]. These modifications have been made to enhance the surface area, reducing electron-hole recombination, decreasing the band gap and increasing visible light activity of TiO_2 photocatalyst (enhance the solar efficiency of TiO_2 under solar irradiation which is low cost and easily available).

1.2.1 Superhydrophilicity

UV illumination of a surface coated with TiO_2 particle may induce a phenomenon called superhydrophilicity, attributed a high wettability properties of photo-excited TiO_2 which has been well described by Fujishima

et al. [30]. A possible application of this phenomenon is anti-fogging and self-cleaning windows [24]. In this phenomenon, the photo-generated electron-hole pairs react in a different route. The electrons tend to reduce the Ti(IV) cations to the Ti(III) state, and the holes oxidize the O^{2-}anions to O_2. Such trapped holes weaken the bond between the associated titanium and lattice oxygen, allowing oxygen atoms to be liberated, thus creating oxygen vacancies (Fig. 1.2). Water molecules can then occupy these oxygen vacancies, producing adsorbed OH groups, which tend to make the surface hydrophilic. The longer the surface is illuminated with UV light, the smaller the contact angle for water becomes; the contact angle approaches zero, meaning that water has a tendency to spread perfectly across the surface [27, 30]. This phenomenon of TiO_2 coated on the surface of reactor wall provides a homogeneous and stable liquid falling film in the falling film reactor.

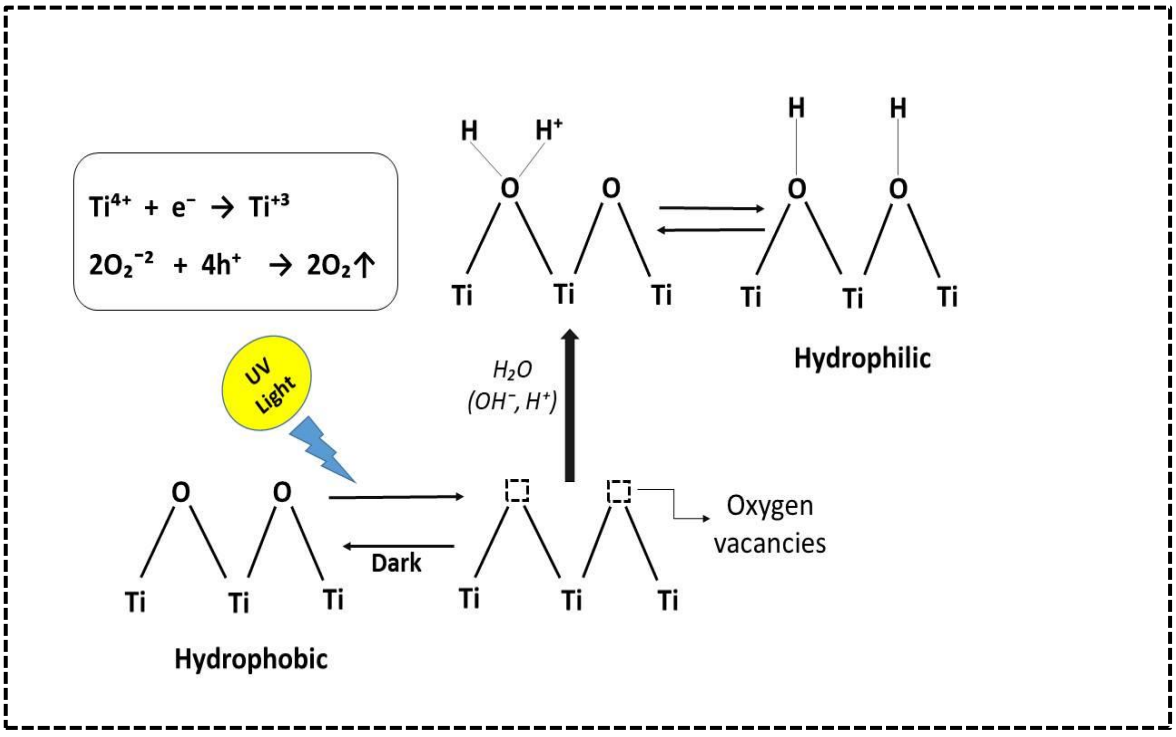

Figure 1.2 Mechanism of photo-induced superhydrophilicity of TiO_2

1.2.2 Heterogeneous photocatalytic oxidation

Photocatalytic oxidation is an advanced oxidation process consists of a combination of a photo-active catalyst like TiO_2 (either as the solid photo-catalyst powder or coated on a support sheet like glass) and UV light in the presence of oxygen. The fundamental mechanism of photocatalysis consists in the generation of electron–hole pairs, which determine the occurrence of redox reactions of species adsorbed on the photocatalyst surface. This method has been successfully used for wastewater treatment [31]. In spite of high efficiency, the separation of TiO_2 powder in aqueous suspension has been the main disadvantage. Though the coated film of TiO_2 on a support plate is the developed step forward to overcome this disadvantage. This process leads to the generation hydroxyl and superoxide ion radicals (see Fig. 1.1) that can be utilized in oxidation and decomposition of organic pollutants. The presence of oxygen which acts as electron scavenger can prevent the photo-generated electron-hole pairs recombination and consequently improves the degradation efficiency [32]. Degradation of various organic pollutants in aqueous solution has been investigated in many reports by using photocatalytic oxidation technique [33-35].

1.3 Ozone (O_3) oxidation

Ozone is a highly toxic gas and a strong oxidizing agent with the standard redox potential of 2.07 V, after fluorine (3.06 V), hydroxyl radical (2.80 V) and atomic oxygen (2.42) [36]. The solubility of ozone is much higher than oxygen in water according to Henry's constant [37]. This is the advantages of ozone because the production of ozone is usually in gas phase and has to be dissolved in aqueous solution. Ozone is widely used as an effective oxidant in water and wastewater treatment. Ozonation process has been widely used for water disinfection treatment including bacteria sterilization, odor, algae, and trihalomethane removal as well as degradation of organic pollutants. Despite

of several advantages of ozonation, its application to wastewater treatment is limited due to high cost of ozone production and only partial degradation of organic pollutants present in water [38, 39]. Ozonation can proceed via two routes: direct reaction in darkness at acidic solution and indirect attack via generation of active species like OH radicals either in alkaline solution or in combination with photocatalyst. Normally under acidic condition (pH ≤ 4) in darkness, the direct ozonation is dominant. When the pH ranges between 4-9, both are present. For pH ≥ 9, the indirect pathway prevails [38]. Ozonation at alkaline medium and photocatalytic ozonation can be placed in a group of AOP methods. In alkaline pH, ozone molecules decompose by hydroxyl ions eventually producing the strong oxidizing agent OH radicals (R 10-13) [31].

$$O_3 + OH^- \rightarrow O_2\bullet^- + HO_2\bullet \qquad (R\,10)$$

$$O_3 + HO_2\bullet \rightarrow 2O_2 + \bullet OH \qquad (R\,11)$$

Or alternatively

$$2HO_2\bullet \rightarrow O_2 + H_2O_2 \qquad (R\,12)$$

$$H_2O_2 + O_2\bullet^- \rightarrow O_2 + OH^- + \bullet OH \qquad (R\,13)$$

1.4 Photocatalytic ozonation

Photocatalytic ozonation (P.C. Ozonation) is an effective method for the decomposition of toxic and recalcitrant organic pollutants in water. It was shown that photolytic ozonation is more powerful for the removal of some organic pollutants than either UV-photolysis or ozonation alone. Ozone decomposition in water leads to the formation of hydroxyl radicals which can be effectively accelerated by UV irradiation. The molar absorptivity of ozone at 253.7 nm is (3300 M^{-1} cm^{-1}) which is much higher than that of H_2O_2 at the same wavelength. The decay rate of ozone is around 1000 times higher than that of H_2O_2 [38]. P.C. Ozonation is more efficient than P.C. Oxidation.

Ozone acts as a very strong electrophilic agent forming ozonide ($O_3\bullet$) radicals which results in the production of OH radicals (R 14-15). Addamo et al. [31] estimated the formation of an hydroxyl radical for each trapped electron (R 14-15), while three electron are needed for the generation of one hydroxyl radical when oxygen acts as the electron acceptor. Moreover, EPR studies confirmed that oxygen is less electrophilic than ozone for photo generated electrons onto TiO_2 surface. Therefore, when the catalyst is irradiated in the presence of ozone, a greater amount of hydroxyl radicals is formed with respect to that produced in the presence of oxygen. The major chain reactions of ozone with photo-generated electrons over the surface of photocatalyst are given in reaction (R 14-17). Hydroxyl radicals generated in these chain reactions non-selectively attack target pollutants and mineralize them into water, CO_2 and harmless mineral acids.

$$O_{3\ ads} + e^- \rightarrow \bullet O_3^- \qquad (R\ 14)$$

$$\bullet O_3^- + H_2O \rightarrow O_2 + \bullet OH + OH^- \qquad (R\ 15)$$

$$\bullet O_3^- + H^+ \rightarrow + HO_3\bullet \qquad (R\ 16)$$

$$\bullet OH + Pollutants \rightarrow\rightarrow\rightarrow H_2O + CO_2 \qquad (R\ 17)$$

1.5 Hydrogen peroxide oxidation

Degradation of organic pollutants by hydrogen peroxide is based on the production of OH radicals via the decomposition of H_2O_2 either by UV light or ferrous ions (so called Fenton's oxidation). Fenton oxidation is a widely used and studied catalytic process based on electron transfer between H_2O_2 and the homogeneous ferrous catalyst [38].

$$H_2O_2 + Fe^{2+} \rightarrow Fe^{3+} + \bullet OH + OH^- \qquad (R\ 18)$$

The Fenton's process is an efficient source for generating hydroxyl radicals. However, it involves a utilization of one Fe^{2+} molecule per one OH radical produced. Nevertheless, H_2O_2 decomposition can be catalyzed by Fe^{3+} as well (Fenton-like reaction). This process maintains a steady-state concentration of ferrous ions during H_2O_2 decomposition [20].

$$H_2O_2 + Fe^{3+} \leftrightarrow FeOOH^{2+} + H^+ \qquad (R\ 19)$$

$$FeOOH^{2+} \rightarrow Fe^{2+} + HO_2\bullet \qquad (R\ 20)$$

$$Fe^{3+} + HO_2\bullet \rightarrow Fe^{2+} + O_2 + H^+ \qquad (R\ 21)$$

Moreover, the degradation efficiency of organic pollutants by Fenton system could be significantly improved by the combination with UV light irradiation (Photo assisted Fenton process).

1.6 Non-thermal plasma

One part of AOP methods is formed by non-thermal plasma generated in various types of electrical discharge in liquid and gas-liquid interface. Plasma is a fully or partially ionized gas which is regarded as the fourth state of matter. It consists of electrons, free radicals and ions, as well as neutral species. And it can be produced by a variety of electrical discharge. When a significant amount of energy is applied to the gas through mechanisms such as an electric discharge, the electrons that escape from atoms or molecules not only allowing ions to move more freely, but also produce more electrons and ions via collisions after accelerating rapidly in an electric field. Eventually, the higher the number of electrons and ions, change will occur in the electrical property of the gas which leads to ionized gas or plasma. All varieties of plasma systems are traditionally defined into two major categories, namely thermal and non-thermal, in terms of electronic density or temperature. Thermal plasma (usually arc discharges, torches or radio frequency) is associated with sufficient energy introduced to allow plasma constituents to

be in thermal equilibrium. While non-thermal plasma is obtained using less power (usually corona discharge, dielectric barrier discharge, gliding arc discharge, glow discharge and spark discharge), which is characterized by an energetic electron temperature much higher than that of the bulk-gas molecules. In this plasma, the energetic electrons can collide with background molecules (N_2, O_2, H_2O, etc.) producing secondary electrons, photons, ions, radicals and neutral molecule species as well as UV light [40, 41]. Owing to the ability to form reactive species in situ, i.e. without the addition of chemicals, and the variety of physical effects induced simultaneously with the chemical reactions, electrical discharge generated in water and gas-liquid interface are considered to be a novel, effective and environmentally friendly tool for water treatment. In the present work, non-thermal plasma generated in DBD in a planar falling film reactor has been applied and studied for the removal of organic pollutants from aqueous solution. DBD also referred to as silent discharge which is based on the use of at least one dielectric barrier (e.g. glass, quartz, ceramics and alumina, etc.) in the discharge gap between ground and high voltage electrodes. DBD produce highly non-equilibrium plasmas in a controllable way at atmospheric pressure and at moderate gas temperature. They provide the effective generation of reactive species such as atoms, radicals and excited species by energetic electrons. Based on DBD technology, ozone gas has been industrially generated with oxygen and air feed, and applied for wastewater treatment [40, 42].

1.7 Application of non-thermal plasma for water treatment

Plasma generated by electrical discharges in liquid and gas-liquid environments have been studied for pulsed power application and high-voltage insulation, and increasing interest has been shown to application in water contamination treatment, nano-technology, sterilization of medical equipment and food and medical applications. The removal of organic

pollutants from wastewater by AOPs has been widely studied as an alternative to conventional wastewater treatment methods. Among them, non-thermal plasma treatment of polluted water with various organic compounds such as pharmaceuticals, organic dyes and pesticides has also been extensively investigated. The reviews by Jiang et al. [40] and Hijosa-Valsero et al. [43] showed that plasma treatment is a successful and promising technique for water remediation at least at laboratory and pilot plant scale. The authors found that the type of plasma, reactor configuration, gas composition atmosphere in case of plasma discharge in contact with liquid and the solution properties like pH and conductivity are the main factors that affect the efficiency of the method for degradation and removal of the pollutants.

It was suggested that plasma in contact with a thin layer of water is advantageous because mass transfer limitations between the generated plasma and liquid are minimized [44]. Dielectric barrier discharges (DBDs) with falling liquid film usually in coaxial and planar configuration were developed and studied. In this configuration designs, the polluted solution is flowing down through the inner walls of the reactor or on the surface of the ground electrode, and significant improvements in energy efficiency were reported [44]. A wide range of water pollutants were treated via this type of plasma configuration such as pharmaceutical pollutants [45, 46], pesticides [18, 47] and organic dyes [48].

1.8 Degradation of aqueous organic pollutants

The decomposition and removal of toxic organic pollutants from wastewater has become a serious global issue in environmental research and technology, since these pollutants accounts for an increasing environmental threat. Among the large number of water treatment technologies that can be apply for removing organic pollutants from water and wastewater, AOPs have been widely studied as an effective technology for destruction of those

organic pollutants which cannot be treated by conventional wastewater treatment methods due to their chemical stability and resistance against biological degradation.

1.8.1 Pharmaceuticals

Pharmaceutical residues in surface and ground waters have been a major environmental concern. The structures of Diclofenac 2-[2-(2,6-dichloroanilino)phenyl]acetic acid and ibuprofen 2-[4-(2-methypropyl) phenyl] propanoic acid are shown in figures (1.3 and 1.4). These are typical representatives of analgesic non-steroidal anti-inflammatory pharmaceutical compounds (NSAIDs) that have been recently detected in the aquatic environment at trace concentrations (ng to µg/L) [13, 14]. This is one of the reason that diclofenac (including the synthetic hormone 17-alpha-ethinylestradiol (EE2), the natural hormones 17-betaestradiol (E2) and Estrone (E1), and three macrolide antibiotics (azithromycin, clarithromycin and erythromycin)) are now included in EU first watch for emerging water pollutants [4, 49]. The ecotoxicity of NSAIDs such as DCF alone is relatively low, but prolonged exposure to environmentally relevant concentrations or to combinations of various NSAIDs present in water, increases the toxicity considerably and has a negative effect on aquatic life [50].

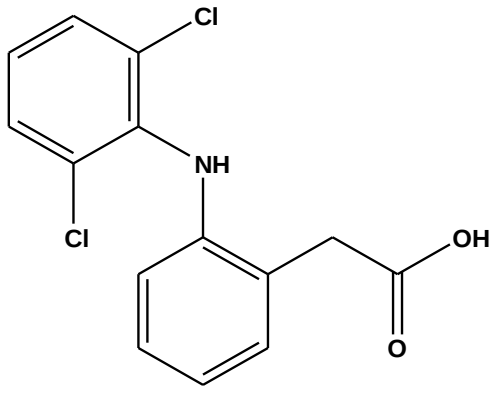

Figure 1.3 Molecular structure of diclofenac (DCF)

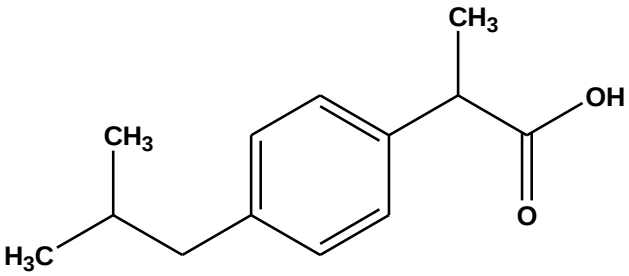

Figure 1.4 Molecular structure of ibuprofen (IBP)

Many pharmaceutical compounds have been detected in surface water and drinking water around the world. This indicates their ineffective removal from water and wastewater using conventional treatment methods. Among different treatment options, ozonation and AOPs are successful and promising methods for the efficient degradation and removal of pharmaceutical pollutants found in water bodies. Various AOPs have been reported in literatures for the degradation and removal of residual pharmaceuticals from aqueous solution [51, 52].

Degradation of DCF was investigated in several reports using photolysis and photocatalytic degradation [53-58], ozonation [59], sonolysis [60], and their combined applications [61-64], UV/H_2O_2 [65], Fenton and photo-Fenton oxidation [66-68], pulsed corona plasma [69, 70] and dielectric barrier discharge plasma [71].

IBP has already been treated by several oxidation processes including photolysis and photocatalysis [72-74], sonolysis and sono-catalytic degradation [75-77], ozonation and photocatalytic ozonation [78, 79], Fenton and photo-Fenton process [80, 81] and non-thermal plasma [82-85]. Decomposition of DCF and IBP in aqueous solution obtained by different methods, including ozonation, photocatalysis and nonthermal DBD-plasma using a planar falling film reactor with a common design which has been investigated and compared in the present work. Besides the removal of DCF and IBP, special attention was paid to the degree of mineralization and the

formation of byproducts. The intermediates formed during the degradation of both pharmaceuticals which were identified by GC/MS. The transformation pathways were also proposed.

1.8.2 Pesticides

Pesticides are chemical compounds that are classified on the basis of their potential against unwanted living organism such as weeds, disease, and pets to improve crop yields. Herbicides, insecticides and fungicides are the most common pesticides [86, 87]. Widespread consumption of these chemicals worldwide has been considered as a major source of water pollution. Due to their adverse effect, the accumulation of these chemicals in water environments can be toxic and harmful for human health and aquatic life [8, 87]. The concentration of pesticides in surface and ground water is considered to be very small (trace or ultra-trace concentration). However, out flowing from agricultural area and pesticide formulating or manufacturing plants contains a high concentration of pesticide which may reaches up to 500 mgL^{-1} [88]. Therefore, a powerful wastewater treatment is necessary to treat these point sources of pesticides so as to decrease their risks on the environment. 2,4-dichlorophenoxyacetic acid (2,4-D), has the chemical structure shown in (Fig. 1.5) is a common phenoxy herbicide widely used for controlling broad-leaf weeds and grasses in forests, gardens and crops [89]. After application of 2,4-D, the residues can be discharge or it can be washed during precipitation and pollute nearby water bodies. Due to its carcinogenic and mutagenic activity, the presence of 2,4-D residues in agricultural product and environment can be extremely harmful to both human and animal [9]. The production of 2,4-D is based on reaction 2,4-dichlorophenol (2,4-DCP) with chloroacetic acid and, in addition the main degradation by-product of 2,4-D is 2,4-DCP [90]. Thus, both emerging water pollutants occur in the environment simultaneously.

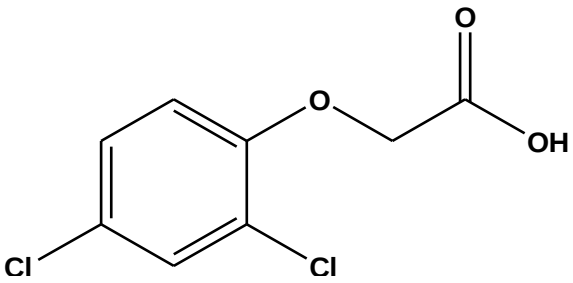

Figure 1.5 Molecular structure of 2,4-D

Several methods have been used for the removal of 2,4-D and 2,4-DCP in aqueous solutions including oxidation via persulfate [90] and adsorption processes [91, 92]. Advanced oxidation processes (AOPs) have been extensively examined for the removal of 2,4-D herbicide and 2,4-DCP from aqueous solutions [93]. Owing to the high toxicity and potential carcinogenic effects of 2, 4-D and 2, 4-DCP [94], the only oxidation of these pollutants would not be a sufficient treatment. Therefore, it is necessary to sufficiently mineralize the mentioned pollutants via efficient treatment methods. Ozone as a powerful oxidant selectively attacks organic pollutants at neutral or acidic medium, but in many cases poor mineralization of these pollutants is observed [88, 95]. This disadvantage makes the application of ozonation alone undesirable. For this reason, various ozone-based AOPs have been studied for the removal of 2,4-D from aqueous solutions such as photocatalytic ozonation [19, 95-97], ozone-hydrogen peroxide [98], AOPs based on photocatalytic degradation [99-102], Fenton and photo-Fenton oxidation [103-105] and electro oxidation process [106]. AOPs based on plasma in contact with liquid water has been emerging as a powerful and novel advancement water purification technology for the removal of most recalcitrant micro pollutants [5]. Recently the degradation of 2,4-D has been reported by combination of ozonation with non-thermal corona discharge to enhance the degradation efficiency [107], and a multiple-pin plane configured pulsed corona discharge reactor [108].

Several oxidation processes have been reported for the removal of chlorophenol from water including ozontion and photocatalysis [109-111], non-thermal plasma induced by corona discharge [112, 113] or dielectric barrier discharge [114] and Fenton and photo-Fenton treatment [115, 116]. In the present work ozonation and different AOPs involving photocatalysis and non-thermal DBD plasma under various gas atmosphere for the degradation and mineralization of 2,4-D and 2,4-DCP from their aqueous solution have been investigated and compared, using a planar falling film reactor.

1.8.3 Organic dyes

Organic dyes and pigments are widely used in various industries such as textile, paper, plastic, leather, ceramic, cosmetic and food processing. Therefore, a significant amount of unfixed dyes are discharged into water environment during synthesis and industrial processing which resulting in serious environmental problems worldwide [117, 118]. These organic dyes can affect the aquatic life by minimizing the sunlight penetration into the stream and reducing photosynthetic process. Furthermore, the majority of these organic dyes are chemically stable, less adapted to the biological treatment and are toxic to the environment due to their resistance to the aerobic degradation and formation of carcinogenic aromatic amines during the anaerobic degradation [119-122]. Therefore, decomposition and removal of these pollutants from wastewater is a necessary step before being discharged into the aquatic ecosystem.

Various treatment technologies in the literature has been reported and reviewed for removing organic dyes from water such as physicochemical, biological, chemical, electrochemical and advanced oxidation processes [122-127].

Biological treatment is commonly used for the removing of organic pollutants from textile wastewater. These methods are environmentally

friendly, produce less sludge, and are relatively inexpensive [128], but it requires a large area of land and it is a very slow treatment process. There is some toxic organic dye which resist against biological degradation which limits the application of this technique.

The physiochemical techniques involve (coagulation-flocculation, adsorption and membrane separation) are effective methods for removing organic dyes. Nevertheless, production large amount of sludge, adsorbent reactivation, decomposition of pollutants after separation, membrane clogging, high capital cost and high disposal cost are the main limitations [126, 129]. Chemical methods such as ozonation and advanced oxidation processes are powerful methods and provide fast decolorization and degradation of organic dyes.[48, 130-132].

Table 1.1 Ozonation and various AOPs reported for MB degradation

Type of oxidation process	Conditions	Reference
Ozonation	Continuous reactor system.	[136]
	Batch bubble column.	[137]
Fenton	Photo-Fenton and sono-photo-Fenton were compared.	[138]
	Under the exposure to UV or Vacuum-UV in a micro photo-reactor.	[139]
	CdS/multi-walled carbon nanotube-TiO_2 under the visible light.	[140]
Photocatalysis	TiO_2/UV-based photocatalysis.	[141]
	UVA/TiO_2 nanoparticle in a self-made photocatalytic reactor.	[142]
	copper (II) oxide synthesized by thermal decomposition of Flubendazole complexes.	[143]
	Synthesized copper, zinc, tin, and sulfide nanoparticles under the visible light.	[144]
	Photocatalysis using ZnO:Eu nanoparticles.	[145]
Non-thermal plasma	Liquid film over the inner electrode using DBD in cylindrical reactor.	[146]
	Pulsed corona discharge in a multi wire plate geometry.	[147]
	DBD at the gas water interface.	[148]
	DBD plasma jet in air, nitrogen and argon gas atmospheres.	[149]
	Coaxial DC corona discharge in air, N_2, He and CO_2.	[150]
	Double-chamber DBD reactor in air and oxygen carrier gases.	[151]
	Microwave plasma jet at atmospheric pressure in argon.	[152]

MB (Fig. 1.6) is one of the most commonly colored compounds used during the dyeing process of cotton, wood and silk [133]. Removing methylene blue from aqueous solution was intensively investigated in the literature. The removal of methylene blue is done either by adsorption on activated carbon [134, 135], or by oxidation via ozonation and various AOPs (Table 1.1).

In the present work, degradation and mineralization of methylene blue as a model dye pollutant was examined by ozonation and various advanced oxidation process in a planar falling film reactor.

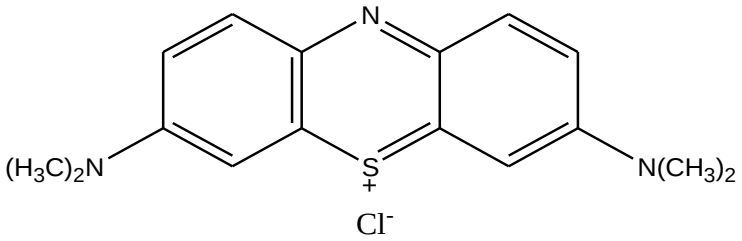

Figure 1.6 Molecular structure of a methylene blue (MB)

1.9 Objectives of this study

Due to the differences in the reactor design and experimental set up used in literature comparative observation of the results by various AOPs is difficult. Therefore, the main objective of the present work is the investigation and comparison of the efficiency of ozonation and different AOPs in the removal of various organic pollutants including DCF and IBP pharmaceuticals, 2,4-D phenoxy herbicide and its degradation by-product 2,4-DCP, and MB dye, from their aqueous solutions, using a planar falling film reactor with a common design. The use of a planar falling film reactor has the advantage of higher transfer rate of generated reactive species from gas into liquid due to the large surface to volume ratio. The performance of the studied treatment methods have been compared in terms of energy yield at 50% conversion and total organic carbon (TOC, degree of mineralization) removal for the treatment of all pollutants. Furthermore, the study includes the efficiency of each examined methods in the degradation of the main by-products formed during the degradation process. In fact, this is generally an important aspect because some of the by-products might be more toxic and carcinogenic than the initial pollutant. Therefore, a maximum mineralization of the pollutants is necessary before releasing them into the ecosystem. Hence, this comparative study helps to elucidate the most efficient remediation methods that can be used for commercial applications.

Chapter Two

Experimental

Chapter Two

2. Experimental

2.1 Materials

All solvents and chemicals used in this work were analytical grade and used without further purification.

Table 2.1 List of the chemical compounds; MW = molar weight

Chemical	MW	Purity (%)	Manufacturer
Acetonitrile for HPLC	41.05	≥ 99.9	Chemsolute, Germany
Ammonium sulfate	132.14	≥ 99.5	Merck, Germany
Diclofenac sodium salt	318.14	> 98.5	Alfa Aesar, Germany
2,4-dichlorophenoxyacetic acid	221.04	98	Alfa Aesar, Germany
2,4-dichlorophenol	163	99	Aldrich
Ibuprofen sodium salt	228.26	≥ 98	Fluka
Iron(II) sulfate heptahydrate	278.02	≥ 90	Sigma-Aldrich
Glacial acetic acid	60.05	99.7	Amresco
Glycolic acid	76.05	99	Sigma-Aldrich
Glyoxylic acid	74.035	98	Sigma-Aldrich
Liquid hydrogen peroxide	34.01	30	Merck
Hydrochloric Acid	36.46	35-38	Chemsolute, Germany
Methylene blue (C.I. 52015)	319.85	---	Merck
Methanol for LC-MS	32.04	99.95	Chemsolute, Germany
Malonic acid	104.06	99	Abcr, Germany
Maleic acid	116.07	≥ 99	Merck
Oxalic acid	126.07	99.5	Merck
Phosphoric acid	98	85	Sigma-Aldrich
Potassium nitrate	101.1	99.99	Merck
potassium titanium oxide oxalate dihydrate	354.13	≥ 90	Sigma-Aldrich
Sodium chloride	58.44	99.5	Merck
Sodium thiosulfate pentahydrate	248.18	≥ 99	Fluka
Sodium azide	65.01	99.5	Chemsolute, Germany

Sodium carbonate, eluent (concentrate for IC)	105.99	0.1M	Sigma-Aldrich
Sodium bicarbonate, eluent (concentrate for IC)	84	0.1M	Sigma-Aldrich
Sulfuric acid	98.08	95-97	Merck
Sodium hydroxide	40	≥ 98.8	Chemsolute, Germany
Succinic acid	118.09	≥ 99	Fluka

2.2 Reactors and equipment

Two planar falling film reactors have been used in the present work (Figs. 2.1 and 2.3). Each reactor with approximately 10 liters volume (height 68 cm, width 29 cm, diameter 5 cm) consists of two Pilkington Activ™ glass sheets as sidewall of the reactor connected by an interior frame of polyvinyl chloride (PVC) which is surrounded by aluminum made exterior frame. The Pilkington Activ™ glass (TiO_2 coated glass) acts as a heterogeneous photo-catalyst and its great superhydrophilicity provides a homogeneous and stable falling liquid film with a thickness of about 150 µm at 1L/min liquid flow rate along the glass sheets. The advantage of the reactor with a thin falling liquid film is to provide the larger surface-to-volume ratio in a thin film as compared with deep layers, resulting in a faster rate of transfer of reactive species from gas into the liquid [44].

2.2.1 Photocatalytic reactor

The photocatalytic reactor (Fig. 2.1) contains seven UVA lamps (LT 15 W/009 UV, produced by NARVA Lichtquellen GmbH & Co.KG, Germany) with the incident light intensity of 1 mW/cm² at the maximum irradiation wavelength of 350 nm, fixed inside the reactor. The relative intensity of the UVA lamps has been verified by a UVA photodiode sensor (Gerus GmbH, Germany). There was no significant aging effect during the experimental period. The spectrum of this type of UVA lamps is shown in Fig. 2.2. The

demanded ozone for all experiments performed in this reactor was supplied by an ozone generator (OZ 502/10 Fischer Technology, Germany). It delivers about 130±5 mg/L ozone gas at a power of 30 W and an oxygen gas flow rate of 10 L/h (controlled by a Brooks Mass Flow Controller 5850E, Netherland) which is continuously flowed into the reactor during the experiments.

The ozonation experiments were carried out in this reactor (Fig. 2.1) in darkness. However, for P.C. Ozonation and P.C. Oxidation experiments the seven UVA lamps were switched on.

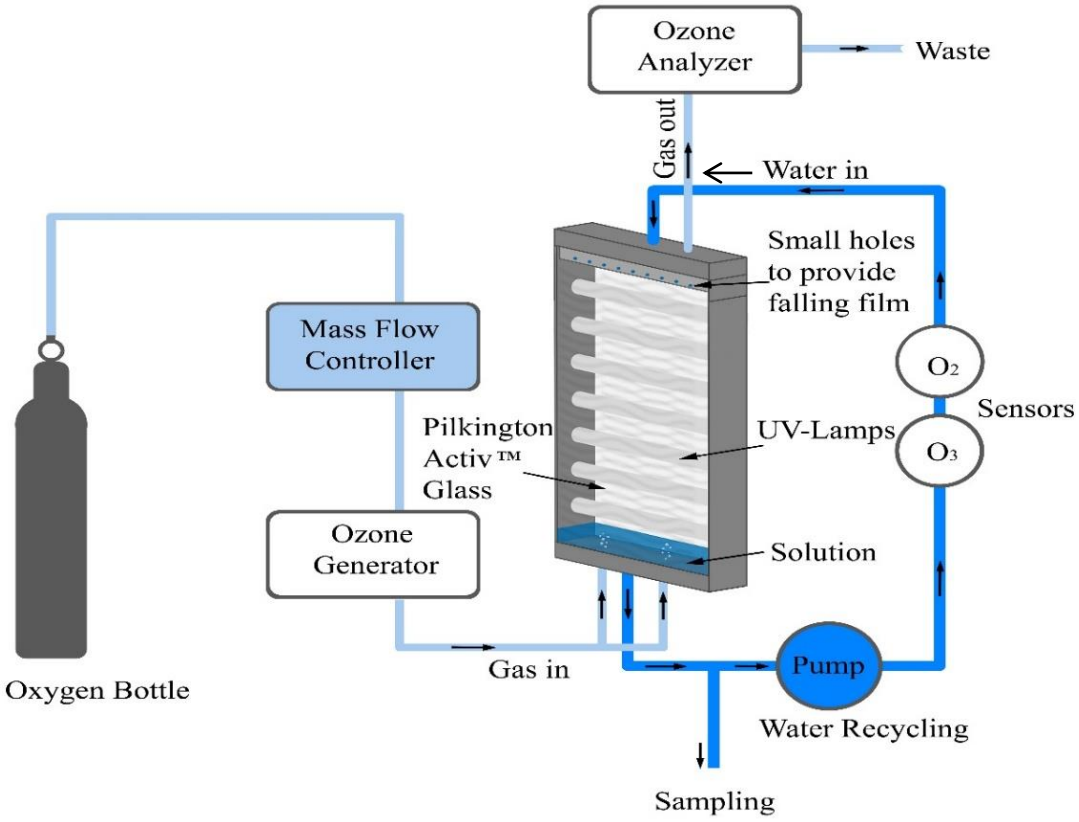

Figure 2. 1 Schematic diagram of the photocatalytic reactor

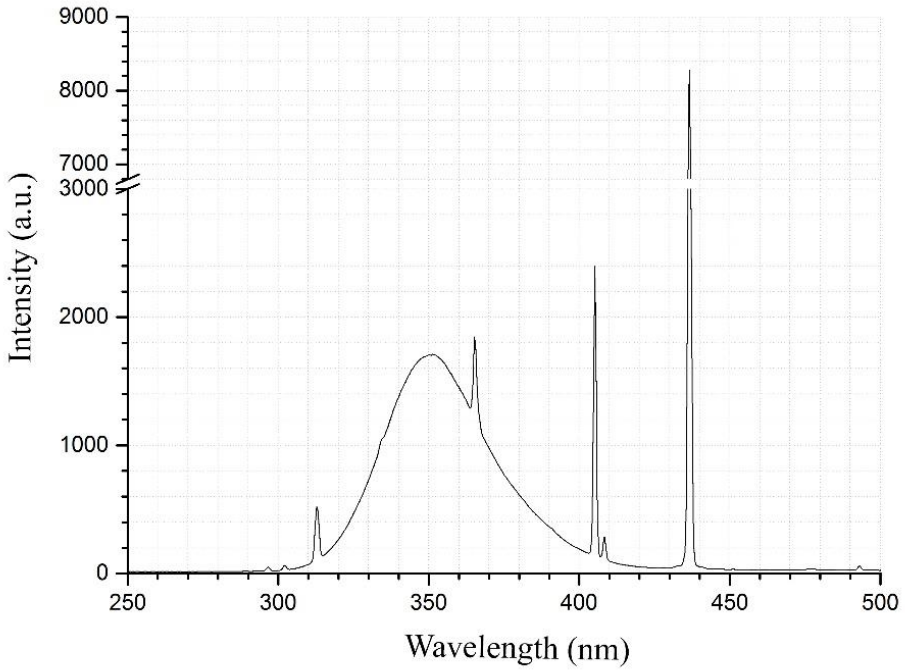

Figure 2.2 Spectrum of UVA lamps

2.2.2 Dielectric barrier discharge (DBD) reactor

In the non-thermal DBD plasma reactor (Fig. 2.3), two dielectric ceramic plates (3 mm thickness) are situated inside the reactor, parallel to the glass sheets between the high voltage and the ground electrodes. The high voltage electrode consists of a self-adhesive aluminum foil (19 × 47 cm) fixed on the inner side of the dielectric plate, while the ground electrode is made of self-adhesive copper strips stuck over a Pilkington Activ™ glass inside the falling film. Minipuls 6 (GBS Elektronic, Rossendrof, Germany) pulse generator providing up to 21 KV (RMS) at frequencies between 5 and 20 KHz was used to generate high voltage. The power of plasma was measured by using the current and voltage wave form. It was regulated online by a homemade Lab view program. The desired gas was introduced to the reactor by mass flow controller at a flow rate of 20 L/h for about two hours until atmospheric saturation of the reactor was achieved. During the degradation process the gas

was circulated in a batch operational mode at a flow rate of about 20 L/h using a membrane pump.

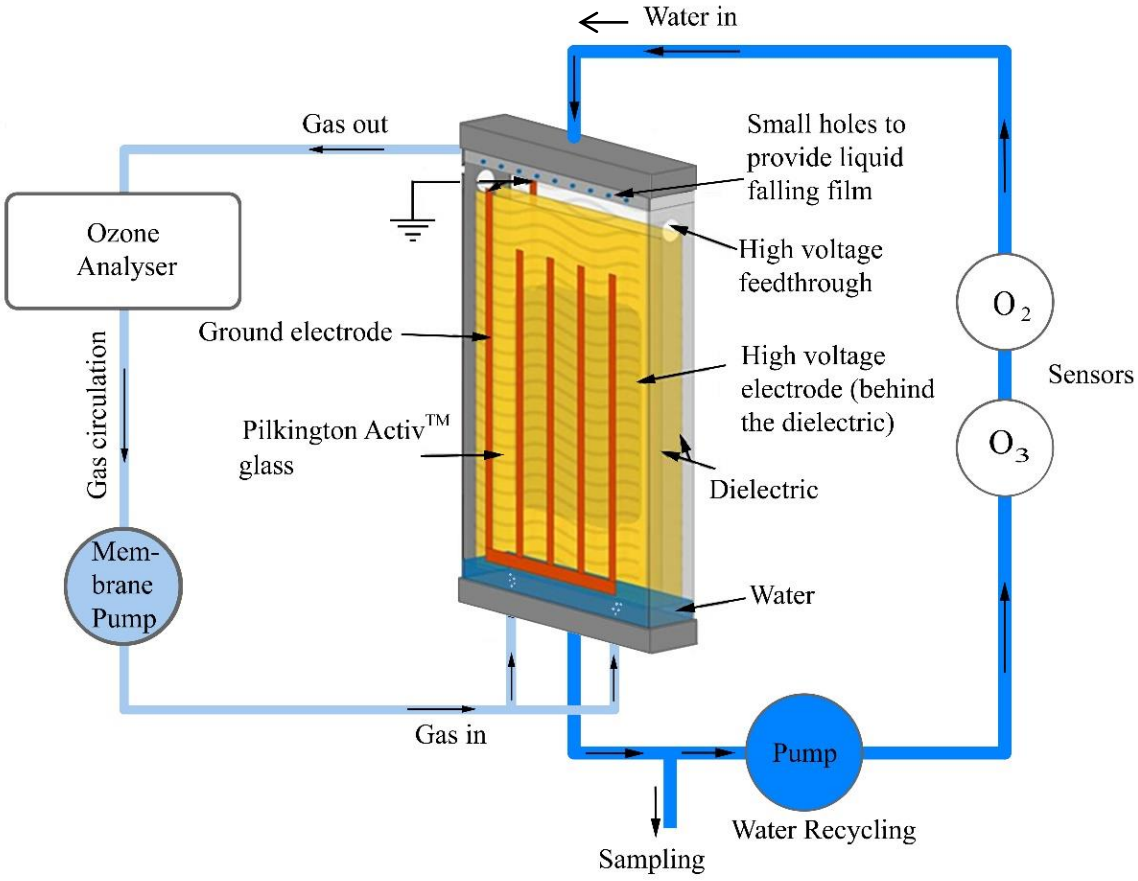

Figure 2.3 Schematic diagram of the DBD reactor

2.2.3 Instruments and devices

The liquid and gas flow rates were controlled by an Ismatec Reglo-z digital gear pump and a Brooks Mass Flow Controller 5850E, respectively. The concentration of both dissolved oxygen and ozone in liquid phase was measured by means of Hach Orbisphere 410 equipped with Orbisphere A1100 and C1100 electrochemical oxygen and ozone sensors, respectively. Ozone concentration in the gas phase inside the reactors was monitored via UV-Photometry method at 253.7 nm by an Anseros Ozomat ozone analyzer GM-

RT1, Germany. The pH and conductivity of the solutions were measured by a Microprocessor pH and conductivity meter (pH-196 and LF-96, WTW, Germany), respectively.

2.3 Experimental conditions

In all experiments presented in this work, 0.5 liter of liquid solution containing the target pollutant is pumped through the polytetrafluoroethylene (PTFE) tubes (3.8 mm diameter) by means of gear pump which is introduced to the top of the reactor and circulated at flow rate of 1 L/min where it flows downward through the Pilkington Activ™ glass as a falling liquid film. The Pilkington Activ™ glass sheet (self-cleaning window) used in the present work is a colorless transparent glass sheet with a thickness of 4 mm coated with a nano-layer of 12 nm anatase TiO_2 nanoparticles with an average crystalline size of 18 nm an average agglomerate size of 95 nm [153, 154]. It acts as photo-catalyst and provides the advantages of large surface to volume ratio (up to 1400 m^2/m^3 per cycle) and its great superhydrophilicity (water contact angle 0˚) provides a homogeneous and stable falling liquid film (~150 µm thickness at 1L/min liquid flow rate) along the glass sheets. In photocatalytic reactor the oxygen gas or a mixture of ozone-oxygen in case of ozone used experiments was continuously flowing into the reactor from the bottom with a rate of 10 L/h in an open system, while in DBD plasma reactor the desired gas was circulated at 20 L/h during the degradation process.

The solutions of treated pollutants and all other standards were prepared by dissolving appropriate amount of the target compounds in deionized water. The energy yields (G_{50}) for the degradation of each pollutant treated in this work at 50% conversion (g/kWh) and estimated by the following equation (Eq. 2.1):

$$G_{50} = \frac{30 \times [C]_0 \times V}{P \times t_{50}} \quad (2.1)$$

where $[C]_o$ represents the initial concentration of target pollutant (mg/L), V is the volume of the treated solution (L), *P* is the power of input energy (W), and t_{50} is the time (min) required for 50% degradation of pollutants.

The yield of photocatalysis was calculated as 105W by summarizing the demanded energy of seven UVA lamps (7 x 15 = 105 W) and the ozone generator yields about 130 ± 5 mg/L ozone gas at a power of 30 W and an oxygen gas flow rate of 10 L/h was used. Ozonation and photocatalytic experiments were performed in photocatalytic reactor Fig. 2.1.

It should be noted that the t_{50} is calculated from the degradation curves, taking into account that the DBD experiments are performed in burst modus: The plasma is usually applied as 1 second on / 1 second pauses in order to restore the falling liquid film which is disturbed by the discharge. Each experiment reported in this work has been repeated for at least two times and the RSD of measurements is not more than ±5%.

2.4 Analytical methods

2.4.1 High-performance liquid chromatography (HPLC)

The concentration of diclofenac (DCF), ibuprofen (IBP), 2,4-dichlorophenoxyacetic acid (2,4-D) and 2,4-dichlorophenol (2,4-DCP) was measured by HPLC (Gynkotek HPLC system equipped with M480G gradient pump, GINA 50 Autosampler with a 10µL injection loop, and a UVD 1705 Dual-Channel UV-VIS Detector). The stationary phase is a NUCLEOSIL 100-5 C18 (125 × 2 mm, 5µm) column. The mobile phase consists of 50% acetonitrile and (50% of 0.01% acetic acid (HAC) for DCF and 1% HAC for IBP prepared in ultra-pure water) at 254 and 230 nm, respectively. In case of 2,4-D and 2,4-DCP the mobile phase was a mixture of methanol and 0.1%

H_3PO_4 solution, with a ratio of 50:50 at λ=280. The mobile phase was flowed at 250 µL/min in all analysis.

In order to calculate the concentrations of DCF, IBP, 2,4-D and 2,4-DCP from the obtained peak area chromatograms their calibration curves are drawn by plotting peak area vs. concentration (Figs. 2.4, 2.5, 2.6 and 2.7)

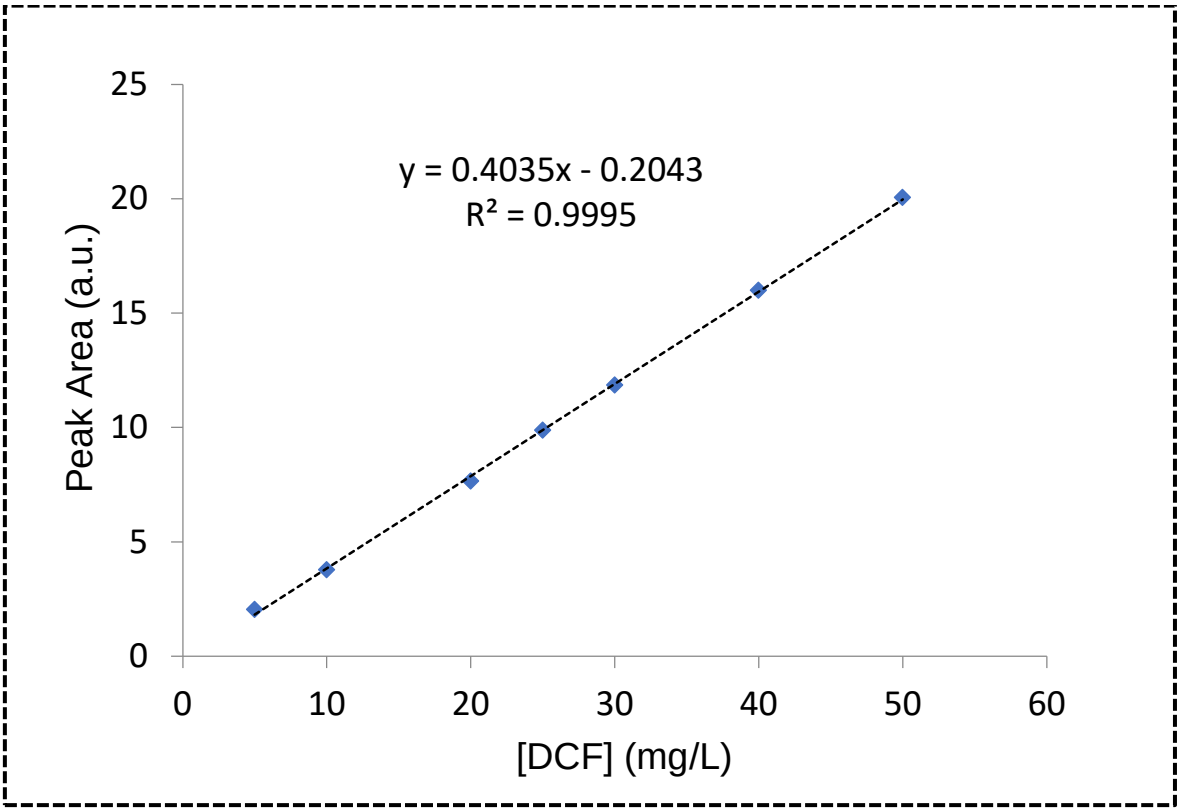

Figure 2. 4 Calibration curve of diclofenac concentration vs. peak area

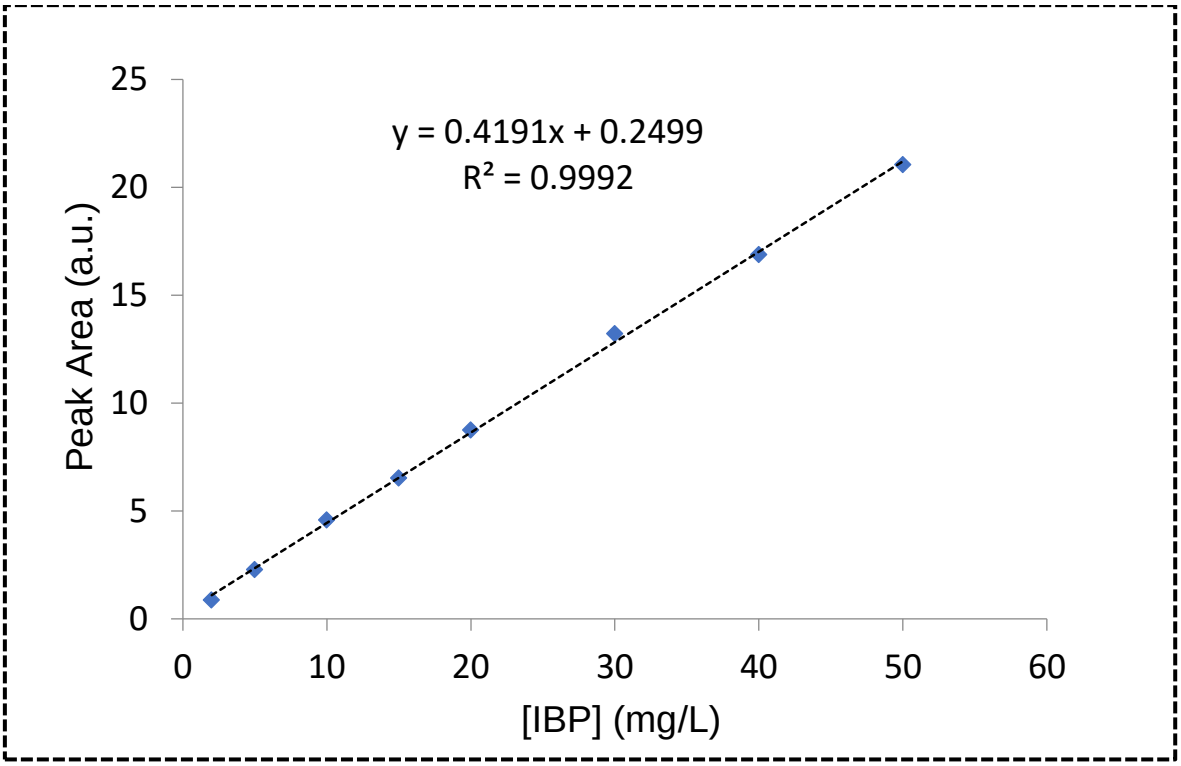

Figure 2. 5 Calibration curve of ibuprofen concentration vs. peak area

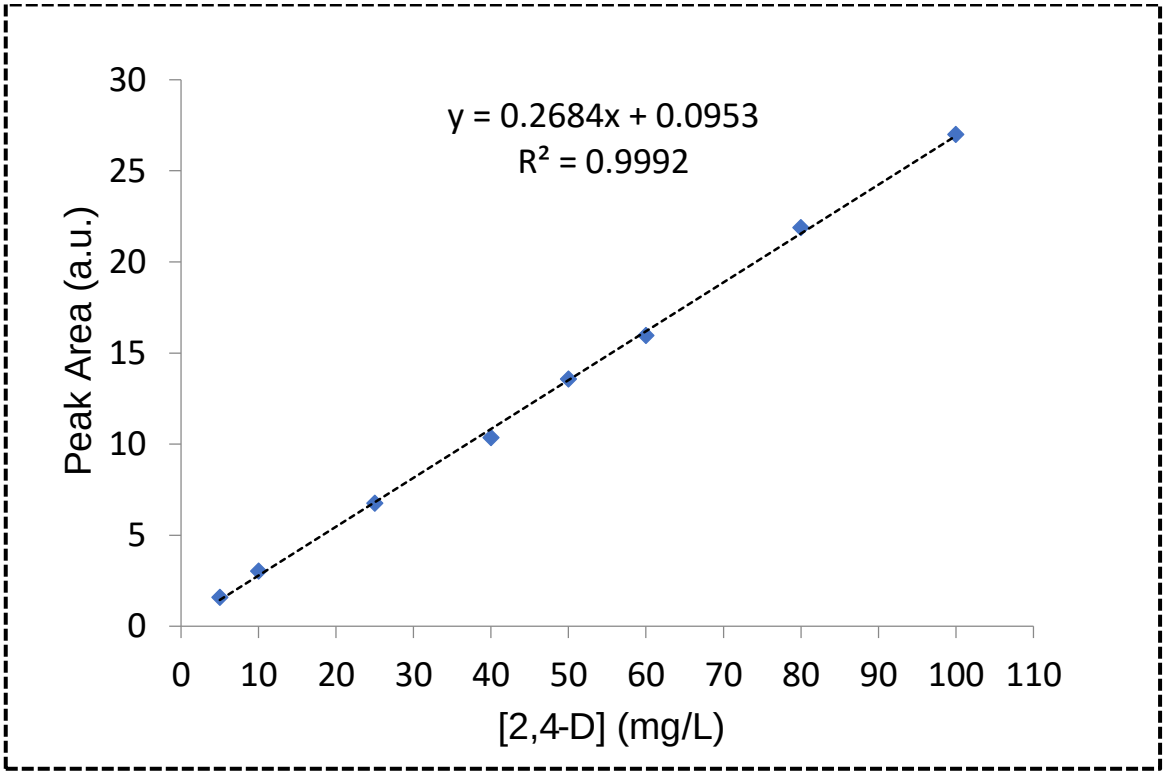

Figure 2.6 Calibration curve of 2,4-D concentration vs. peak area

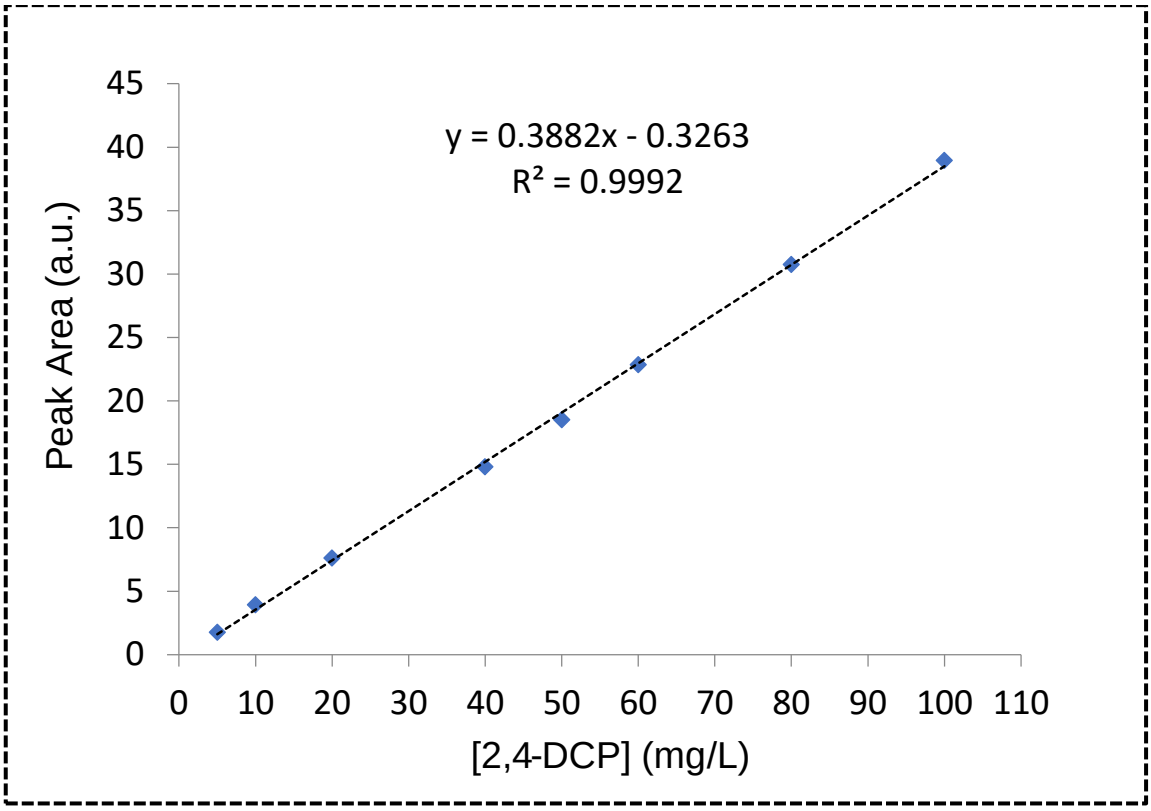

Figure 2.7 Calibration curve of 2,4-dichlorophenol concentration vs. peak area

2.4.2 Ion chromatography (IC)

Anionic by-products produced during the degradation process such as acetic acid, oxalic acid, glyoxylic acid, glycolic acid, chloride ion as well as sulfate ion were determined by ion chromatography, using a Dionex DX 500 equipped with a CD20 conductivity detector connected to an Ion Pac AS14 (4 × 250 mm) column and an AG14 (guard column) with the injection volume of 25 µL. The mobile phase is consisted of a mixture of $NaHCO_3$ (1.0 mM) and Na_2CO_3 (3.5 mM), at a flow rate of 1.2 mL/min. The concentration of each ion was calculated from their calibration curves, which were drawn by plotting peak area vs. concentration. The concentration of acetic acid Rt = 2.9 min., oxalic acid Rt = 8.5 min., glyoxylic acid Rt = 3.1, Glycolic acid Rt = 2.75, chloride Rt = 3.85 min. and sulfate ion Rt = 7.7 were calculated by fitting the concentration to the obtained peak areas using a linear regression giving the following equations shown in (Figs. 2.8 to 2.13).

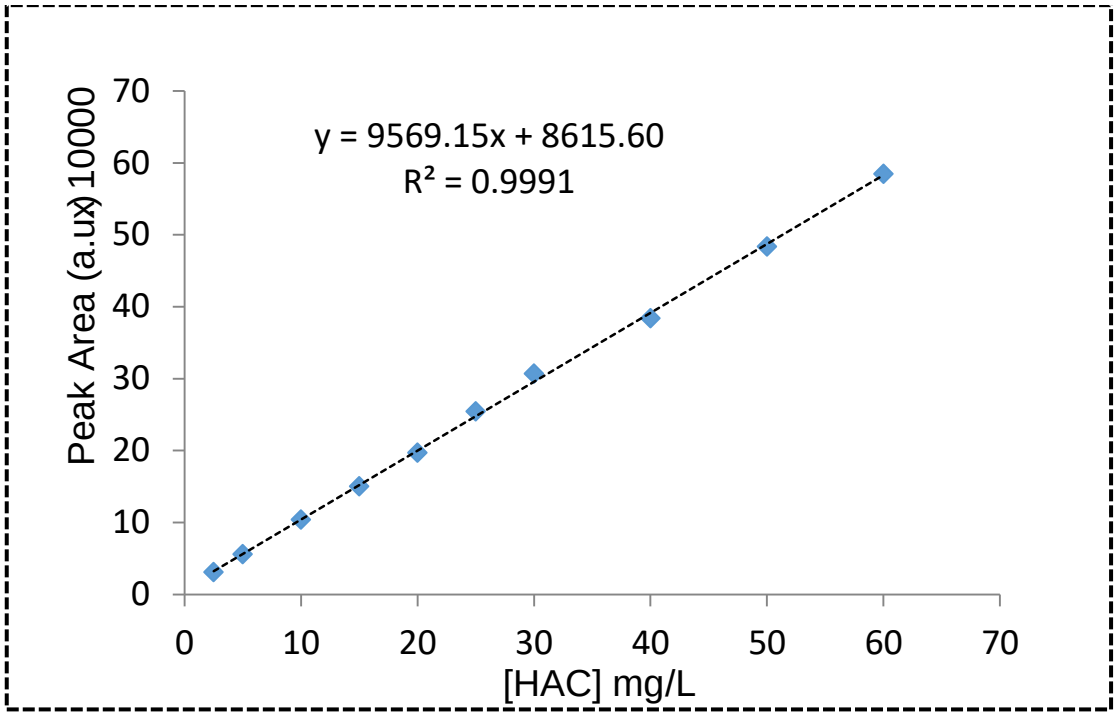

Figure 2.8 Calibration curve of acetic acid concentration vs. peak area

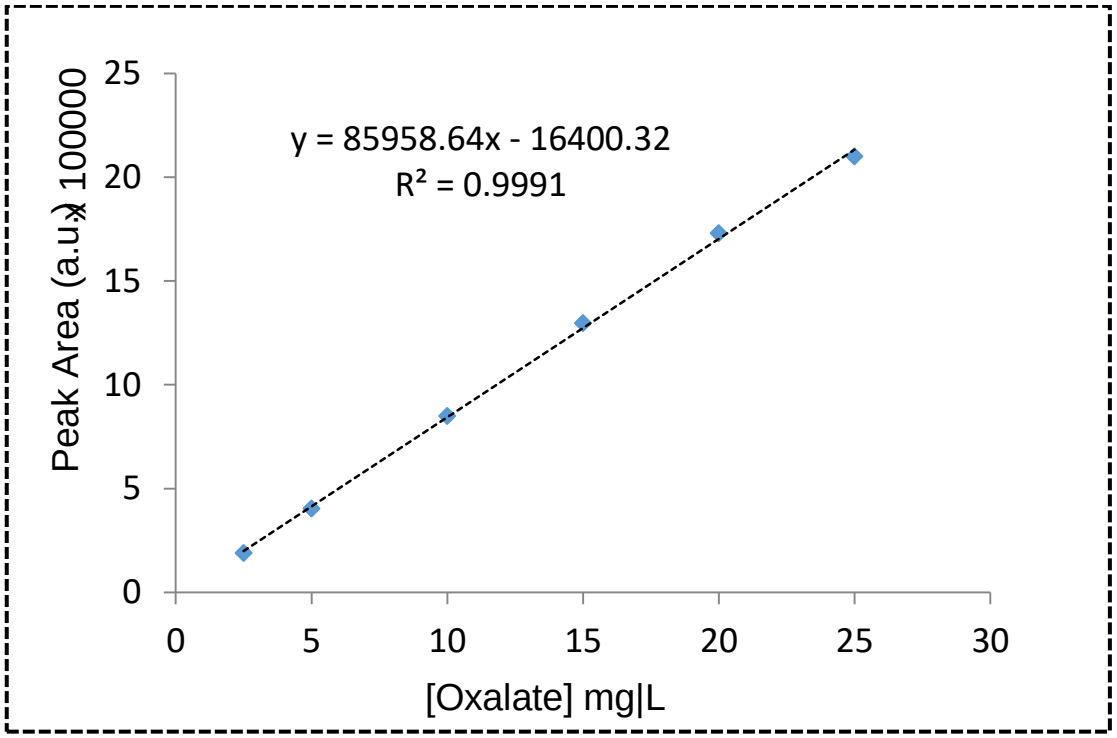

Figure 2. 9 Calibration curve of oxalic acid concentration vs. peak area

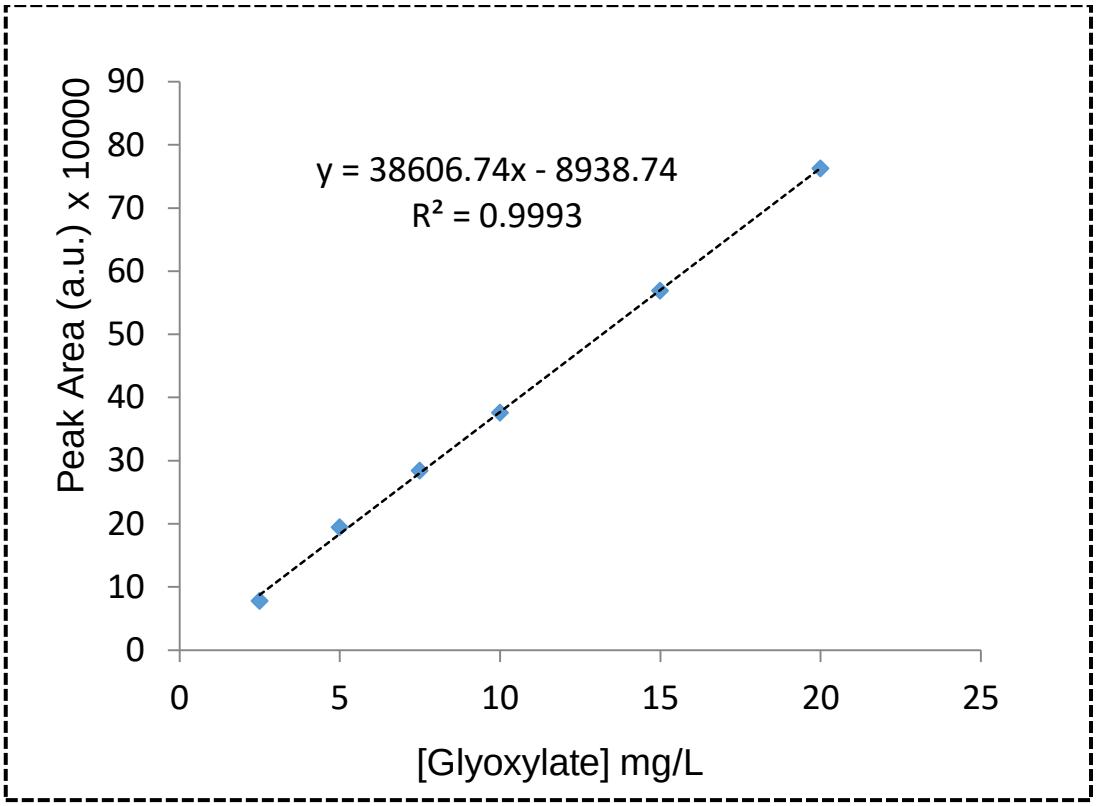

Figure 2. 10 Calibration curve of glyoxylic acid concentration vs. peak area

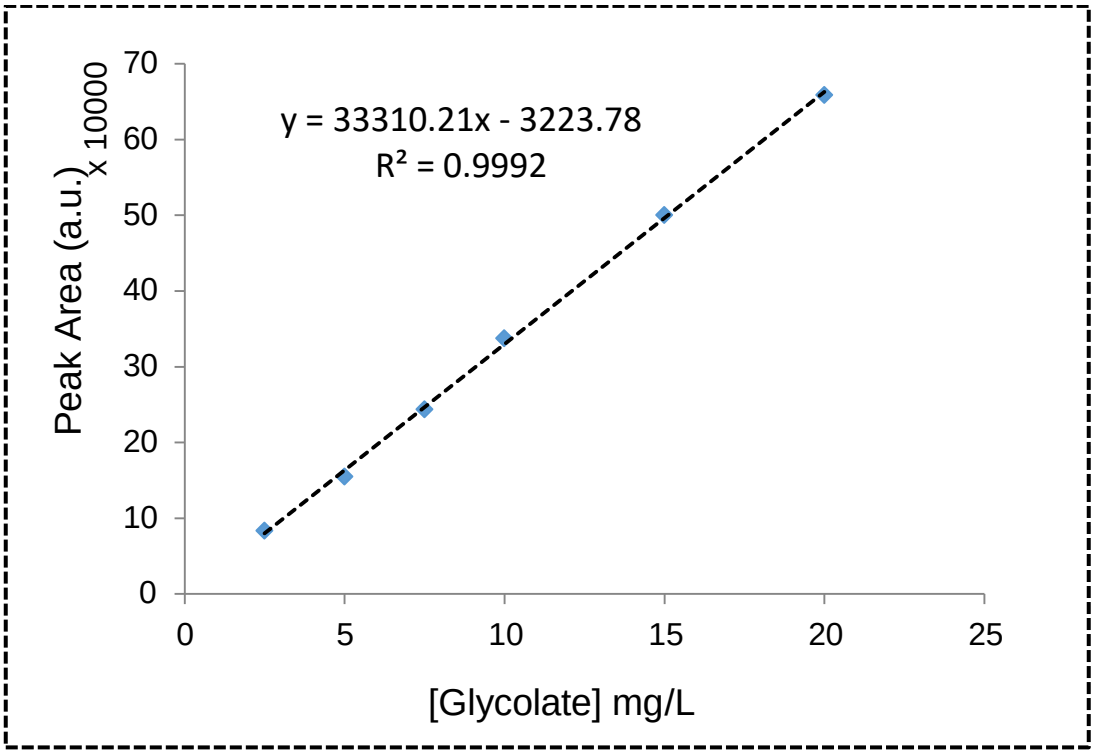

Figure 2.11 Calibration curve of glycolic acid concentration vs. peak area

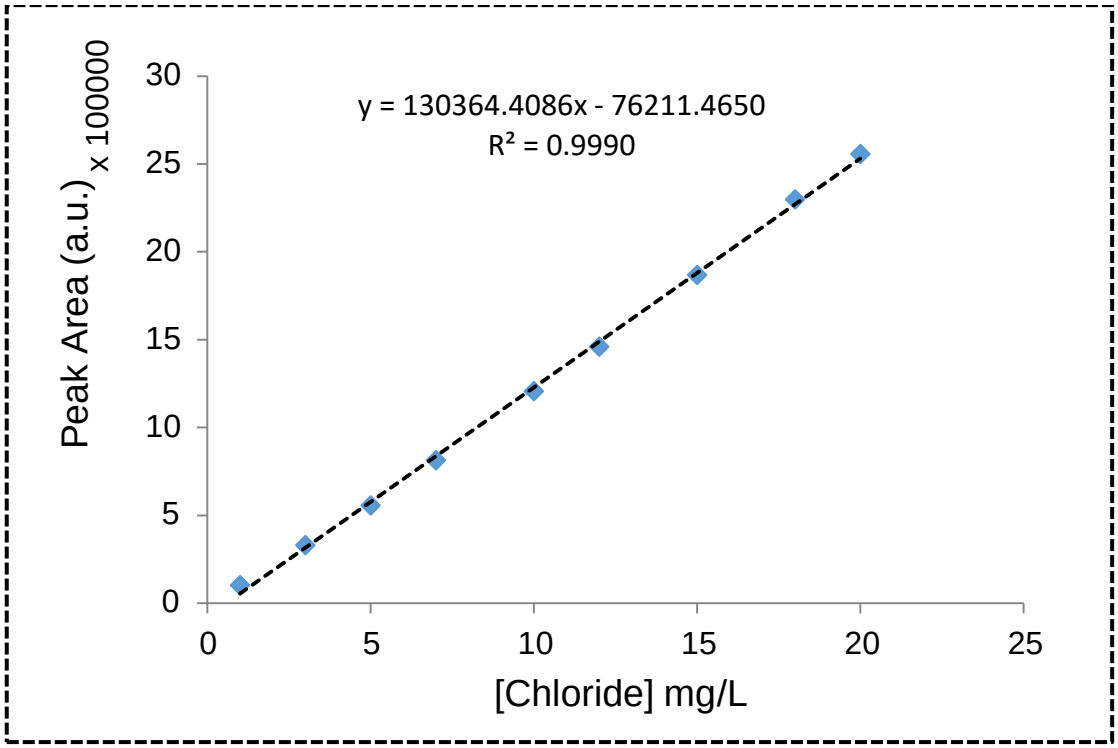

Figure 2.12 Calibration curve of chloride concentration vs. peak area

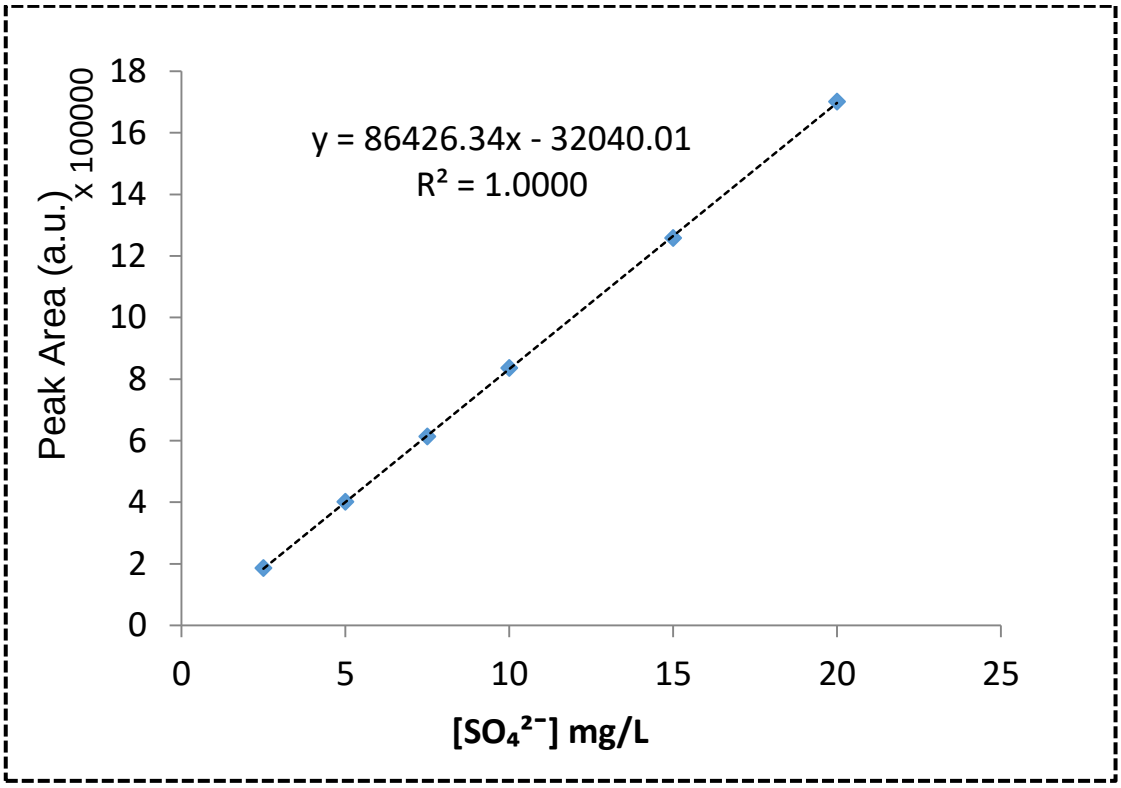

Figure 2.13 Calibration curve of sulfate concentration vs. peak area

2.4.3 Total organic carbon (TOC) analysis

The evaluation of mineralization of the treated samples was performed by means of TOC analyzer, using a Shimadzu TOC-5000 (Japan). Mineralization efficiency *M* (in %) is calculated by the following equation (Eq. 2.2)

$$M\% = (1 - \frac{[TOC]t}{[TOC]_o}) \times 100 \qquad (2.2)$$

where $[TOC]_o$ and $[TOC]_t$ are the TOC concentration (in mg/L) of the solution at reaction times 0 and *t* (in min), respectively.

2.4.4 Spectrophotometry

A UV-visible scanning spectrophotometer (Shimadzu UV-1601 CE, Japan) was used to determine the concentration of the methylene blue at λ=665 nm (Fig. 2.14) and generated hydrogen peroxide as a result of DBD plasma treatment using spectrophotometric potassium titanium (IV) oxalate method [155, 156] at λ = 390 nm. Titanium (IV) oxalate method is an effective and successful method for the determination of hydrogen peroxide in treated water sample by AOPs [156]. This method is based on the reaction of hydrogen peroxide and titanium (IV) in acid solution resulting in the formation of an intensively yellow colored pertitanic acid complex and possesses a maximum absorbance at 390 nm.

Preparation of reagents and analysis procedure

1. A solution of 50 g/L potassium titanium oxide oxalate was prepared by dissolving 25 gram of $K_2TiO(C_2O_4)_2 \cdot 2H_2O$ in 400 mL of deionized water and diluted to 500 mL with deionized water in a volumetric flask.
2. 20 mL of concentrated sulfuric acid (d = 1.84 g/mL) was added to 340 mL deionized water slowly, the yielded concentration was placed in a 1 L

beaker and then allowed to cool and used as a solution of (1:17) H_2SO_4:H_2O.

3. A stock solution of 1000 mg/L H_2O_2 was prepared by diluting about 6.7 mL of concentrated H_2O_2 (ACS reagent, 30%) to a 2 liter volumetric flask with deionized water. In order to determine the actual concentration of H_2O_2 the prepared solution was standardized by using the potassium permanganate titration method.
4. The calibration curve and analysis of treated samples were performed as follows: a volume of 1 mL of 50 g/L potassium titanium oxide oxalate reagent was added to a mixture of a series H_2O_2 standard solutions or a suitable volume of the treated sample solutions with 1 mL (1:17) solution. The mixture was mixed well and diluted to 25 mL in a volumetric flask using deionized water, allowing the solution for 5 min. The absorbance of the resulted pertitanic acid was measured against the reagent blank at 390 nm. The calibration curve was drawn between absorbance and H_2O_2 concentration and the concentration of H_2O_2 in treated sample solutions was obtained from the calibration curve (Fig. 2.15).

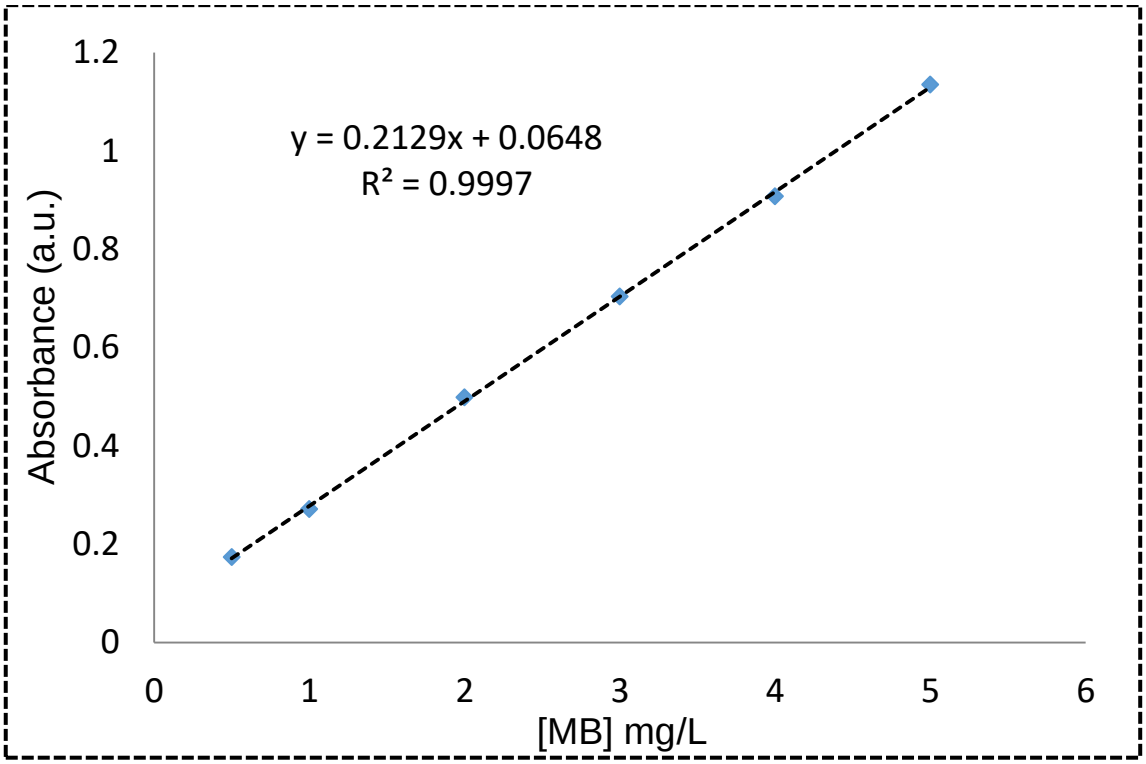

Figure 2.14 Calibration curve of methylene blue concentration vs. peak area

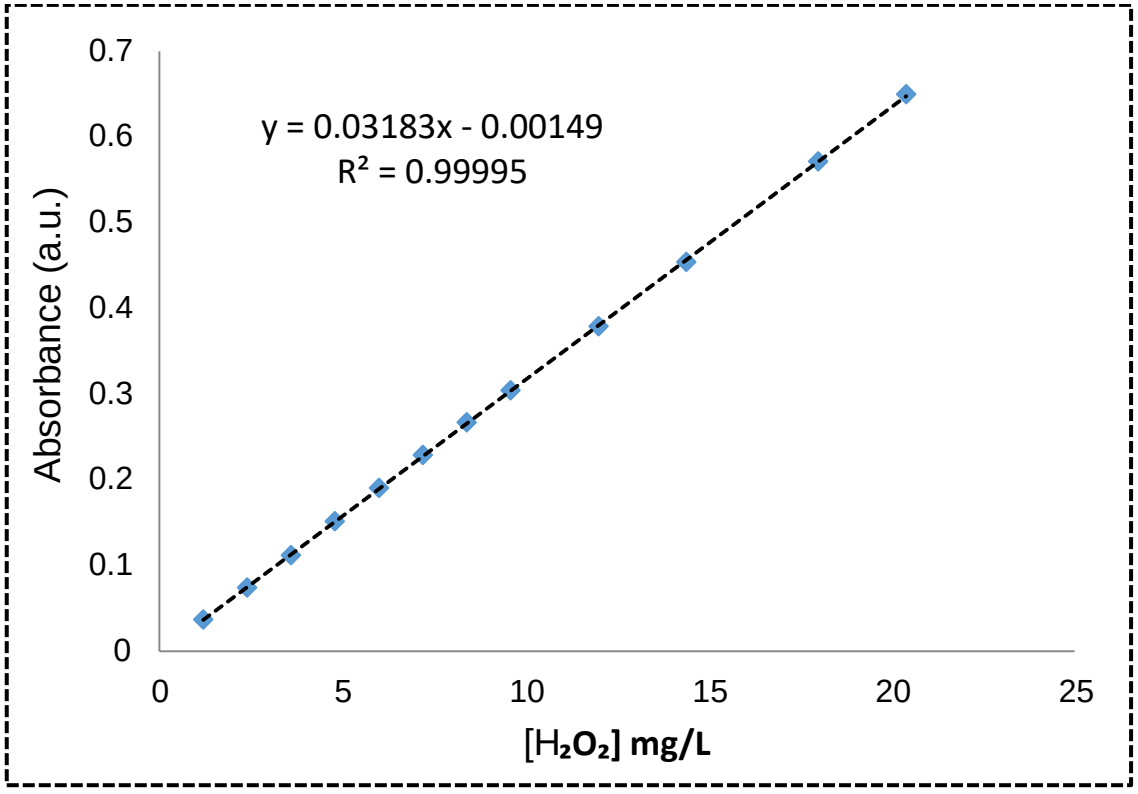

Figure 2.15 Calibration curve of hydrogen peroxide concentration vs. peak area

2.4.5 Gas chromatography-mass spectrometry (GC/MS)

The intermediate degradation products formed during the degradation of diclofenac and ibuprofen were identified by gas chromatography-mass spectrometry (GC-MS). An Agilent (GC: 6890, MS: 5975) was equipped with a capillary column DB-5MS (10 m x 0.25 mm ID x 0.1 µm film thickness). The carrier gas was helium at a flow rate of 6.0 mL/minute. The GC/MS system was operated in electron impact ionization scan mode using the NIST14 spectra library. The analysis was performed by PiCA Prüfinstitut Chemische Analytik GmbH, Germany. Each sample was analyzed by both acidic and alkaline extraction procedure with MTBE solvent after spiked with internal standard (i.a.PCB209) solution.

For each pollutants, two treated samples (200 mL of initial concentration 50 mg/L) were collected and analyzed: the first sample was collected and mixed after (5, 15, 30 and 60 minutes photocatalytic oxidation then followed by 1, 3 and 5 min photocatalytic ozonation) treatment time in photocatalytic reactor whereas the second sample was collected and mixed after 1, 3, 5, 10, 15, 20, 30, 40 and 60 minutes treatment time in DBD plasma reactor under argon gas atmosphere. Each sample solution was treated with 0.025 g sodium thiosulfate to stop the action of hydrogen peroxide or dissolved ozone in the solution.

2.4.6 Real wastewater treatment by DBD plasma

The proposed DBD plasma under argon gas atmosphere at power of 150 W and treatment time of 30 minutes was also used for treatment of real wastewater.

Procedure

The DBD reactor was filled with a 500 mL of the deionized water which was circulated at 1 L/min. An argon gas with a flow rate of 20 L/h was continuously introduced to the reactor for 2 hours to achieve atmospheric

saturation of the reactor with argon gas. After filling the reactor with argon gas atmosphere the deionized water was exchanged by 500 mL real wastewater, the gas inlet and outlet were connected to each other and circulated at 20 L/h in a batch mode followed by plasma treatment of real wastewater for 30 min. at power of 150 W.

In order to stop the action of hydrogen peroxide generated during the discharge plasma and bacteria growth, the collected samples after treatment were protected by addition of 0.025g sodium thiosulfate and 5g sodium azaide. The analysis of treated samples was performed by SGS Institute Fresenius GmbH, Germany using standard analytical gas chromatography methods DIN EN ISO 10301, SOP M2949 DIN 38407-16 and DIN 38407-F16 for chlorobenzene, chloroaniline and non-chlorinated aniline compounds, respectively. The conductivity and pH of the treated wastewater samples were 1600 µS/cm and 6.7 at 24 ˚C, respectively. Both treated samples were taken from the same source (sample (1) without biological treatment and Sample (2) after biological treatment).

2.5 Average thickness of the liquid falling film

Among various methods for measuring the average liquid film thickness, collecting and measuring the volume of distinct amount of the liquid flowed down through the surface of reactor is the simplest method [157]. The average thickness liquid falling film is calculated by dividing the average volume of the water collected by the surface area of the reactor wall. Due to the difficulty of disassembling the planar reactors used in this work in order to collect the exact amount of the drained water and because of the collected water from the outlet of the reactor is not accurate; the same technique was applied with a small modification. The thickness of liquid falling film in a planar reactor used in this work was calculated according to the following equation (Eq. 2.3)

$$\sigma = \frac{Q\ x\ t}{A}\ x\ 10^4 \qquad (2.3)$$

where 1 (μm) is the average liquid film thickness, *Q* (mL/s) liquid flow rate, *t* the time (in second) required for water to cover the whole surface area of the reactor wall, and *A* (in cm²) is the total surface area of the reactor wall covered by liquid falling film. *A* and *Q* are constant throughout the experiment, *Q* was controlled by the gear pump, while *A* was calculated from the surface area of two Pilkington glass sheet (29 x 68 cm). The required time (t) for covering all Pilkington surface area with the liquid was measured by stop watch which was repeated for several times. The obtained liquid film thickness of 500 mL water circulated at a flow rate of 1 L/min in a planar falling film reactor used was 145±5 μm.

2.6 Calibration and optimization of ozone generator

Electrical discharge technology is the most widely used method for commercial ozone production using air or pure oxygen as the feed gas. The concentration of produced ozone depends on the applied power input and the feed gas flow rate [158]. The calibration and optimization of ozone generator used in the present study was performed by investigation of the relation between oxygen feed gas flow rate and the applied electrical power to the ozone generator. From the results shown in Fig. 2.16, it can be observed that the higher input feed gas flow rate was required higher electrical power demands and the optimum ozone production of 130 ± 5 mg/L was obtained at electrical power of 30 W.

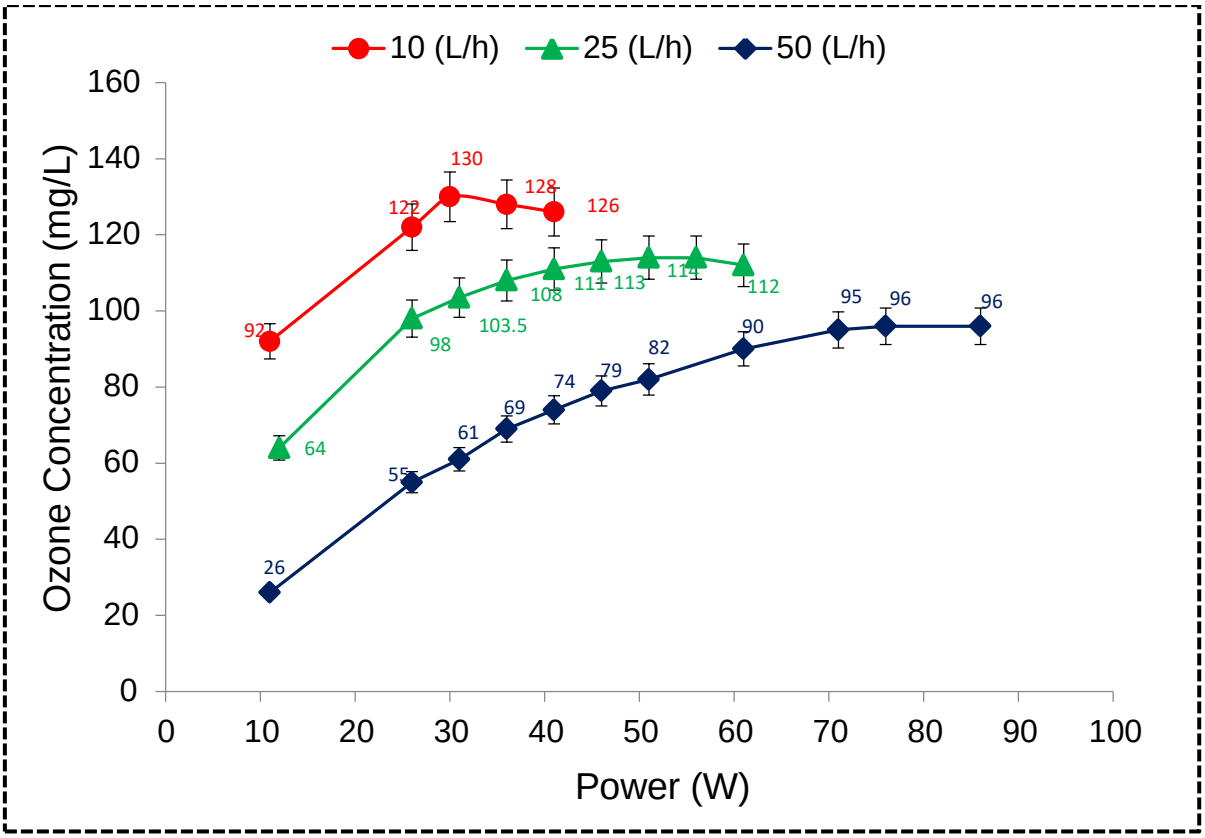

Figure 2.16 Calibration and optimization of ozone generator

2.7 The effect of UVA lamp on ozone decomposition

The influence of UVA lamp irradiation on the decomposition of ozone inside the photocatalytic reactor was investigated. To obtain that goal, 0.5 L of the deionized water (pH = 5.5) was recirculated in the reactor with a constant flow rate of 1 L/min., ozone gas with a flow rate of 10 L/h and the initial concentration of 130 mg/L at power of 30W was continuously introduced to the reactor from the gas inlets at the bottom of the reactor. The concentration of ozone in gas phase and dissolved ozone in deionized water was monitored during the experimental operation over a time period of 2 hours. The same experiment was repeated under seven UVA lamps irradiation for the same time and conditions. According to the results presented in Fig. 2.17, the decomposition of ozone molecule in both gas and liquid phase inside

the reactor was accelerated by illumination with UVA light and after 20 min. of irradiation the condition was reached to steady state.

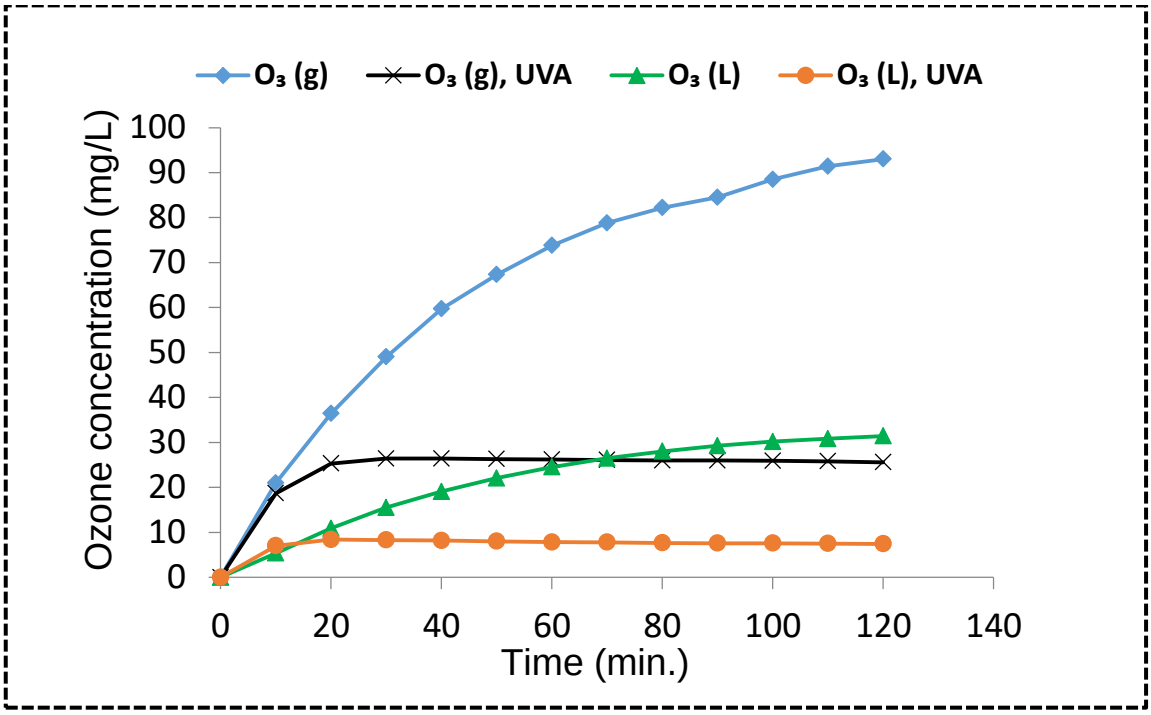

Figure 2.17 Effect of UVA light irradiation on decomposition of ozone; 0.5L DI, T = 24˚C, pH = 5.5 and O3 feed gas = 130±5 mg/L.

2.8 The effect of ozone on the reactor frame made of polyvinylchloride

The influence of ozone molecule on the degradation of polyvinylchloride (PVC) made interior frame of the falling film reactor was investigated. To this end, two preliminary experiments were performed on a photocatalytic reactor. The reactor was filled with a 0.5 L of the deionized water (pH = 5.5) which was circulated with a flow rate of 1 L/min. A mixture of ozone-oxygen gas (Initial concentration 135 mg/L at flow rate of 10 L/h) was continuously introduced to the reactor in the darkness. The concentration of produced chloride and acetate ions were measured by ion chromatography during the period of 2 hours (Fig. 2.18). The same experiment was repeated in the same condition with illumination by seven UVA lamps as photocatalytic ozonation. The results are presented in Fig. 2.18 shows that the reaction of ozone with

PVC is only moderate and does not have great effect on the reactor frame. A very low concentration of produced chloride and a maximum amount of 12 mg/L of acetate ion was observed. Due to the very slow oxidation rate of acetic acid by ozonation alone [159] the measured acetate concentration was increased with treatment time. However, the concentration of acetate ion by photocatalytic ozonation was remained low during the period of 2 hours probably due to the degradation of acetic acid by photocatalytic ozonation [160].

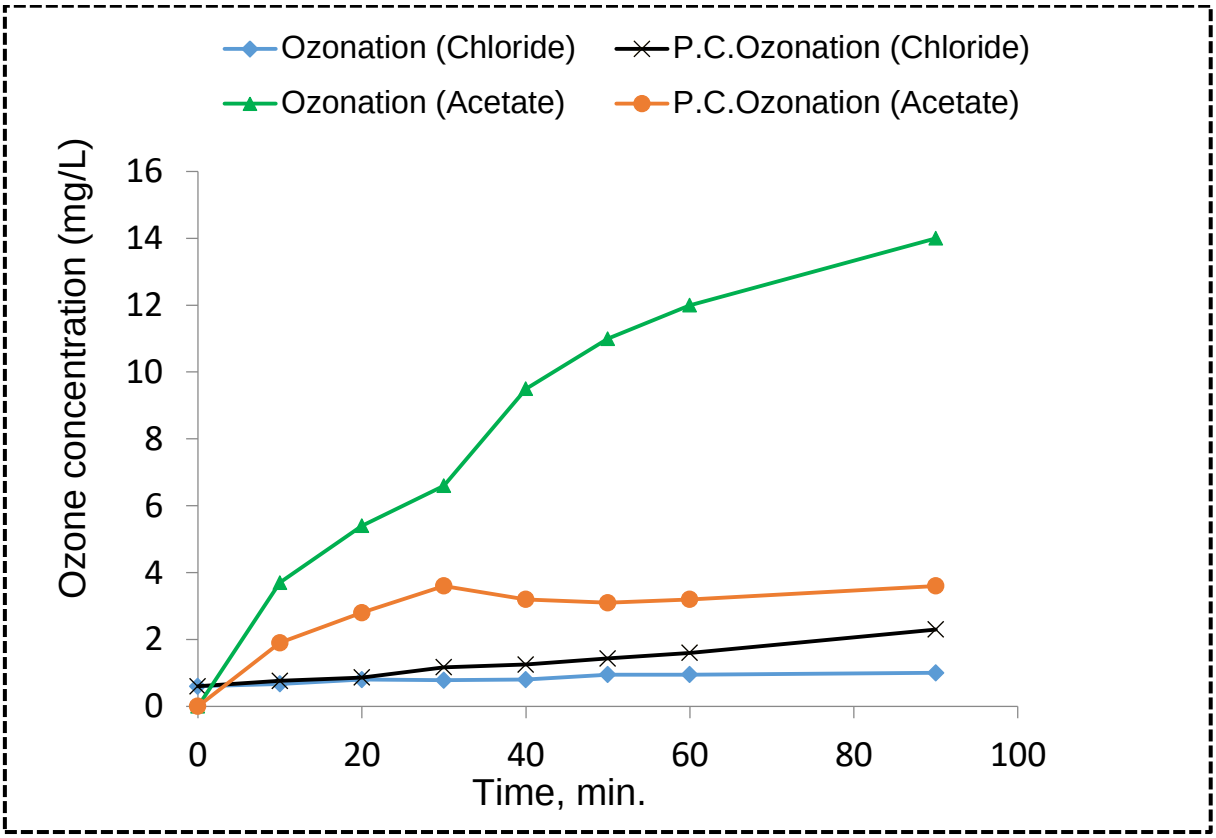

Figure 2.18 Effect of UVA light irradiation on decomposition of ozone; 0.5L D.I, T = 24˚C, pH = 5.5 and O_3 feed gas = 130±5 mg/L.

2.9 The effect of H_2O_2 concentration on methylene blue degradation by UVA/TiO_2/H_2O_2 and optimization the amount of Fe^{2+} in Fenton processes

The optimum concentration of H_2O_2 in the TiO_2/H_2O_2/UVA method for the decolorization of 50 mg/L MB was examined (Fig. 2.19). The results indicate that almost the same decolorization rate was observed when 100, 130 and 200 mg/L of H_2O_2 was added to the solution; therefore, 130 mg/L was chosen as the optimum concentration of H_2O_2.

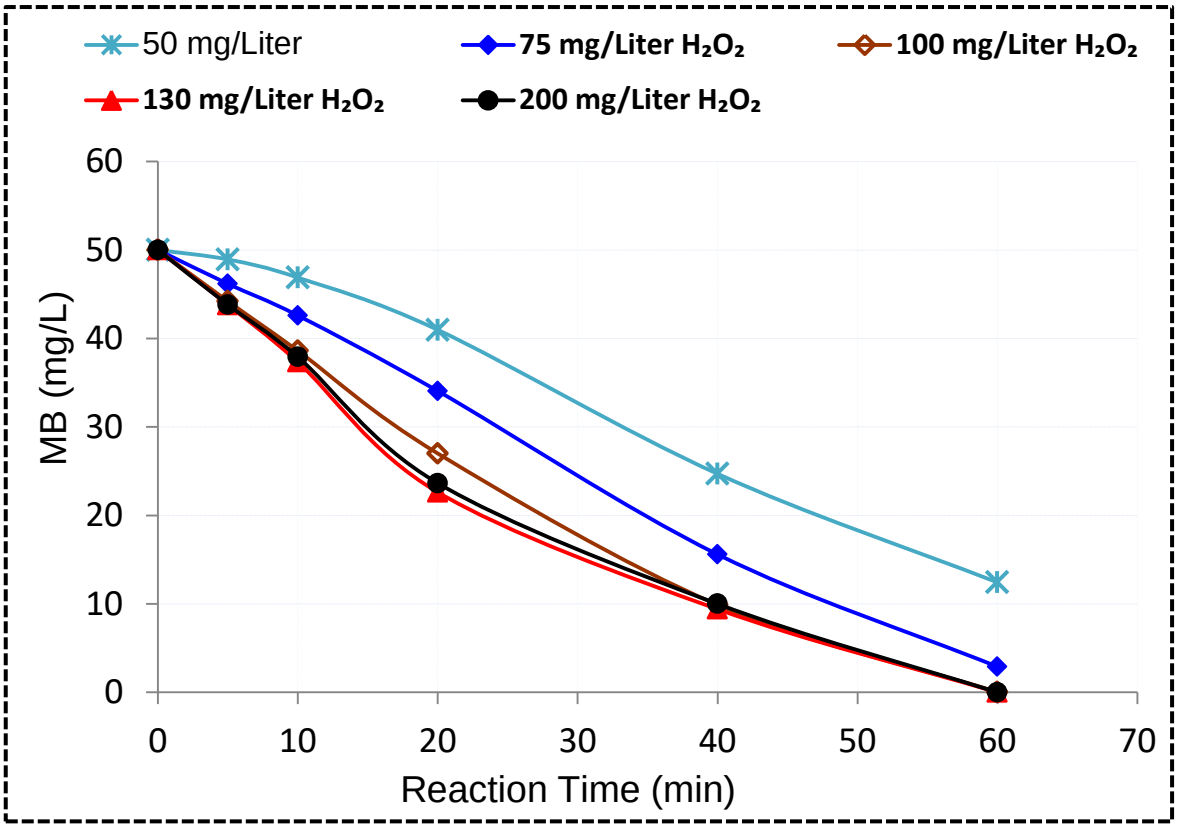

Figure 2.19 Effect of H_2O_2 concentration on decolorization of MB (50 mg/L) by UVA/TiO_2/H_2O_2.

The same condition was used to optimize the amount of Fe^{2+} catalyst in Fenton oxidation process. As shown in Fig. 2.20, 100 percent decolorization was attained either in the presence of 20 or 25 mg/L Fe^{2+}. To optimize the initial concentration of H_2O_2, the same experiments at the same condition (20 mg/L Fe^{2+}) were performed. The result presented in Fig. 2.20 indicates that 100 percent decolorization of MB is achieved when the concentration of added H_2O_2 reaches to 100 mg/L.

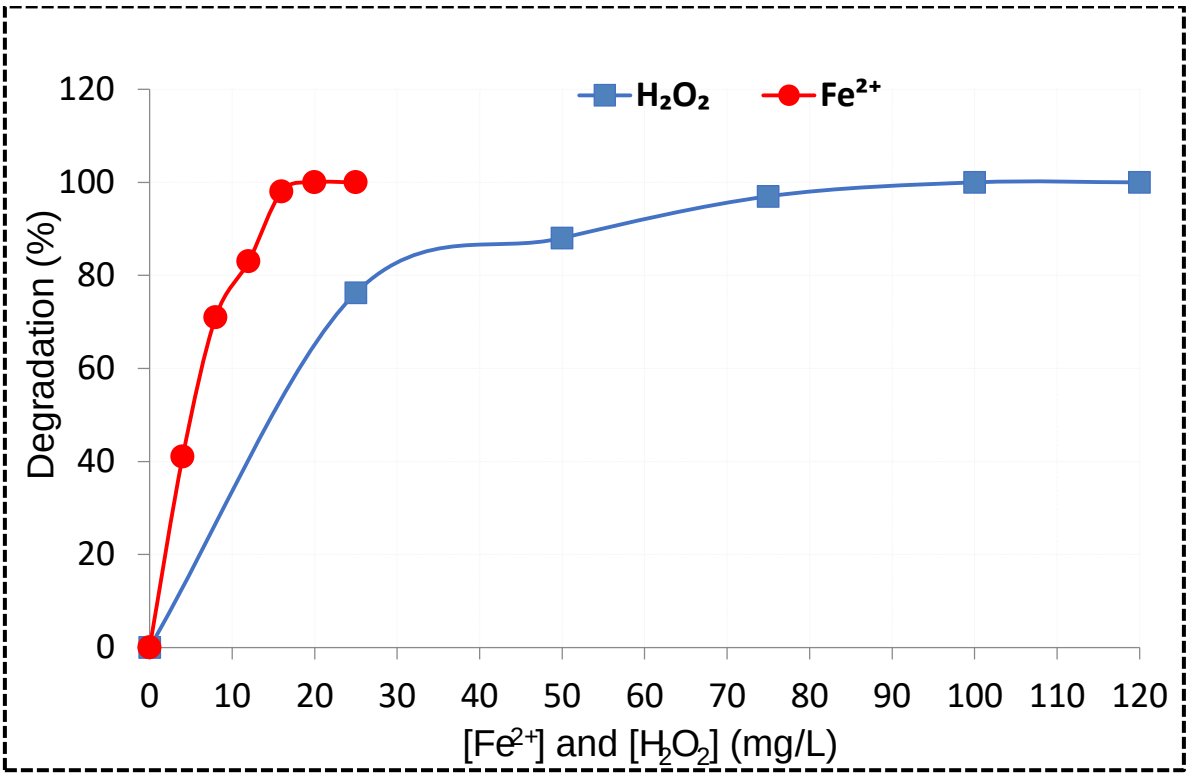

Figure 2.20 Optimization of the concentrations of H_2O_2 and Fe^{2+} on decolorization of 50 mg/L MB in Fenton oxidation.

Hence, 20 mg/L of Fe^{2+} and 100 mg/L of H_2O_2 were chosen as the optimum condition for the decolorization of MB solution (50 mg/L) by Fenton oxidation.

Chapter Three

Results

&

Discussion

Chapter Three

3. Results and discussion

3.1 Formation of reactive species in the DBD reactor

Advanced oxidation processes based on non-thermal plasma generated by electrical discharge in gas-liquid interface, gas atmosphere, induces ultrasonic waves, ultraviolet radiation, and of particular importance, generation various reactive species at ambient condition such as neutral molecules (H_2, O_2, O_3, and H_2O_2), negative and positive ions, and most importantly free radicals ($^{\bullet}OH$, $^{\bullet}O$, $^{\bullet}H$, and $HO_2^{\bullet}$).These reactive species can decompose most of the organic pollutants. The amount and the feature of these reactive species are influenced by many factors such as the type of discharge, input energy, the nature of the gaseous atmosphere as well as the composition of the solution and its pH, conductivity and temperature. The formation mechanisms of active species by the discharge are as follows [44, 48, 161, 162]:

$$* e^- + H_2O \rightarrow \bullet H + \bullet OH + e^- \quad (R\ 3.1)$$

$$* e^- + 2H_2O \rightarrow H_2O_2 + H_2 + e^- \quad (R\ 3.2)$$

$$2 \bullet OH \rightarrow H_2O_2 \quad (R\ 3.3)$$

$$\bullet O + H_2O \rightarrow 2 \bullet OH \quad (R\ 3.4)$$

$$H_2O_2 + \bullet OH \rightarrow HO_2 \bullet + H_2O \quad (R\ 3.5)$$

$$HO_2 \bullet + \bullet OH \rightarrow H_2O + O_2 \quad (R\ 3.6)$$

$$\bullet H + \bullet OH \rightarrow \bullet O + H_2 \quad (R\ 3.7)$$

When oxygen is present in the gas atmosphere:

$$* e^- + O_2 \rightarrow 2 \bullet O + e^- \quad (R\ 3.8)$$

$$O_2 + \bullet O \rightarrow O_3 \quad (R\ 3.9)$$

$$O_3 + H_2O + h\nu \rightarrow H_2O_2 + O_2 \quad (R\ 3.10)$$

$$H_2O_2 + O_3 \rightarrow \bullet OH + O_2 + HO_2 \bullet \quad (R\ 3.11)$$

$$HO_2 \bullet + O_3 \rightarrow \bullet OH + O_2 + O_2^- \quad (R\ 3.12)$$

$$H_2O_2 + h\nu \rightarrow 2 \bullet OH \quad (R\ 3.13)$$

Among them, hydroxyl radical ($^{\bullet}$OH) is the main desired powerful, non-selective and unstable oxidant (E^o = 2.85 V/SHE) that play an important role in oxidizing recalcitrant organic pollutants that present in water. It reacts with most organic pollutants either by hydrogen abstraction with saturated aliphatic hydrocarbons and alcohols, or electrophilic addition with unsaturated hydrocarbons [161]. Hydrogen peroxide (E^o = 1.77 V/SHE) is another important species formed mainly by decomposition of water molecules in gas-liquid plasma system followed by the recombination of generated hydroxyl radicals in oxygen free water [161, 163]. Hydrogen peroxide at ambient conditions is relatively stable in an aqueous solution. It can also be used, consequently, as an efficiency measure of the hydroxyl radical generation in the DBD discharge in an argon gas atmosphere. The formation of hydrogen peroxide in DBD process is affected by various parameters such as gas composition, flow rate, input energy power and the shape of electrode [163, 164]. In order to characterize the efficiency of the

DBD reactor, the formation of H_2O_2 in deionized water under an argon gas atmosphere at different input energies power was studied. Fig. 3.1 shows the concentration of H_2O_2 in the liquid phase generated in dependence on time and introduced input power.

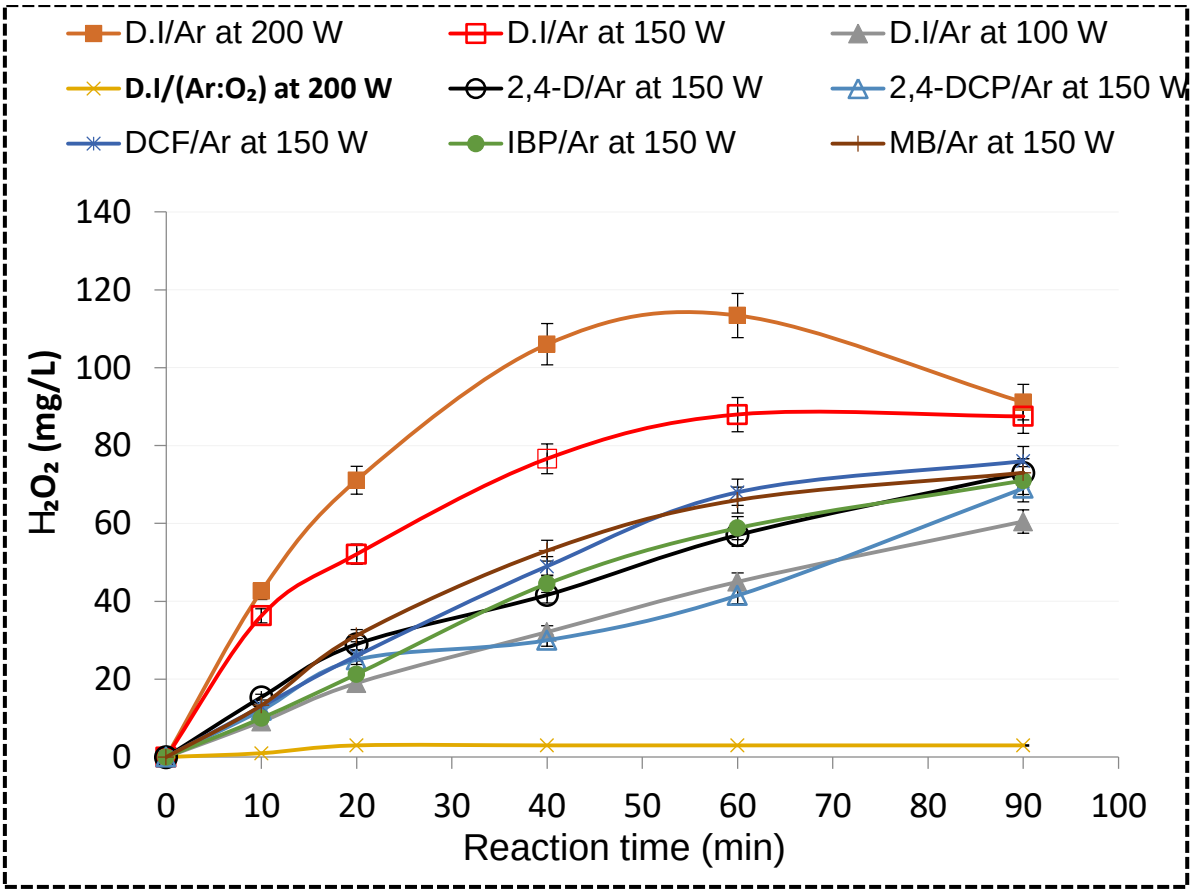

Figure 3.1 Formation of H_2O_2 in deionized water and in solutions containing (C_o=100 mg/L 2,4-D or 2,4-DCP) and (C_o=50 mg/L DCF, IBP or MB) by DBD plasma at different input powers, in Ar and Ar/O_2 (80:20) atmosphere (the treatment time includes also the pause intervals without discharge which is explained in experimental part)

The concentration of H_2O_2 increases with increase of discharge time and introduced energy up to a saturation level. At higher energy even a decrease is observed with progressive time. This is caused by decomposition of H_2O_2 in the solution at high concentration by its reaction with active species generated during the discharge [44, 165] and by the possible effect of discharged water

temperature which was raised from 23 to 29, 33 and 36.5 °C at power of 100, 150, and 200 W after 90 min discharge respectively.

From the initial formation rate the estimated energy yield for H_2O_2 production in deionized water by DBD under the argon atmosphere obtained in the present work was 1 to 1.1 g/kWh depending on the power applied. This energy yield is in the same range reported by Lock et al. [163] which is generally in the range of 0.5-1 g/kWh. Similarly, in previous works several methods have been used for estimation of H_2O_2 production which involve pulsed corona discharge in water [147], microwave plasma under argon atmospheric pressure [152], low power pulsed water spray plasma reactor [166] and plasma reactor with coaxial geometry corona discharge in water [84] to give different yields with 0.47, 0.0027, 10-20 and 1.6 g/kWh, respectively. These variations of energy yields are attributed to the use of different reactor technique.

In the presence of the pollutants Fig. 3.1 the production of H_2O_2 is affected. Scavenging of OH radical by the pollutants which prevent their recombination to H_2O_2 is the main cause of the reduction of H_2O_2 yield in the treated solutions of each 100 mg/L (2,4-D or 2,4DCP) or 50 mg/L of each DCF, IBP or MB.

The presence of oxygen in the gas atmosphere as in Ar/O_2 (80:20) mixture induces the reaction between the generated active electrons and oxygen, which results in the production of •O and O_3 (R 3.8-9). Also in Ar/O_2 atmosphere only a very low production of H_2O_2 was observed (Fig. 3.1), due to the decomposition of H_2O_2 by generated ozone (R 3.8-9) in peroxone process (R 3.11). Furthermore, in the case of argon combined with the Fenton reaction a part of the generated H_2O_2 was subjected to the Fenton oxidation.

Ozone generation is one of the most successful commercial applications of non-thermal plasma. Ozone itself is a powerful oxidant (E^o = 2.07 V/SHE) and can react with organic pollutants either directly or indirectly after decomposition through a series of reactions [167].

The results shown in Fig. 3.2 illustrate the variation of ozone yields in the deionized water under a mixture of Ar/O_2 (80:20) gas atmosphere. The generated ozone in the gas phase during the discharge is dissolved in deionized water up to a maximum amount of 450 µg/L, while at high power of 200W the concentration will decline (Fig. 3.2) and that is due to the interaction of the radicals formed during the discharge in a chain reaction with ozone in water according to (R 3.14-15) (competition between ozone production and ozone decomposition at high concentration of ozone) [168, 169]:

$$\bullet OH + O_3 \rightarrow HO_2\bullet + O_2 \qquad (R\ 3.14)$$

$$HO_2\bullet + O_3 \rightarrow \bullet OH + 2O_2 \qquad (R\ 3.15)$$

Another effect limiting the dissolved ozone concentration is the temprature of the discharged soluion which is gradually raises from 24 to 31 and 33 ºC after 90 min discharge time at 150 and 200 W input energy. In the presence of pollutants, the generation of ozone was affected (Fig. 3.2). In the solutions containing DCF, 2,4-DCP and MB, no dissolved ozone was detected due to the consumption of generated ozone for the oxidation of pollutants and their intermediate products. However, in the presence of IBP and 2,4-D a small amount of dissolved ozone was detected especially at the beginning of the process. This is probably due to the slower decomposition rate of these pollutants by ozone (table 3.1). The concentration of generated ozone inside the reactor atmosphere has been measured by ozone analyzer and it reached to 3.6 and 4.5 mg/L at 150 and 200 W input energies respectively.

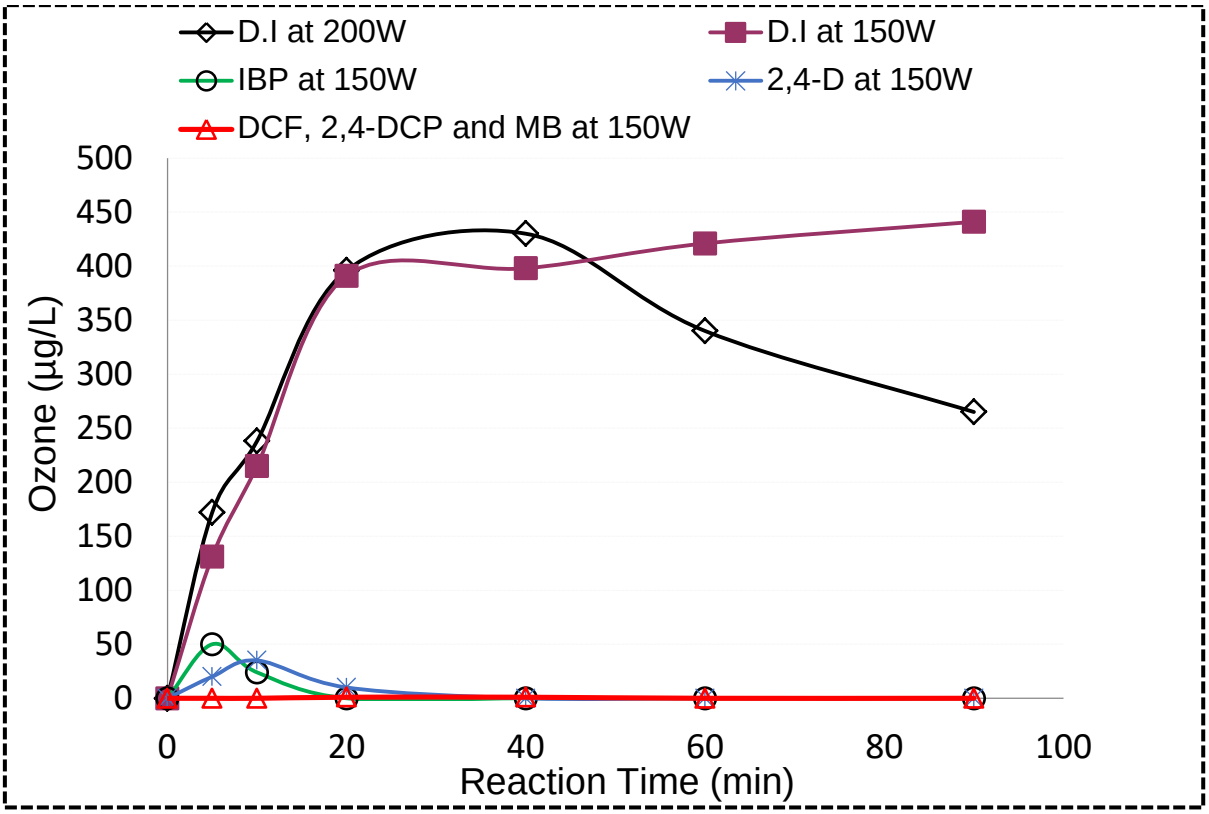

Figure 3.2 Concentration of generated O_3 in deionized water and in solutions containing (C_o=100 mg/L 2,4-D and 2,4-DCP) and (C_o=50 mg/L DCF, IBP and MB) by DBD plasma in Ar/O_2 (80:20) atmosphere (the treatment time includes also the pause intervals without discharge, explained in experimental part).

It is notable that when the discharge is operating in air atmosphere, a poor generation of H_2O_2 was detected only by 3 mg/L in deionized water and o.5 mg/L gaseous ozone. Electric discharge in oxygen-nitrogen mixture like air atmosphere inevitably results in the formation of aqueous nitrite and nitrate anions [170]. Fig. 3.3 shows the variation of generated nitrite and nitrate anion concentrations in deionized water under air atmosphere at 200W input energy.

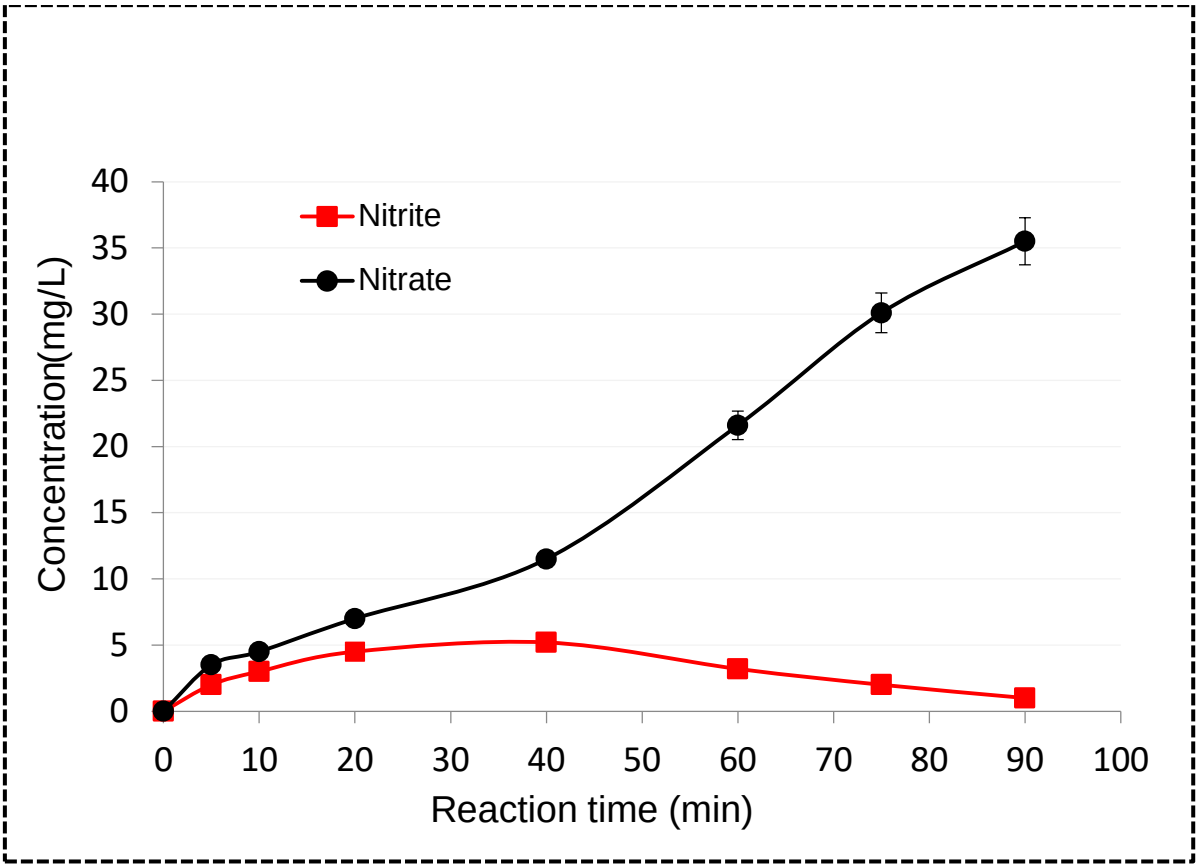

Figure 3. 3 Variation of generated nitrite and nitrate ion concentrations by DBD in deionized water (P = 200W) in air atmosphere (the treatment time includes also the pause intervals without discharge, explained in experimental part).

3.2 Degradation of organic pollutants

Oxidative degradation of 100 mg/L of each 2,4-D, 2,4-DCP and 50 mg/L of each DCF, IBP, and MB in aqueous solutions have been investigated by different advanced oxidation process by using a planar falling film reactor. Plasma in contact with a thin liquid falling film has the advantageous of minimizing mass transfer limitations between the plasma and treated solution [44, 163]. The degradation of DCF, 2,4-D, and 2,4-DCP can be tracked by three different methods: direct determination of pollutant-decay by HPLC, indirectly via the produced chloride ion by ion chromatography, and by the degree of mineralization using measurement of TOC removal. For IBP and

MB indirect determination by chloride is not applicable. However, the behavior of TOC removal with respect to the direct determination of IBP and MB are similar as for mentioned pollutants. In the following discussion, the values determined by direct HPLC analysis is used to obtain the degradation efficiency of examined methods. The degradation of DCF and 2,4-D by DBD plasma in argon atmosphere and P.C. Oxidation are chosen as a representative examples and the results are shown in Fig. 3.4 and 3.5.

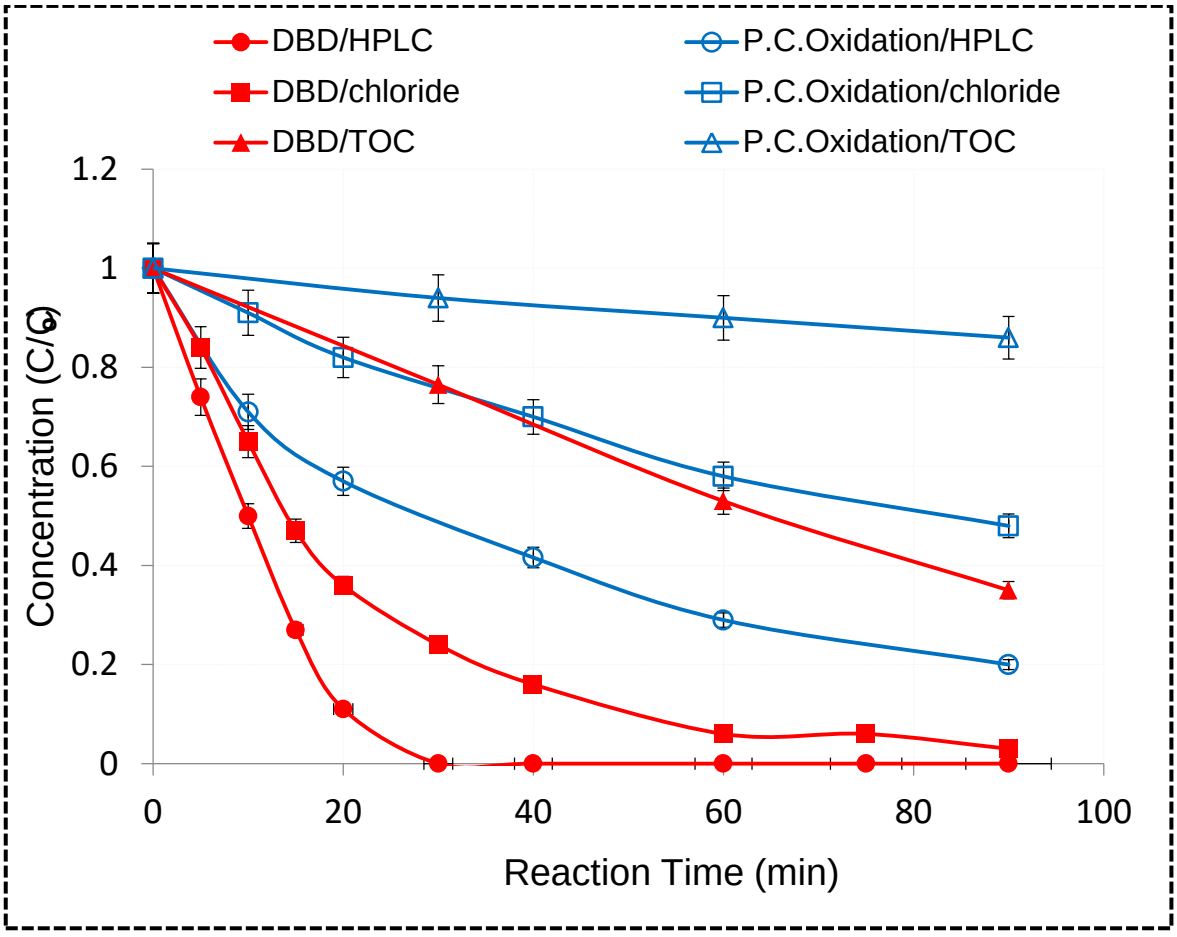

Figure 3.4 Relative concentration profiles of DCF removal (C_0 = 50 mg/L, pH 5.6) by DBD/Ar at 150W and P.C. Oxidation (in DBD the treatment time includes also the pause intervals without discharge).

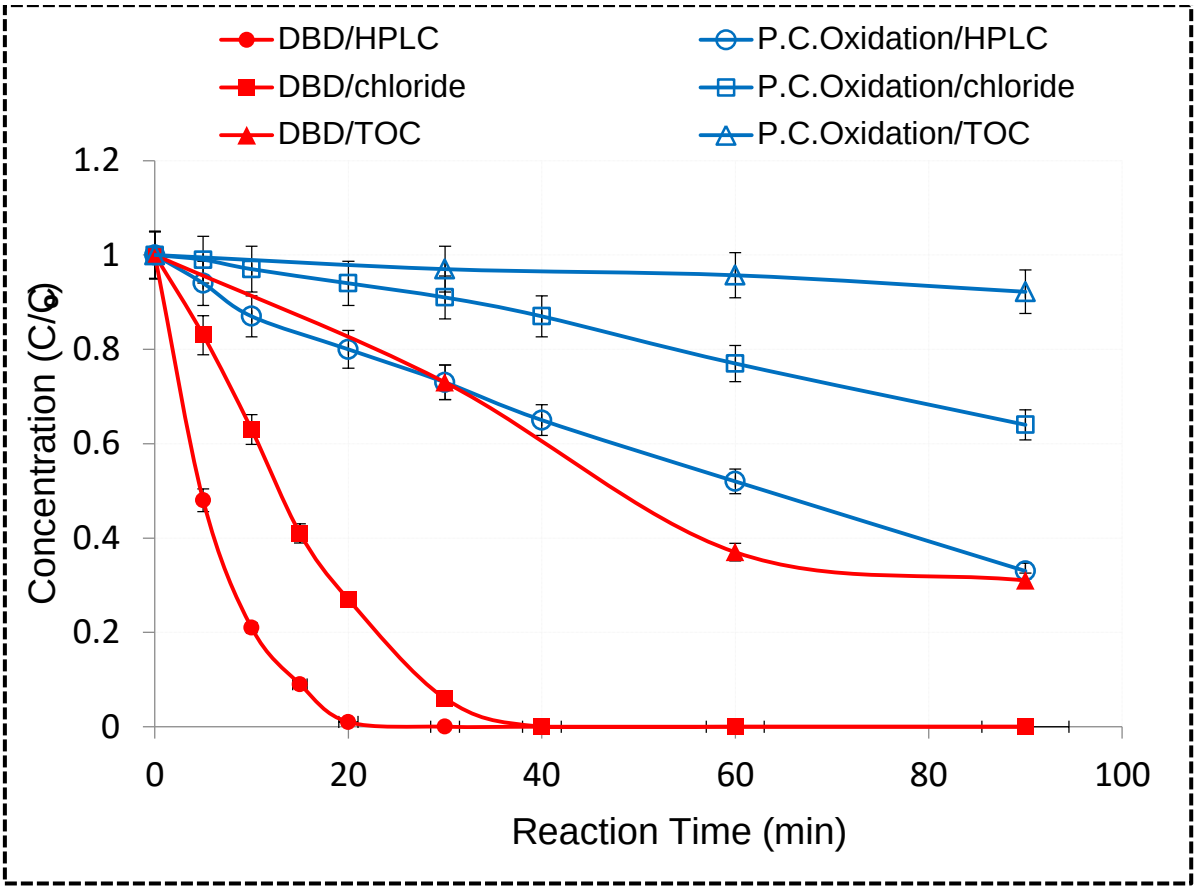

Figure 3.5 Relative concentration profiles of 2,4-D removal (C_0 = 100 mg/L, pH 3.35) by DBD/Ar at 150W and P.C. Oxidation (in DBD the treatment time includes also the pause intervals without discharge).

The degradation processes tracked by indirect measurement of chloride is somewhat retarded compared with direct measurements by HPLC due to the formation of chloride containing intermediates [70, 71, 171]. The decrease of TOC value is also remarkably slower as more stable organic by-products are formed (see by-product and mineralization sections). This behavior was observed in all experiments.

3.3 Degradation by non-thermal DBD plasma

The efficiency of degradation by DBD plasma depends on the gas composition and introduced energy. The TiO_2 photocatalyst coated on PAGs used a falling film liquid generator in the present work. This is also another possible synergistic system of DBD plasma processes to improve the degradation process through the production of active oxidant. The UV light emitted by DBD during the pulsed discharge can irradiate the coated TiO_2 on the glass sheets [40].

$$TiO_2 + h\nu \rightarrow TiO_2\,(e^- + h^+) \qquad (R3.16)$$

$$H_2O + h^+ \rightarrow \bullet OH + H^+ \qquad (R3.17)$$

$$O_2 + e^- \rightarrow O_2\bullet^- \qquad (R3.18)$$

$$O_2\bullet^- + 2H^+ \rightarrow 2 \bullet OH \qquad (R3.19)$$

The effect of the gas composition atmosphere including pure argon, argon: oxygen (80:20) mixture, and air as well as combination Fenton oxidation with DBD plasma under argon atmosphere was investigated for degradation and mineralization of each pollutant.

3.4 Degradation based on ozonation and photocatalysis

The degradation of pharmaceutical diclofenac (DCF), Ibuprofen (IBP), 2,4-dichlorophenol (2,4-DCP), phenoxy herbicide 2,4-dichlorophenoxyacetic acid (2,4-D) and organic dye methylene blue (MB) as model pollutants were investigated via ozonation (O_3), photocatalytic ozonation ($UVA/TiO_2/O_3$), and photocatalytic oxidation ($UVA/TiO_2/O_2$) in a planar falling film reactor. In addition, other advanced oxidation processes such as Fenton, photo-Fenton,

ozonation in alkaline medium, and photocatalytic oxidation in the presence of H_2O_2 (UVA/TiO_2/O_2/H_2O_2) have been also examined for the removal of MB in the same reactor. Degradation of organic pollutants based on ozonation is generally proceeds via two possible routes; (1) direct molecular ozone attack in darkness and (2) indirect process via transformation of O_3 into OH radicals by elevating pH or by UV irradiation pathway. In acidic medium (pH < 4), the direct pathway is assumed. When pH ranges between 4–9, both are present. For pH > 9, the indirect pathway is suggested [38, 172]. Table 3.1 summarizes the rate constants for the reaction of ozone and hydroxyl radicals with DCF and IBP. The reaction of hydroxyl radicals is very fast for all pollutants whereas the reaction of ozone with DCF and 2,4-DCP is much faster than the reaction with IBP and 2,4-D.

These differences are also due to the relation between chemical structures of organic compounds that are resulting from the presence of various substitutions on aromatic ring and their reactivity with ozone.

Table 3.1 Rate constants for reactions of ozone and OH radical with pollutants.

Pollutant	**k (O_3) $M^{-1} S^{-1}$**	**k (•OH) x 10^9 $M^{-1} S^{-1}$**
Diclofenac	≈ 1 X 10^6 [173]	7.5 ± 1.5 [173]
Ibuprofen	9.6 ± 1 [173]	7.5 ± 1.4 [173]
2,4-D	2.4 [158]	5.2 ± 0.4 [174]
2,4-DCP	8 ± 4 x 10^9 [159]	7.4 ± 0.5 [174]

3.5 Degradation of pharmaceutical DCF and IBP

Figure 3.6 illustrates the degradation of DCF and IBP (50 mg/L, pH 5.6) by ozonation and photocatalytic ozonation. Direct attack of the pharmaceuticals by ozone molecules in darkness is expected to be the main degradation mechanism due to the initial pH of the solutions used in this work [175]. A direct ozonation results in a very fast degradation of DCF which is completely disappeared after 4 min. The presence of two chlorine atom in the aromatic ring of DCF results additionally in a fast dechlorination step by ozonation and consequently in an increase of the degradation rate [38]. Then, combination of ozone with UVA has only a marginal effect on the degradation of DCF. On the other hand, the removal of TOC by P.C. ozonation is much faster than by direct ozonation in the darkness (see Section mineralization).

The degradation of IBP at pH = 5.7 by ozonation (direct reaction) is slower than that of DCF (Fig. 3.6). The differences are due to the rate constants for the reactions of ozone with DCF and IBP (Table 3.1).

P.C. ozonation enhances the degradation of IBP (Fig. 3.6). This is due to the oxidation of IBP through the generated hydroxyl radicals, either by ozone photolysis (R3.10-3.15) or via the photocatalysis of ozone molecules by photo-generated electrons on the surface of the TiO_2 coated on the surface of Pilkington active glass (R3.20-22) [63, 95]. In that case, a real synergetic effect is obtained by the combination of ozonation and photocatalysis.

$$TiO_2 + h\nu \rightarrow e^- + h^+ \qquad (R3.20)$$

$$O_{3(ads)} + e^- \rightarrow O_3^- \qquad (R3.21)$$

$$O_3^- + H^+ \rightarrow HO_3^\bullet \rightarrow {}^\bullet OH + O_2 \qquad (R3.22)$$

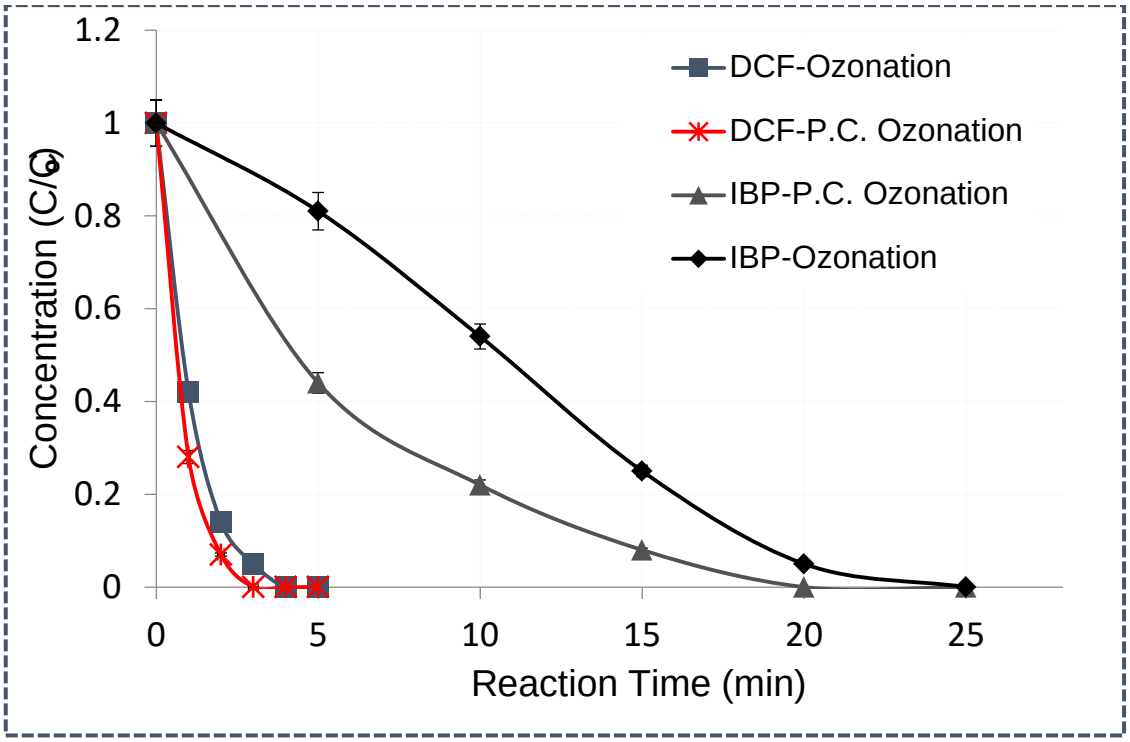

Figure 3.6 Relative concentration profiles during DCF and IBP degradation (C_o= 50 mg/L each, pH = 5.6) by ozonation and P. C. Ozonation.

As shown in Fig. 3.7, the photocatalytic oxidation (UVA/TiO_2/O_2) of both pharmaceuticals is only moderate. This is due to the lower efficiency of the OH radical production in aqueous solution by only slow heterogeneous reactions on TiO_2 [176].

Degradation of both pharmaceuticals by DBD in air atmosphere is only moderate Fig. 3.7. However, in the argon gas atmosphere alone with an input energy of 150W, a complete degradation of IBP and DCF was attained after 20 and 30 min respectively. Moreover, degradation rate was enhanced with increasing power from 150 to 200W (Fig. 3.8). The addition of oxygen to the argon atmosphere has a different impact on the degradation of the selected pollutants under study: for DCF an acceleration of the degradation is observed, whereas for IBP oxygen seems to have a restraining effect (Fig. 3.9).

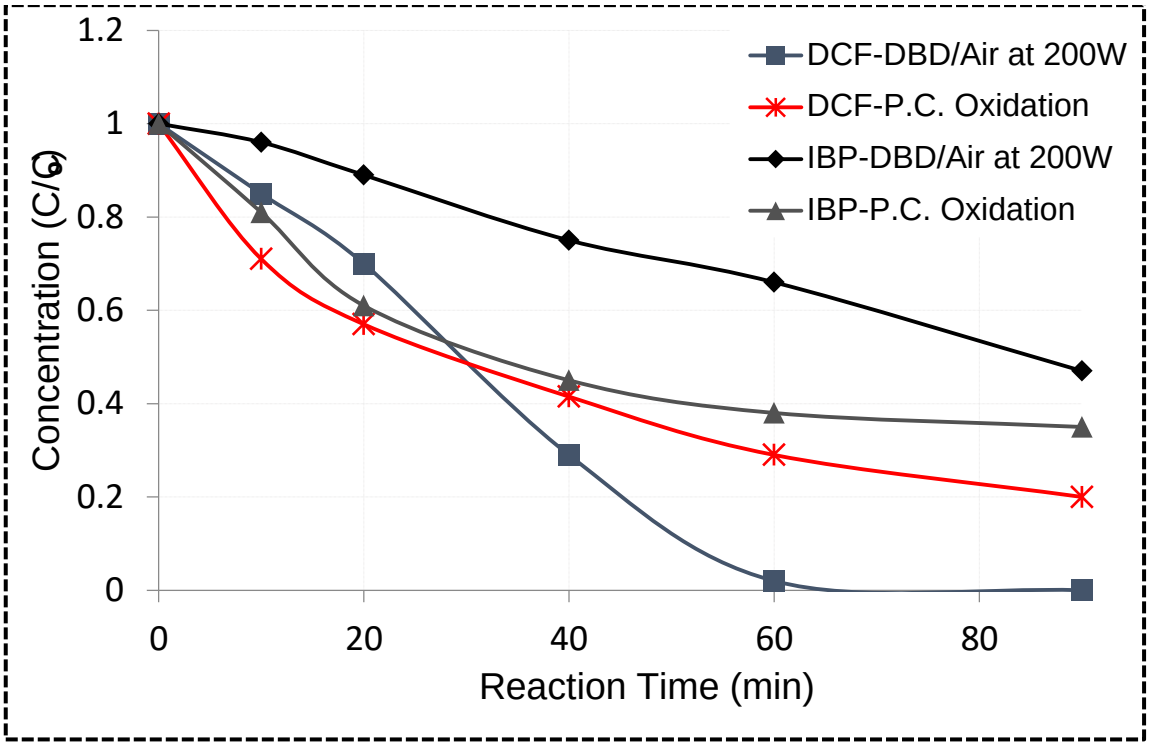

Figure 3.7 Relative concentration profiles during DCF and IBP degradation (C_o= 50 mg/L each, pH = 5.6) by P. C. Oxidation and DBD plasma under air atmosphere.

The main reactive species involved in the degradation process are hydroxyl radicals, hydrogen peroxide, ozone and other reactive species that might be formed during the discharge. The hydroxyl radicals formed in discharge in the humid argon atmosphere near the surface of the falling film can react directly with the contaminants in a fast reaction according to their comparable high rate constants (Table 3.1). In oxygen containing gas atmosphere ozone is generated which react then very fast with DCF but not with IBP because of the low rate constant (Table 3.1). The direct reaction of hydrogen peroxide with organic pollutants is generally slow, but an addition of ferrous ion as a homogeneous catalyst to the aqueous solution improves the degradation process by the formation of hydroxyl radicals (Fenton reaction)

$$H_2O_2 + Fe^{2+} \rightarrow Fe^{3+} + \bullet OH + OH^- \qquad (R3.23)$$

The results of DCF and IBP degradation in the presence of 10 mg/L ferrous ion as $FeSO_4$ salt are shown in Fig. 3.9. The results of TOC reduction (see mineralization section) show that the degree of degradation and mineralization is improved only for DCF. Whereas, for IBP a significant influence of ferrous ion is not observed. These results are due to differences in their chemical structure and their reactivity with Fenton reaction.

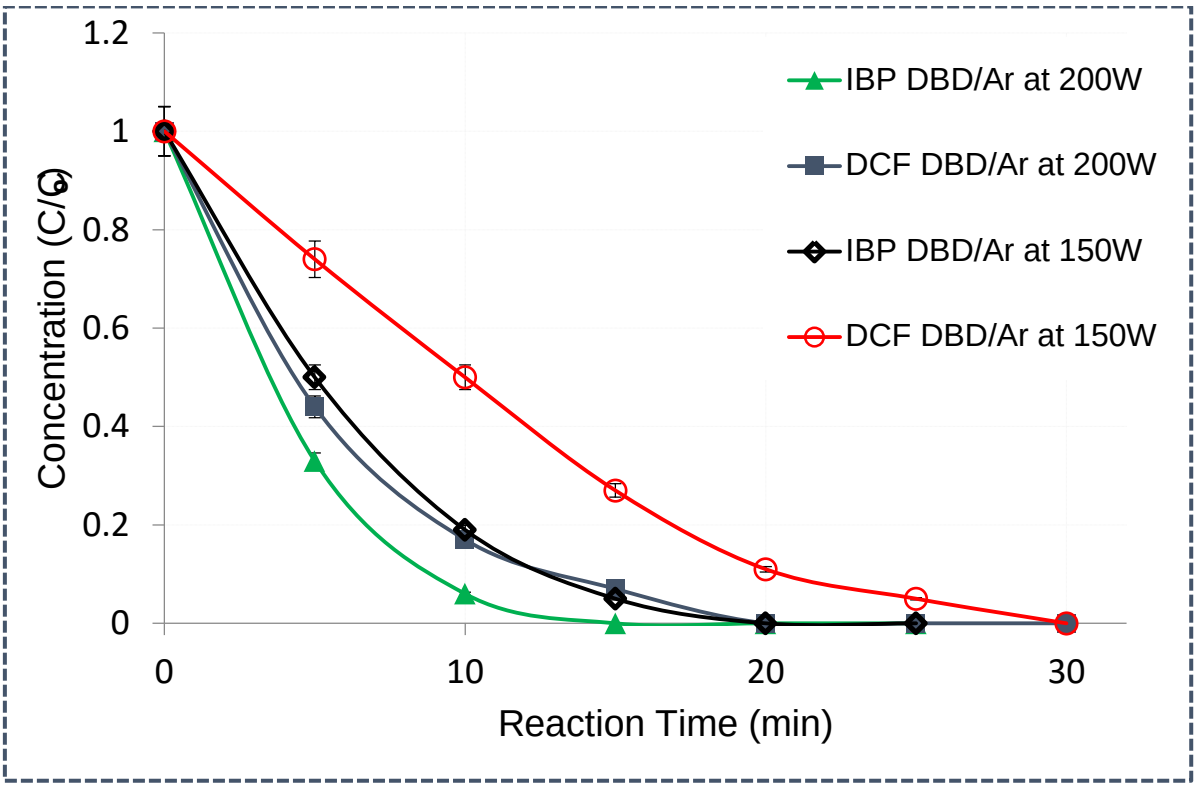

Figure 3.8 Relative concentration profiles during DCF and IBP degradation (C_o= 50 mg/L each, pH = 5.6) by DBD plasma under argon atmosphere at 150 and 200W (the treatment time includes also the pause intervals without discharge).

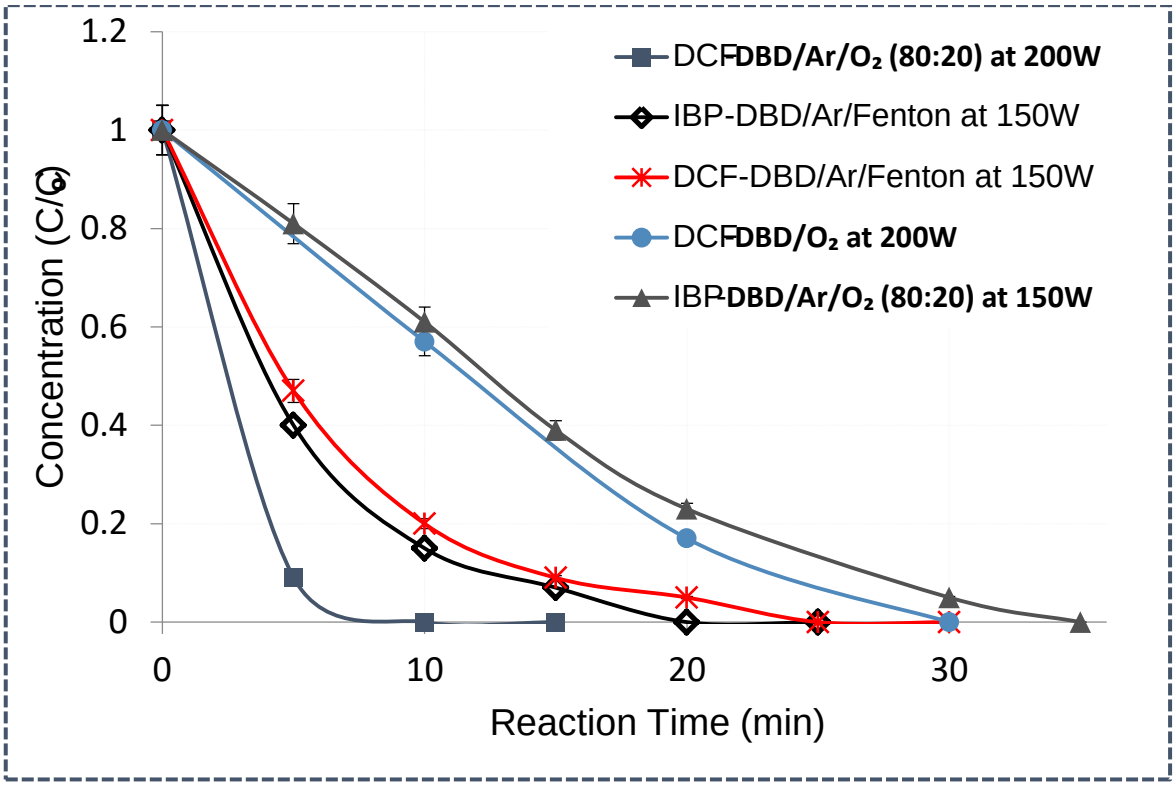

Figure 3.9 Relative concentration profiles during DCF and IBP degradation (C_o= 50 mg/L each, pH = 5.6) by DBD plasma in Ar/O_2 atmosphere and Ar/Fenton at 150 and 200W (the treatment time includes also the pause intervals without discharge).

3.6 Degradation of 2,4-D and 2,4-DCP

Figure 3.10 shows the degradation results obtained by direct ozonation, P.C.Ozonation and P.C.Oxidation. Photocatalytic oxidation did not completely decompose 2,4-D and 2,4-DCP. Even after 90 min of treatment, only 67% of 2,4-D and 73% of 2,4-DCP were decomposed mainly into other organic by-products where by which only 7% and 12% of TOC was removed.

Decomposition of organic pollutants by direct ozonation in acidic medium leads to the partial degradation of organic molecules present in water and the formation of ozone resistant low chain carboxylic acids. Therefore, it results in low degree of mineralization [39, 172]. In the present work, based on the initial pH of treated solutions by direct mechanism for both 2,4-D (initial pH 3.35) and for 2,4-DCP (initial pH 6.85) is expected to be the main degradation

pathway by ozonation in darkness. As shown in Fig. 3.10 the degradation of 2,4-D is slower than 2,4-DCP. A complete degradation of 2,4-DCP and 2,4-D by direct ozonation were achieved after 10 and 20 min respectively. Whereas, the TOC decreases only moderately (see mineralization section). The combination of ozonation with photocatalysis in P.C. Ozonation (TiO_2 on PAGs under UVA illumination) does not show any significant synergistic effect on 2,4-DCP degradation, but only a marginal effect on 2,4-D degradation. Obviously, the reaction of these pollutants with ozone is so fast that the additional formation of OH radicals by direct ozone photolysis with UVA or by ozone interaction with illuminated TiO_2 does not result in a significant degradation improvement. At the same time, a dramatic increase in the mineralization was achieved.

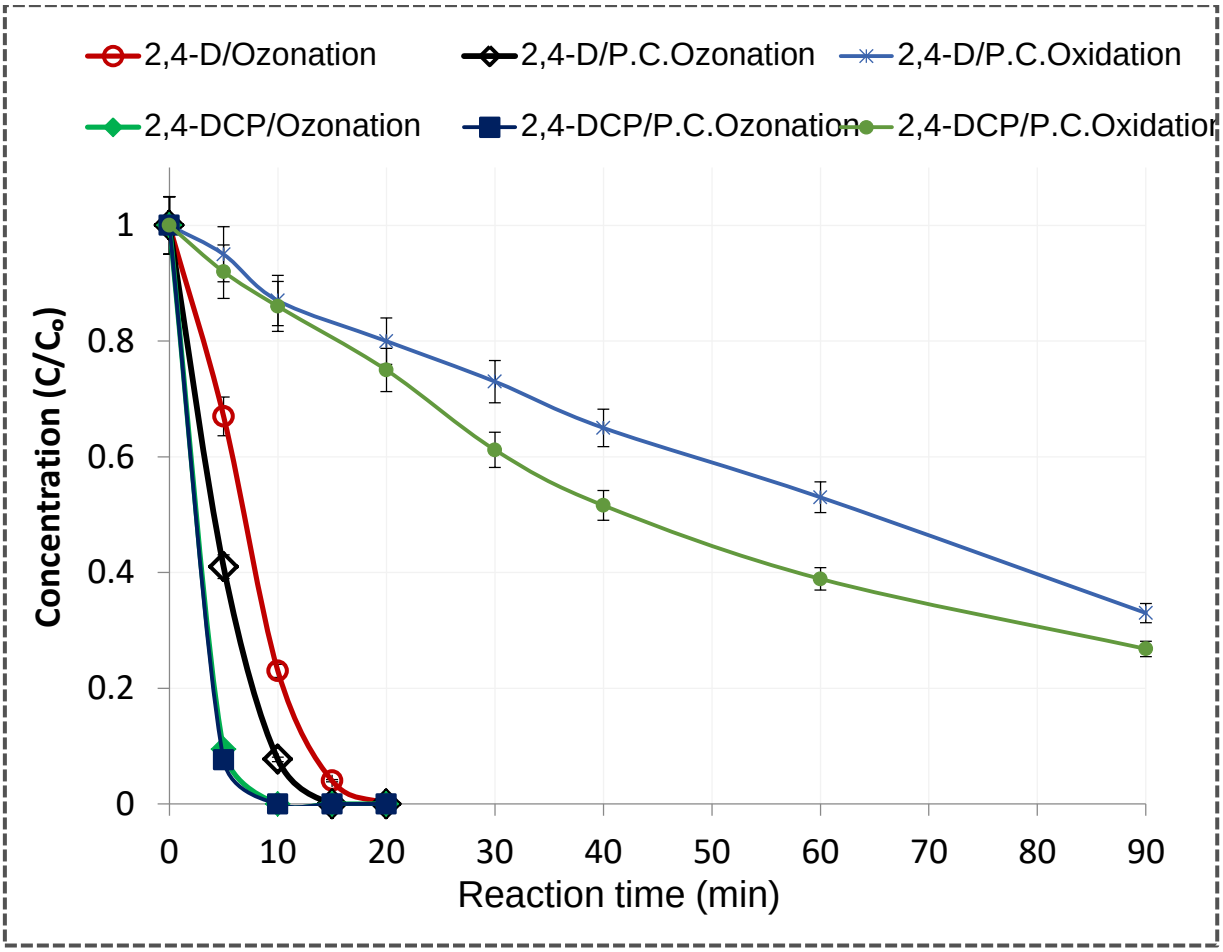

Figure 3.10 Relative concentration profiles of 2,4-D and 2,4-DCP degradation (C_o= 100 mg/L each) by ozonation, P.C. Ozonation, and P.C. Oxidation.

The effect of the gas atmosphere including pure Ar, Ar/O_2 (80:20) and air on DBD process has been studied for the degradation and mineralization of both pollutants. The relative concentration profiles of 2,4-D and 2,4-DCP as a measure of the degradation in DBD plasma at power of 150W under Ar, Ar/O_2, Ar combined with Fenton reagent and air at 200W are shown in Figs 3.11 and 3.12. The degradation of both pollutants under air atmosphere at power of 200W was only moderate. In pure argon, a complete degradation of both pollutants was obtained in about 15 min. Addition of 20% oxygen to argon results in a retardation of the degradation. On the other hand, the mineralization efficiencies are improved. This is due to the acceleration of

intermediate by-product oxidation through the production of additional reactive species like •O and O_3 (Reactions (R3.8) and (R3.9) as well as by the peroxone process (Reactions R3.10 and R3.11). In pure argon atmosphere, hydrogen peroxide is formed during the discharge. Hydrogen peroxide is a stable and long living species produced in DBD plasma and its amount is influenced by several parameters such as gas composition and the design of the reactor. The production of hydrogen peroxide under argon atmosphere in deionized water and in solution of 2,4-D and 2,4-DCP is shown in Fig. 3.1. The combination of two different advanced oxidation processes is an effective approach to enhance the oxidation efficiency due to the additional source of OH radicals. The removal of both pollutants were significantly enhanced in the presence 10 mg/L of ferrous ion due to the additional Fenton oxidation between ferrous ion and generated hydrogen peroxide under argon atmosphere in DBD system.

From the degradation results which are shown in Figs. 3.11 and 3.12 and the energy yields which are shown in the (section 3.8), it is obvious that the effect of this combination is more significant in 2,4-D degradation than 2,4-DCP. This difference may be due to the initial pH of treated solution which is more acidic in 2,4-D and their chemical structure with electronic density [177] (see experimental). Beside of degradation, also the degree of mineralization is improved for both pollutants (Fig. 3.32).

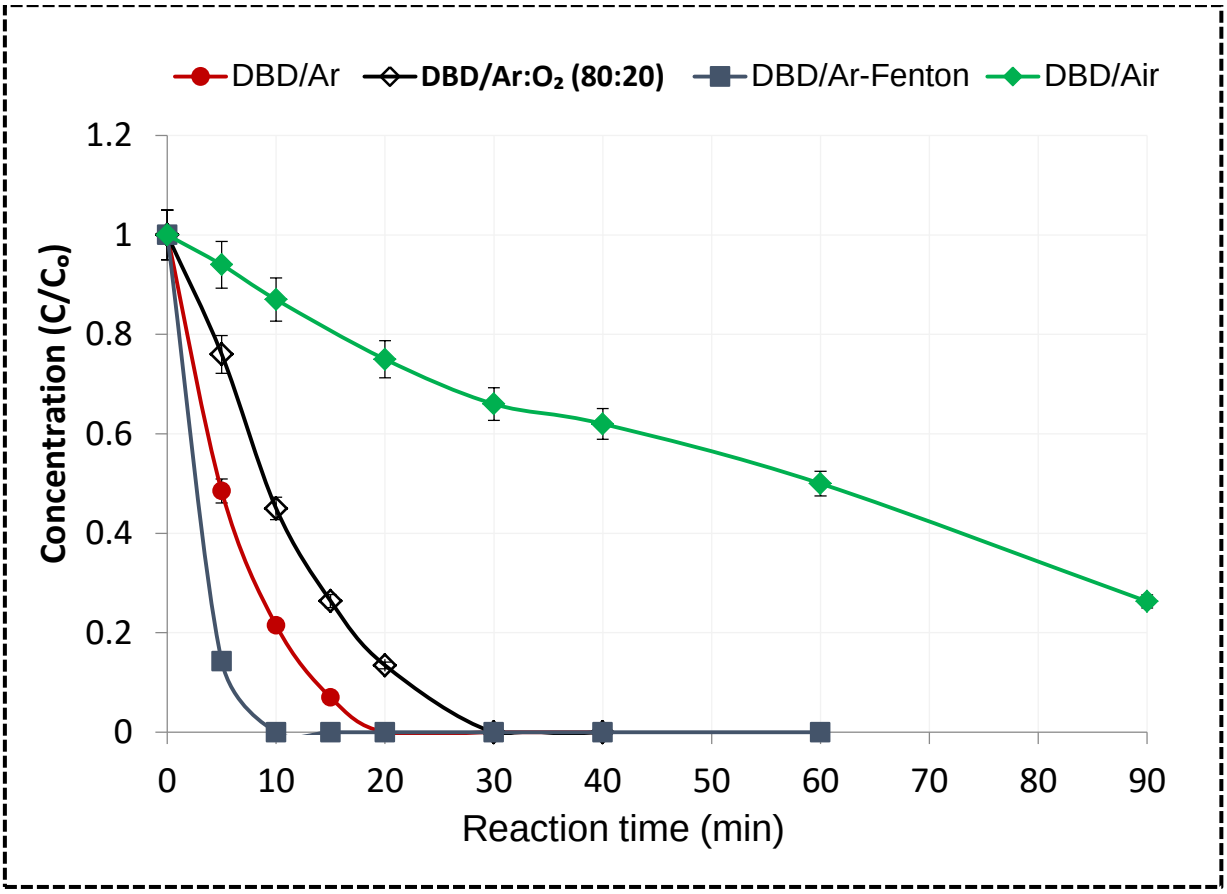

Figure 3.11 Relative concentration profiles of 2,4-D degradation (C_o= 100 mg/L, pH = 3.35) by the DBD plasma at 150W in Ar, Ar/Fenton, and Ar/O_2 (80:20) atmosphere and (P = 200W in air), (the treatment time includes also the pause intervals without discharge).

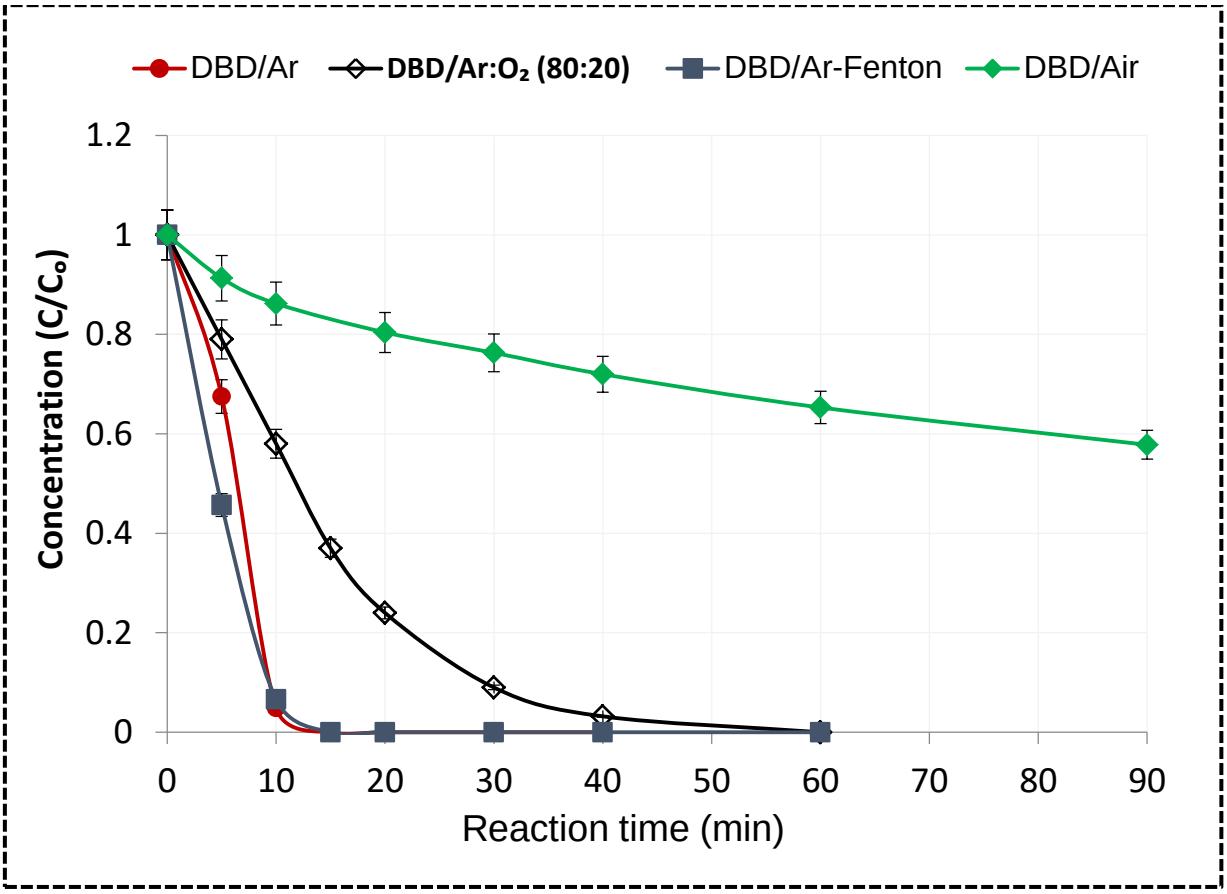

Figure 3.12 Relative concentration profiles of 2,4-DCP degradation (C_o= 100 mg/L, pH = 6.85) by the DBD plasma at 150W in Ar, Ar/Fenton, and Ar/O_2 (80:20) atmosphere and (P = 200W in air), (the treatment time includes also the pause intervals without discharge).

3.7 Degradation of methylene blue

The results shown in Fig. 3.13 illustrate the decolorization of MB (50 mg/L) by ozonation and other applied advanced oxidation process. The decolorization of MB by the photocatalytic oxidation (UVA/TiO_2/O_2) is only moderate (Fig. 3.13A) which is due to the lower efficiency of hydroxyl radical production by only photocatalytic oxidation. However, in the presence of 100 mg/L H_2O_2 (the optimum concentration of H_2O_2 for decolorization of 50 mg/L MB see experimental) a significant enhancement in decolorization is observed and the complete decolorization of MB has been achieved after one-hour treatment by (UVA/TiO_2/O_2/H_2O_2). The variation of H_2O_2 concentration

with time is shown in Figure 3.14. Addition of H_2O_2 into the system provides an additional source for generating OH radicals via decompostion by either photocatalysis (R3.24- R3.27) or UV illumination (Eq. R3.28) [178]. As shown in Fig. 3.14, the decrease in H_2O_2 concentration due to the generation of OH radicals follows the first-order kinetics.

$$TiO_2 + h\nu \rightarrow e^- + h^+ \qquad (R3.24)$$

$$O_2 + e^- \rightarrow O_2\bullet^- \qquad (R3.25)$$

$$H_2O_2 + e^- \rightarrow \bullet OH + OH^- \qquad (R3.26)$$

$$H_2O_2 + O_2\bullet^- \rightarrow \bullet OH + OH^- + O_2 \qquad (R3.27)$$

$$H_2O_2 + h\nu \rightarrow 2\bullet OH \qquad (R3.28)$$

The ozonation of MB at *pH* = 5 (direct reaction of ozone molecule with MB) and *pH* = 11 (indirect reaction of ozone with MB via the radical chain mechanism) as well as the combination with the UVA light results in a complete decolorization of MB after four min (Fig. 3.13B). Neither the combination of ozonation with the UVA irradiation nor increasing the *pH* value from 5 to 11 shows synergistic effect on the decolorization efficiency of MB. This is due to the fast decomposition of MB by the direct reaction of ozone molecules with MB in the ozonation process. The only observed differences are in the TOC removal efficiency which is much higher at alkaline pH and in the presence of UVA light (see mineralization section).

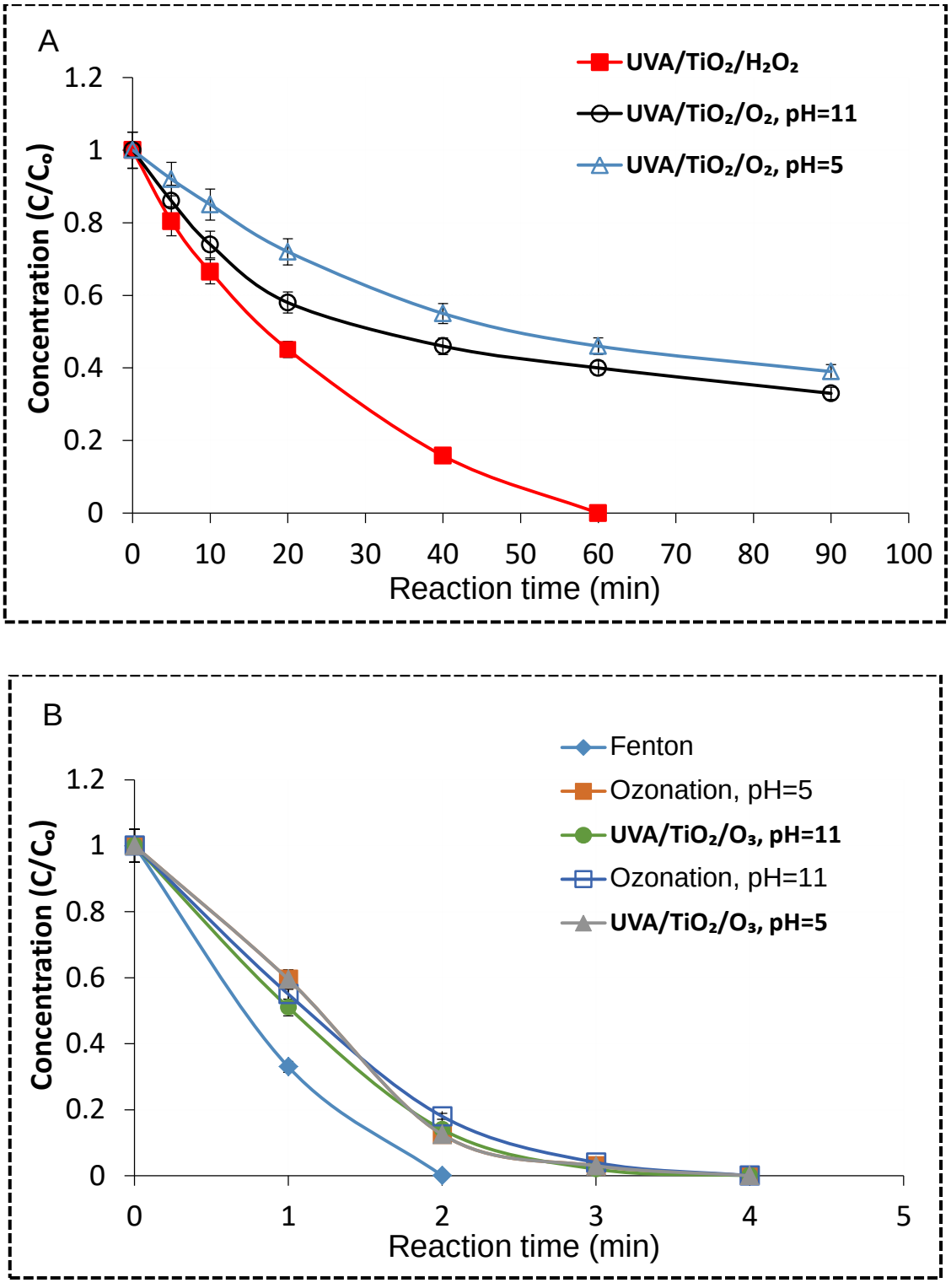

Figure 3.13 Relative concentration profiles of MB decolorization (C_o=50 mg/L, pH = 5) by (A) H_2O_2-photocatalysis, and P.C. Oxidation (B) Fenton, ozonation, and P.C. Ozonation.

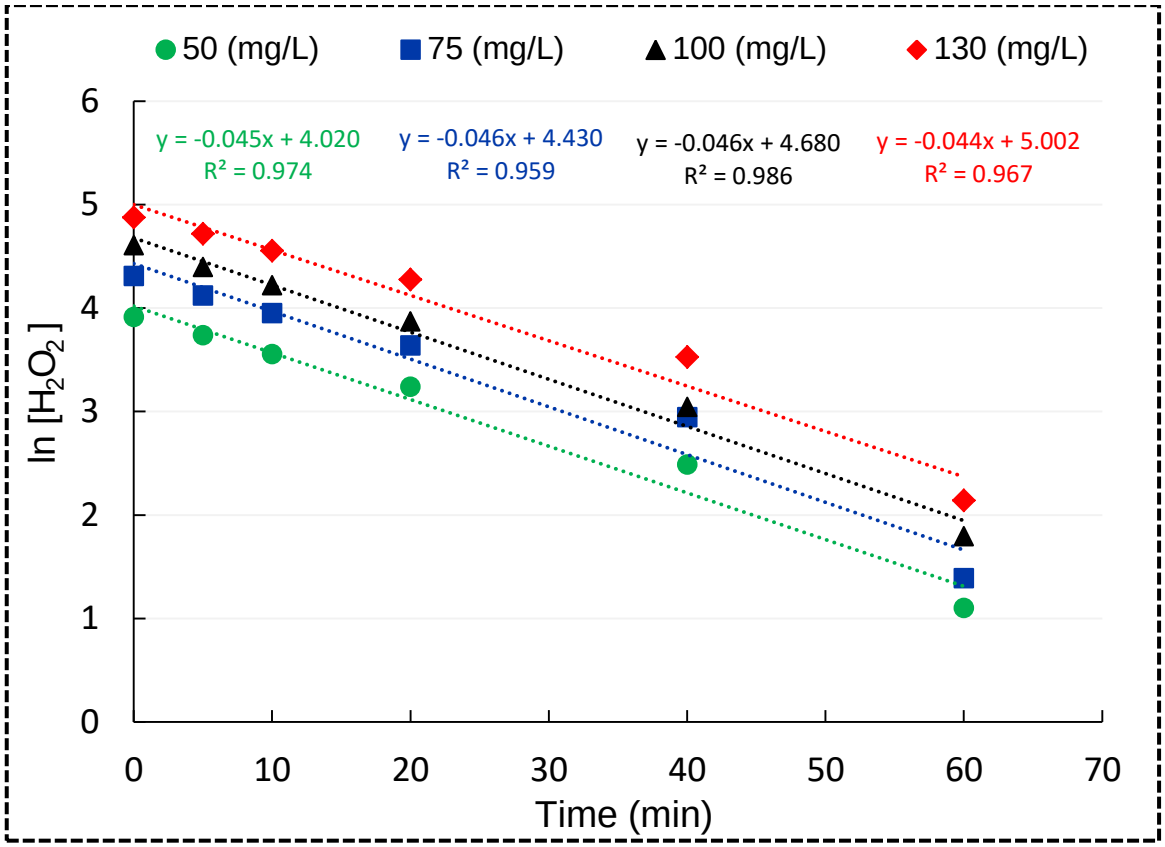

Figure 3.14 The variation of concentration H_2O_2-decay during the degradation of 50 mg/L MB at different initial concentration.

Comparing the decolorization efficiencies of the ozonation and UVA/TiO₂/H_2O_2 processes indicates that the ozonation provides tremendously higher decolorization efficiency than H_2O_2. The lower decolorization efficiency of H_2O_2 in comparison with ozone is due to the much lower molar absorptivity of hydrogen peroxide. The molar absorptivity of H_2O_2 at 253.7 nm is only 20 M^{-1} cm^{-1} which is much lower than that of ozone at the same wavelength (3300 M^{-1} cm^{-1}). Therefore, H_2O_2 needs a longer UV exposure time than the photocatalytic ozonation [38, 179].

Fenton oxidation contaning 100 mg/L H_2O_2 and 20 mg/L Fe^{2+} (as ferrous sulfate) is found to be the fastest process for the decolorization of MB solution as shown in Fig. 3.13B. The oxidation reaction is based on electron transfer from Fe^{2+} to H_2O_2 where ferrous cations act as a homogeneous catalyst. This is resulting in the generation of high reactive $^{\bullet}OH$ radicals

(R3.23) [38]. Because of the high effectivity of Fenton oxidation in generating $^{\bullet}OH$ radicals and consequently in the decolorization of MB, combination of Fenton with the UVA light did not show any synergistic effect on MB decolorization.

From Fig. 3.15, it can be observed that applying the DBD plasma with an input electrical power of 150 W under the argon or a mixture of argon/oxygen atmosphere completely decolorized MB solution after 25 min. Combination of non-thermal DBD plasma with other AOPs such as Fenton reaction can improve the production of active species. Also it enhances the efficiency of MB oxidation. As shown in Fig. 3.15, the presence of 20 mg/L Fe^{2+} as a homogeneous catalyst enhances the decolorization and mineralization efficiencies and improves the energy yield due to the occurrence of Fenton oxidation reaction by means of Fe^{2+} and H_2O_2 which is generated during the DBD process (R3.23).

Considering the results, it can be concluded that the ozonation, photocatalytic ozonation, Fenton and photo-Fenton oxidation displayed higher decolorization efficiencies than the DBD non-thermal plasma. However, the DBD plasma showed higher decolorization efficiency than either the photocatalytic oxidation alone or in the presence of H_2O_2.

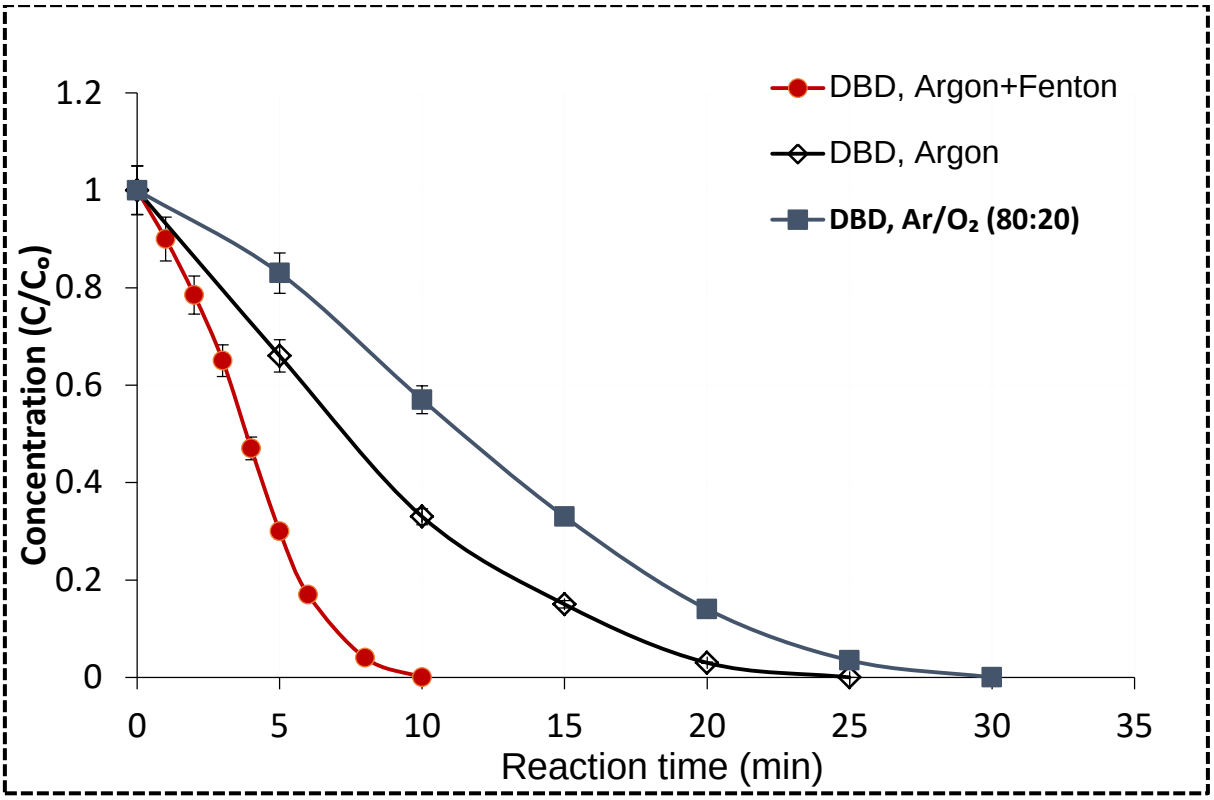

Figure 3.15 Relative concentration profiles of MB decolorization (C_o= 50 mg/L, pH = 5) by DBD plasma in Ar, Ar/O_2, and Ar/Fenton atmosphere at 150W (the treatment time includes also the pause intervals without discharge).

The influence of the initial concentration of MB on the energy yield of decolorization at different degradation levels of MB by DBD plasma (*P*=150W) under the argon atmosphere is studied and the obtained results are shown in Fig. 3.16.

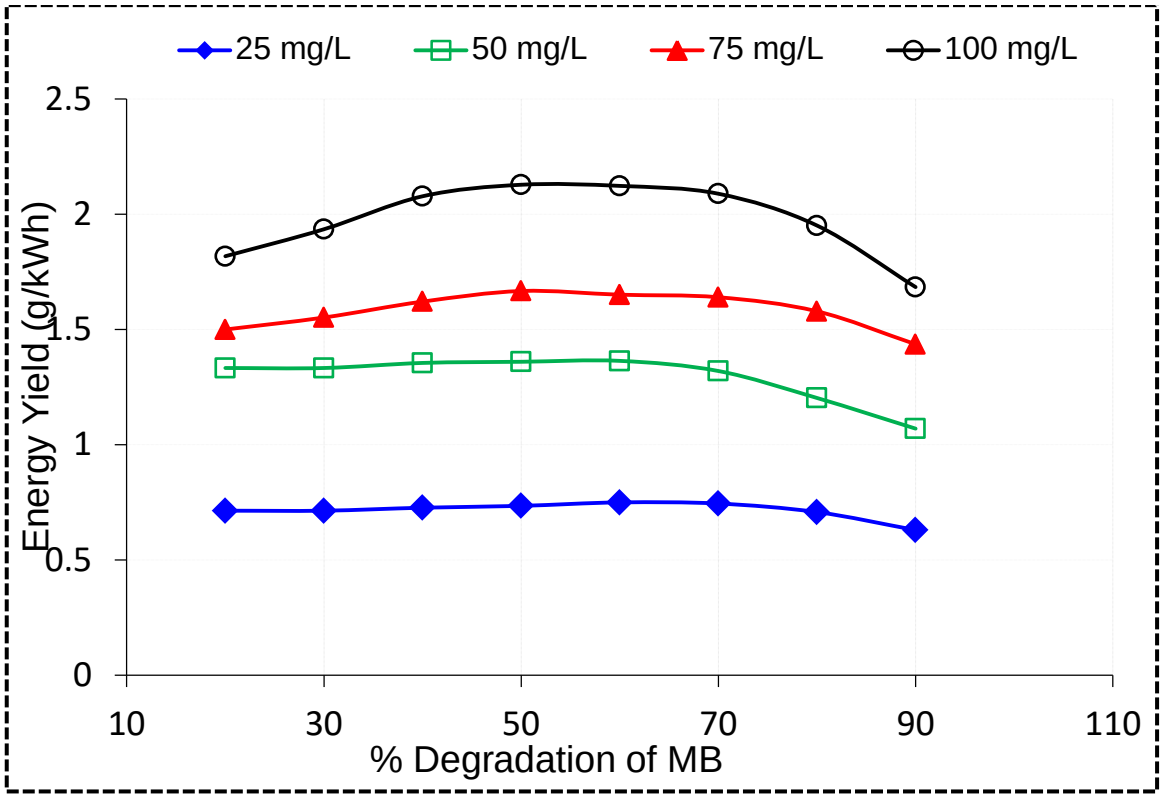

Figure 3.16 Effect of the initial concentration of MB on the energy yield of MB decolorization by the DBD plasma (P = 150W, pH= 5) under the argon atmosphere.

It can be seen that the energy yield of decolorization is proportional with the initial concentration of MB. This is probably due to the presence of higher amount of reactant molecules in the solution affected by the discharge. A maximum energy yield of 2.13 g/kWh at G_{50} of the solution containing 100 mg/L MB is achieved. However, the energy yield decreases to 1.66, 1.36 and 0.7 g/kWh as the initial concentration of MB decreases to 75, 50, and 25 mg/L respectively.

3.8 Energy yield

The energy yields at 50% degradation (G_{50}) for each pollutants examined in the present work were calculated according to the Eq. 2.1. G_{50} is defined as grams of pollutant decomposed per kilowatt-hour and expressed in (g/kWh). For each treated pollutants, the examined methods are compared on the bases of energy yield, i.e the energy necessary for degradation of certain amount of each pollutants. This value is well established measure especially for non-thermal plasma experiments, to compare different plasma methods such as DBD, corona discharge, and electrohydraulic discharge in order to design the most effective experimental process. Moreover, it allows us to compare the energy yield of plasma experiments with ozonation and other advanced oxidation processes because the amount of energy introduced to the system in each oxidation process is known. It should be noted that the comparison of data reported in the literature for degradation of pollutants by various advanced oxidation processes is a challenging study, because the estimated energy yields depend not only on the type of used reactors but also on a variety of other factors such as percent of conversion, the presence of catalyst and additives, initial concentration, pH, nature of gas atmosphere, design of the reactor, and by-products of the pollutants. In the present work the condition of 50% conversion G_{50} has been selected because most energy yield values reported in the literature is available in this conversion and interference from intermediates may not negligible at >50% conversion [44].

3.8.1 Energy yield (G_{50}) of pharmaceutical DCF and IBP

The estimated energy yields G_{50} for the degradation of 50 mg/L DCF and IBP by ozonation and different AOPs are shown in Figs. 3.17 and 3.18. The results reflect the decomposition behavior discussed in 3.5. The highest yield of 28 g/kWh DCF is obtained by direct ozonation. This is much higher than that for DBD plasma assisted DCF decomposition. Dobrin et al. [70] reported energy yield at G_{50} of about 1 g/kWh for decomposition of 50 m/L DCF using a corona discharge in oxygen over the water surface. This value is comparable with our results of DBD in an oxygen atmosphere, whereas in pure argon and Ar/O_2 mixture higher values (up to 5.1 g DCF/kWh) are obtained (Fig. 3.17). Banaschilik et al. [84] calculated the energy yield at G_{90} for lower initial concentration of 0.5 mg/L DCF which is 100 times lower than the initial concentration in the present work by 0.045 g/kWh using corona discharge generated in extended coaxial geometry directly in water.

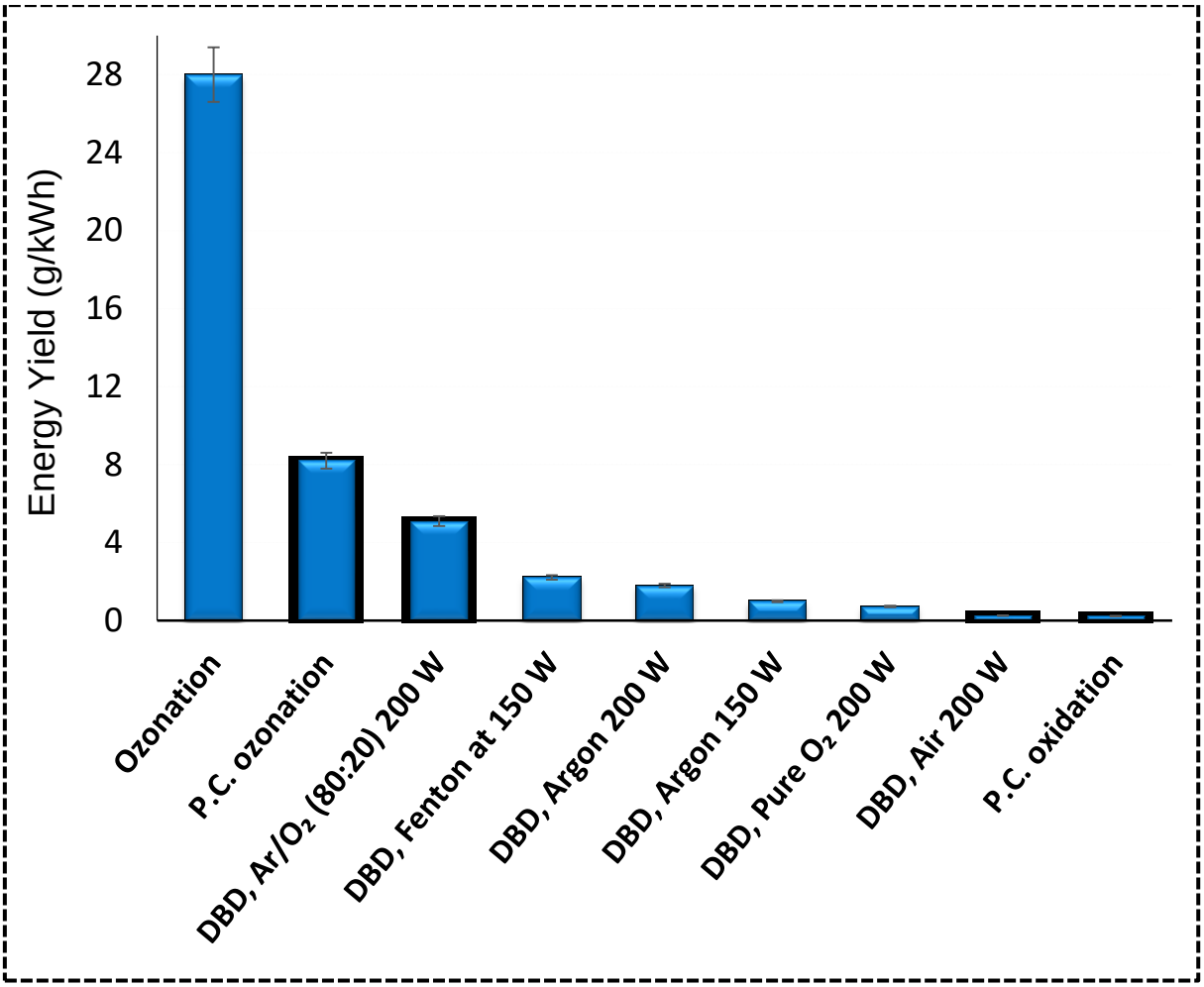

Figure 3.17 Energy Yields (G_{50}) of the ozonation and other applied AOPs for the degradation of DCF (C_o = 50 mg/L).

The energy yield (G_{50}) for the decomposition of IBP by ozonation and other tested advanced oxidation processes are shown in Fig. 3.18. They are in the range of 0.1 g/kWh by DBD plasma in air atmosphere up to 2.5 g/kWh by ozonation.

The yield for the DBD plasma in argon atmosphere with about 2.15 g/kWh is comparable with the energy yield obtained by ozonation. Zheng et al. [85] compared the energy yield (G_{50}) for the IBP degradation obtained for an initial concentration of 20 mg/L using several AOPs. Most of them are below 1 g/kWh and the energy yields reached up to 10 g/kWh by using a cylindrical wetted-wall corona discharge.

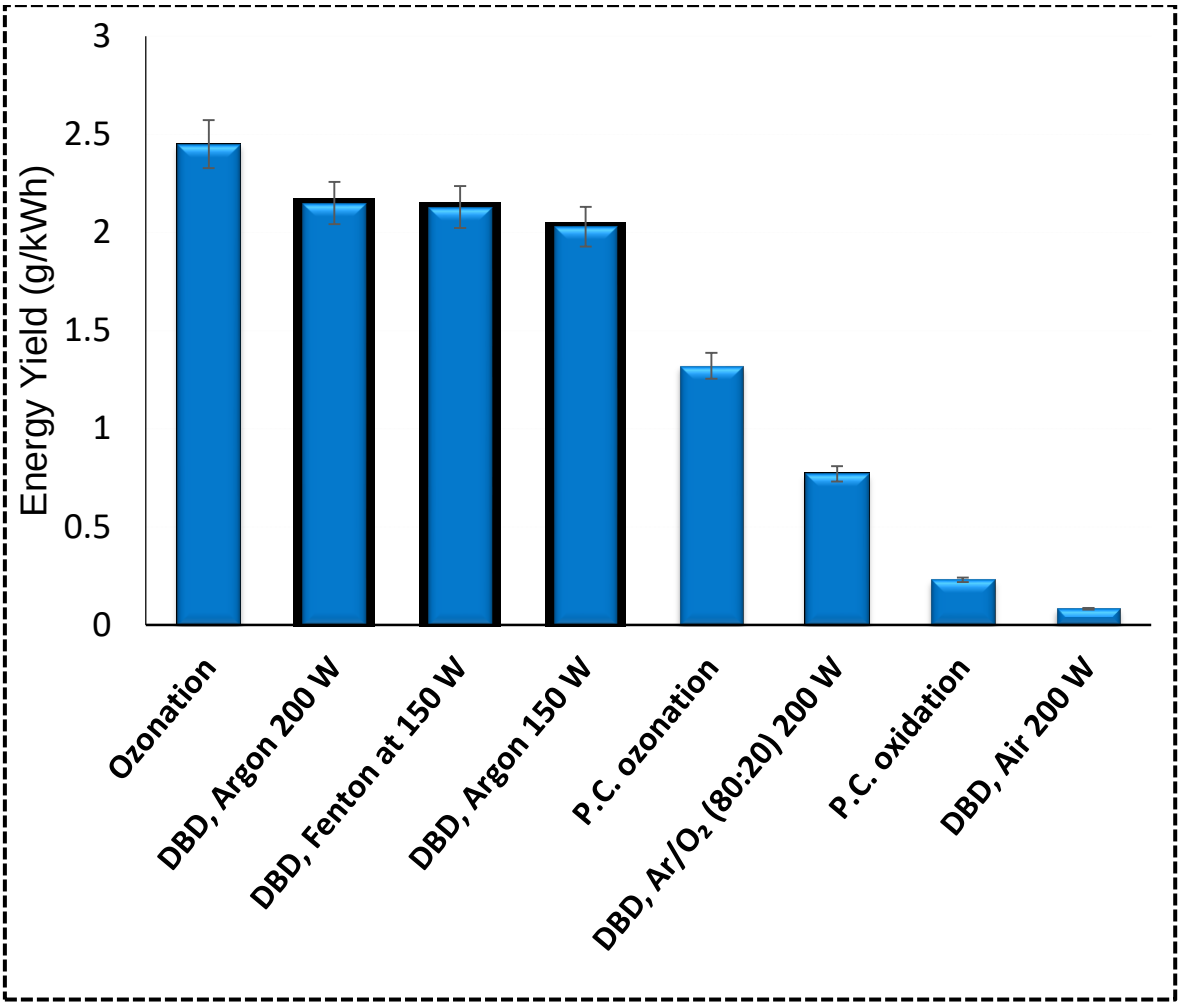

Figure 3.18 Energy Yields (G_{50}) of the ozonation and other applied AOPs for the degradation of IBP (C_o = 50 mg/L).

3.8.2 Energy yield (G_{50}) of 2,4-D and 2,4-DCP

The energy yields (G_{50}) of 2,4-D and 2,4-DCP (C_o= 100 mg/L each) are shown in Fig. 3.19 and 3.20. It can be seen that the highest yield of 24.54 g/kWh for 2,4-DCP and 6.5 g/kWh for 2,4-D are obtained by ozonation and DBD/Ar-Fenton respectively. The order of estimated G_{50} among the investigated methods is;

DBD/Ar-Fenton > ozonation > DBD/Ar > P.C. Ozonation > DBD/Ar:O_2 > DBD/Air > P.C. Oxidation for 2,4-D while, for 2,4-DCP degradation is ozonation > DBD/Ar-Fenton > P.C. Ozonation > DBD/Ar > DBD/Ar:O_2 > P.C. Oxidation > DBD/Air.

In the present work, the estimated energy yield G_{50} for the degradation of 100 mg/L 2,4-D by DBD plasma under air, argon/oxygen mixture, argon alone and their combination with Fenton process is 0.18, 1.5, 2.84 and 6.5 g/kWh (Fig. 3.19) respectively. The concentration of H_2O_2 produced in the 100 mg/L 2,4-D solution under argon atmosphere reaches 57 mg/L after 60 min (Fig. 3.1)

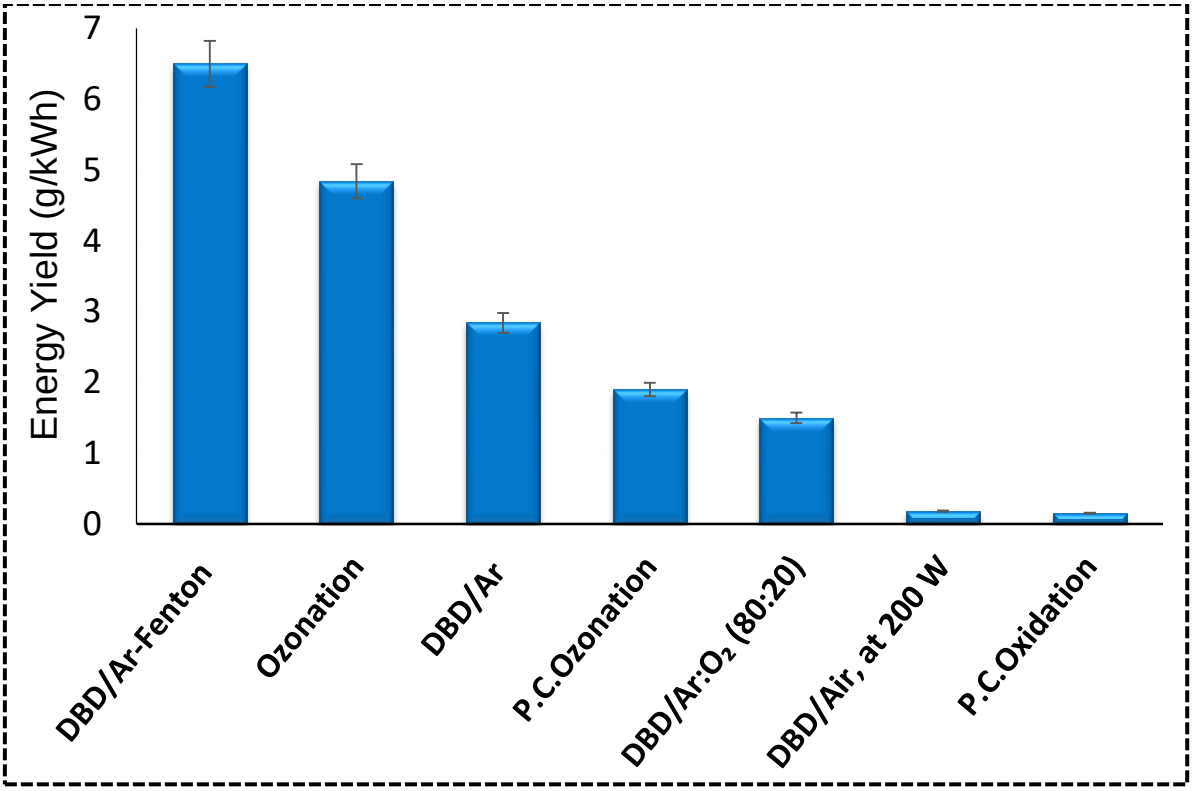

Figure 3.19 Energy Yields (G_{50}) of the ozonation and other applied AOPs for the degradation of 2,4-D (C_o= 100 mg/L).

These values are comparable with corresponding results obtained by other groups. Singh et al. [180] reported the energy yield of 1.6 g/kWh for 90% 2,4-D degradation using multiple pin-plain corona discharge at lower initial concentration of 1 mg/L . Bradu et al. [181] studied the degradation of 2,4-D by combination of corona discharge with ozonation and obtained an energy yield at G_{50} of 5.1 g/kWh and the concentration of H_2O_2 produced in the 25 mg/L 2,4-D solution in the absent of ozone reaches 41 mg/L after 60 min.

The obtained energy yields for 2-chlorophenol degradation at G_{50} (C_o= 65 mg/L) using pulsed streamer corona discharge is 2.9 g/kWh [112] and (C_o= 100 mg/L at pH 6.5) using non-thermal plasma-induced photocatalysis and without catalyst in needle-plate reactor [113] have been reported as 2.15 and 0.95 g/kWh respectively.

The estimated energy yield G_{50} for the degradation of 100 mg/L 2,4-DCP obtained in the present work (Fig. 3.20) is 3.2 and 4.64 g/kWh by DBD under argon alone and their combination with Fenton oxidation respectively.

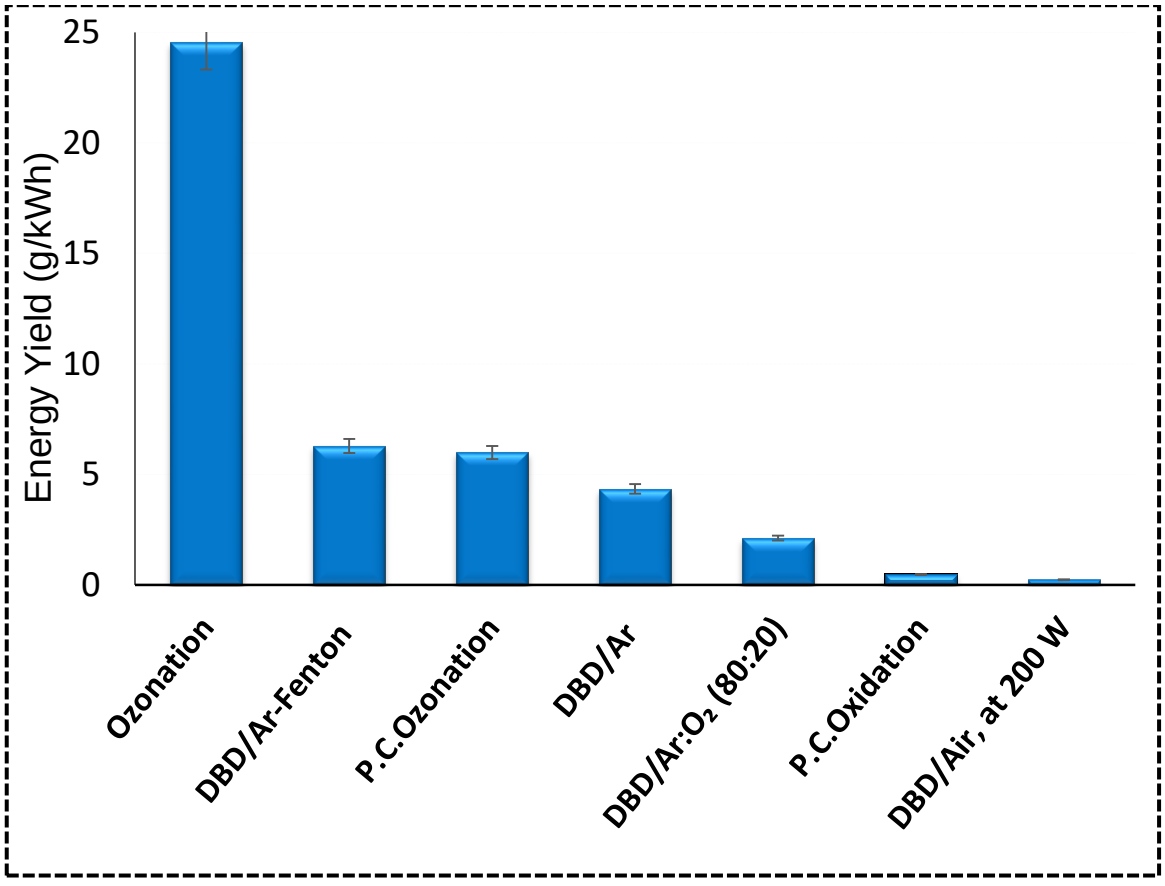

Figure 3.20 Energy Yields (G_{50}) of the ozonation and other applied AOPs for the degradation of 2,4-DCP (C_o = 100 mg/L)

3.8.3 Energy yield (G_{50}) of MB

Fig. 3.21 shows the energy yields at 50% decomposition (G_{50}) of MB. The decolorization of MB by the Fenton oxidation reaction is fast and does not require any sort of energy input. The highest energy yield of 20.5 g/kWh is obtained by the ozonation which is much higher than those of the DBD plasma methods due to the high efficiency of ozonation in decolorization of MB. Previously, several studies have been reported the value of energy yields for MB degradation by non-thermal plasma such as Ikoma et al. [182] who used the pulsed discharge in Ar-O_2 at G_{70} and initial concentration of 15 mg/L MB. Benetoli et al. [164] have used a point-to-plate electrical discharge reactor in O_2 at G_{81} and C_o= 20 mg/L MB. Liu et al. [150] used a DC corona discharge in air at G_{90} and C_o= 50 mg/L MB. Chandana et al. [149] conducted a study using a plasma jet in argon at G_{72} and 50 mg/L MB, the estimated energy yields was 0.073, 0.0244, 1.21 and 0.4 g/kWh respectively. Magureanu et al. [147] used a pulsed corona discharge in O_2, Wang et al. [151] applied a double-chamber DBD in O_2. Garcia et al. [152] conducted a research by using a microwave plasma jet in argon, the authers reported the energy yields for 50 mg/L MB decomposition at G_{50}, G_{100} and G_{50} as 1.3, 0.83, and 0.033 g/kWh respectively. Hsieh et al. used a pulsed electrical discharge which is generated in a tubular reactor under argon carrier gas have also reported the energy yield in the range of 1.7 to 4.1 g/kWh. In the present work, the obtained energy yields G_{50} by the DBD plasma under the different gases atmosphere such as argon/oxygen (80:20), argon alone and their combination with additional Fenton oxidation process at *P*=150W are 0.84, 1.36, and 2.5 g/kWh respectively.

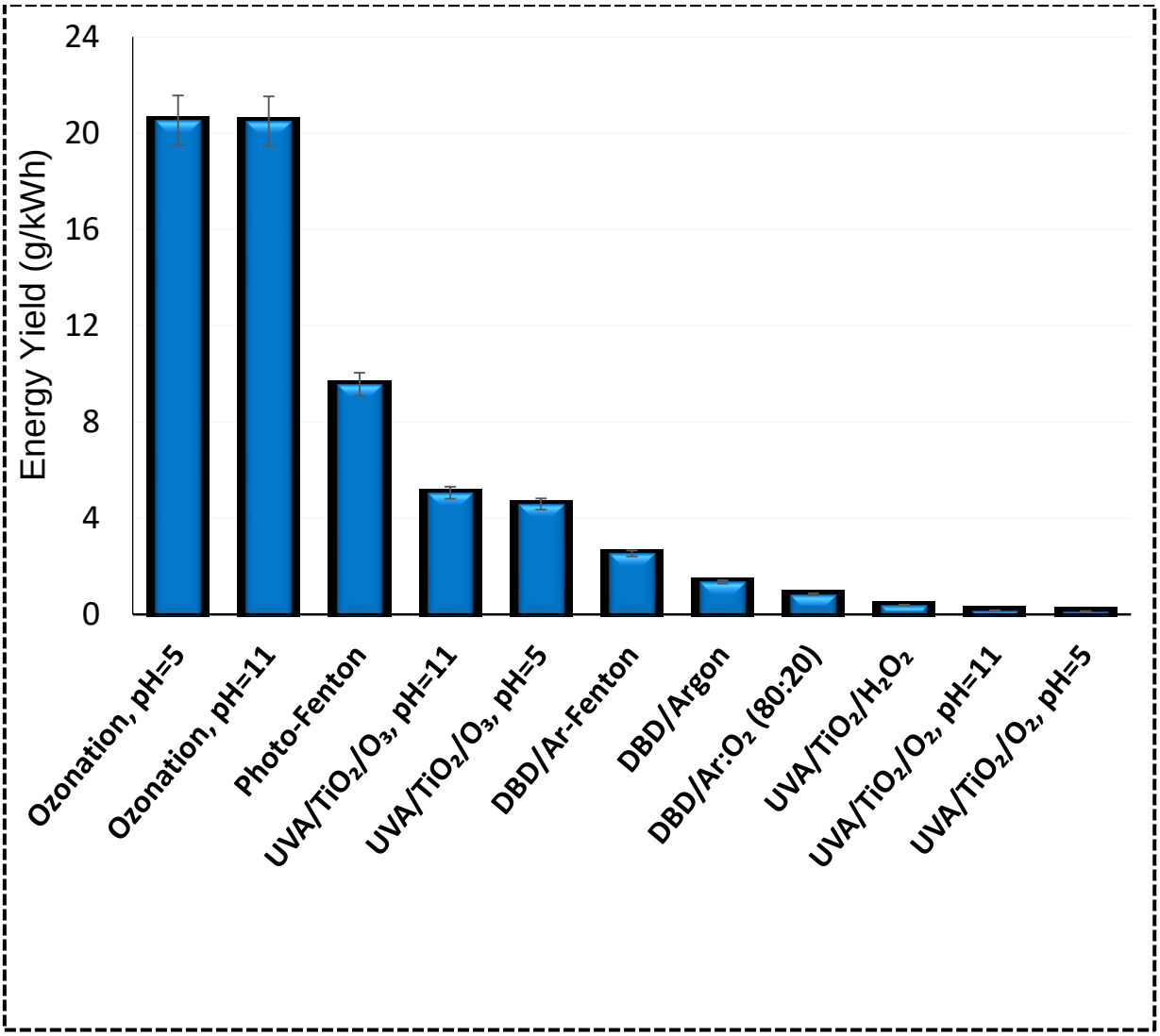

Figure 3.21 Energy Yields (G_{50}) of the ozonation and other applied AOPs for the decolorization of MB (C_o= 50 mg/L).

3.9 Mineralization and by-products degradation

Degradation simply means the transformation of the parent compound into the other lower molar mass compounds, whereas mineralization is complete degradation of target pollutants to CO_2, H_2O, and other harmless inorganic compounds.

Disappearance of target pollutant in wastewater does not guarantee for the successful wastewater treatment method. For instance, the only decolorization of organic dye in polluted water does not guarantee the quality of such wastewater meets the standard limits for disposal. As the decolorization may only be due to the change in chromophore groups of dye molecules which is responsible for color appearance. Moreover, the degradation by-products may be more toxic and harmful than the initial pollutant [76, 183]. Therefore, beside the degradation of initial pollutants, it is also important to follow the degradation of intermediates and by-products and the degree of mineralization. Maximum degree of mineralization is an important key for the successful wastewater treatment system by an advanced oxidation processes. Poor mineralization is the indication of remaining of some non-degradable intermediate by-product in the system. Therefore, a prolonged treatment time is necessary until these intermediate by-products are also decomposed and the solution contains only safe or harmless compounds.

3.9.1 Mineralization and by-products degradation of DCF and IBP

The main ionic by-products which have been identified and measured by ion chromatography during the degradation of DCF and IBP are acetate and oxalate. Chloride (Fig. 3.5), nitrate, and to a minor extent, maleate, malonate and succinate ions are also identified during the degradation of DCF. Figure 3.22 and 3.23 show the variation of the acetic acid and oxalic acid concentrations during the decomposition of both pollutants, respectively. It can be seen that a significant amount of acetate and oxalate ions remain as by-products even after a complete decomposition of two pollutants by ozonation and DBD plasma in an argon and air atmosphere. This is important, especially in the case of ozonation, for which the highest energy yield has been observed. However, the ozone resistant carbonic acids could not be removed. This behavior is also reflected in the TOC values (degree of mineralization) after the decomposition of both pharmaceuticals by ozonation (Fig. 3.24 for DCF and 3.25 for IBP). The direct ozonation results in a fast decomposition of the parent compounds, but ozone resistant byproducts remain in the solution. The TOC value remains also high after P.C. oxidation and DBD plasma in air atmosphere, for which the degradation is slow (Fig. 3.7). The maximum TOC reduction is obtained for both pharmaceuticals by using P.C. ozonation and DBD in Ar/O_2 mixtures.

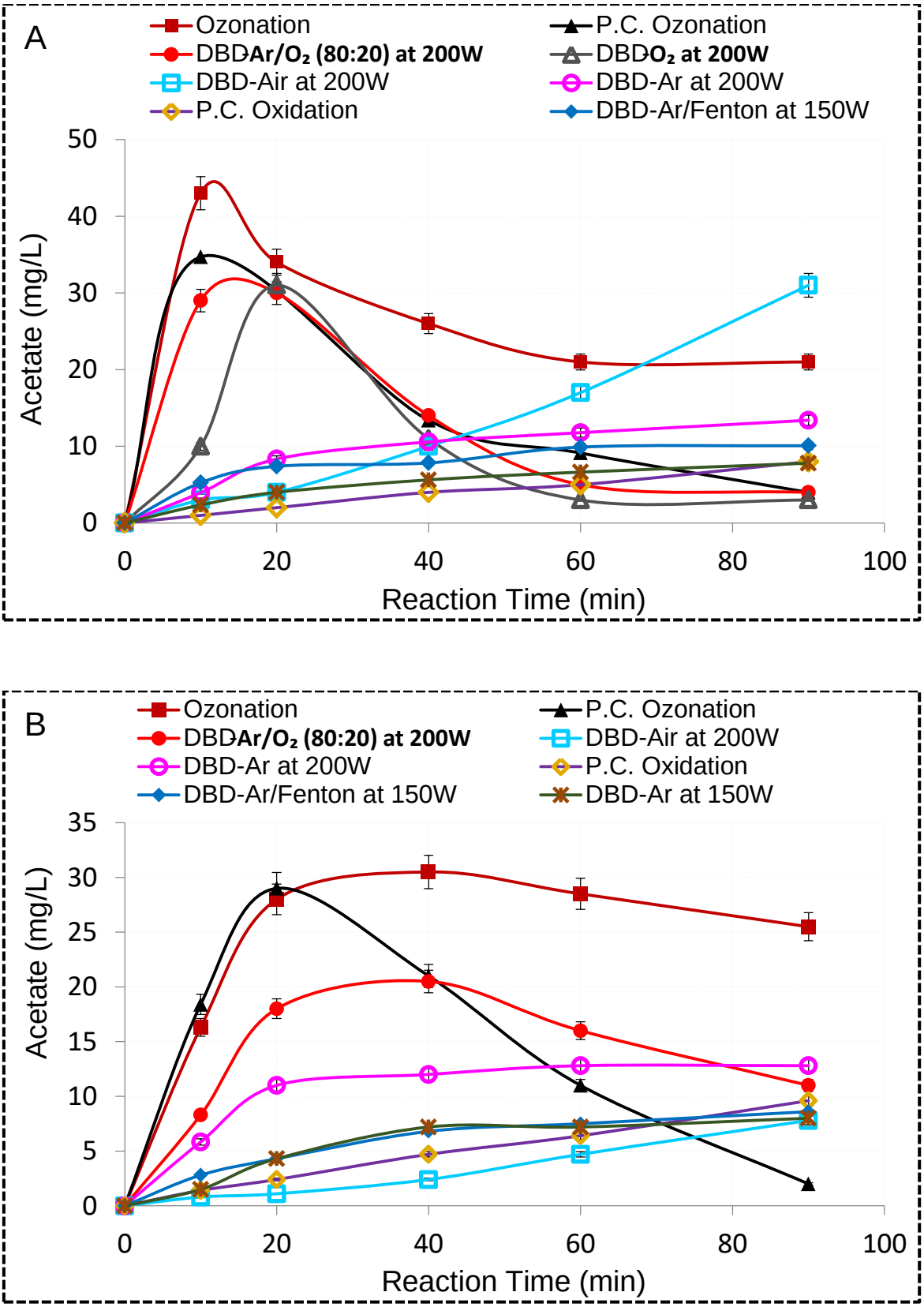

Figure 3.22 Variation of acetate intermediate by-product concentrations during the degradation of 50 mg/L : (A) DCF, (B) IBP.

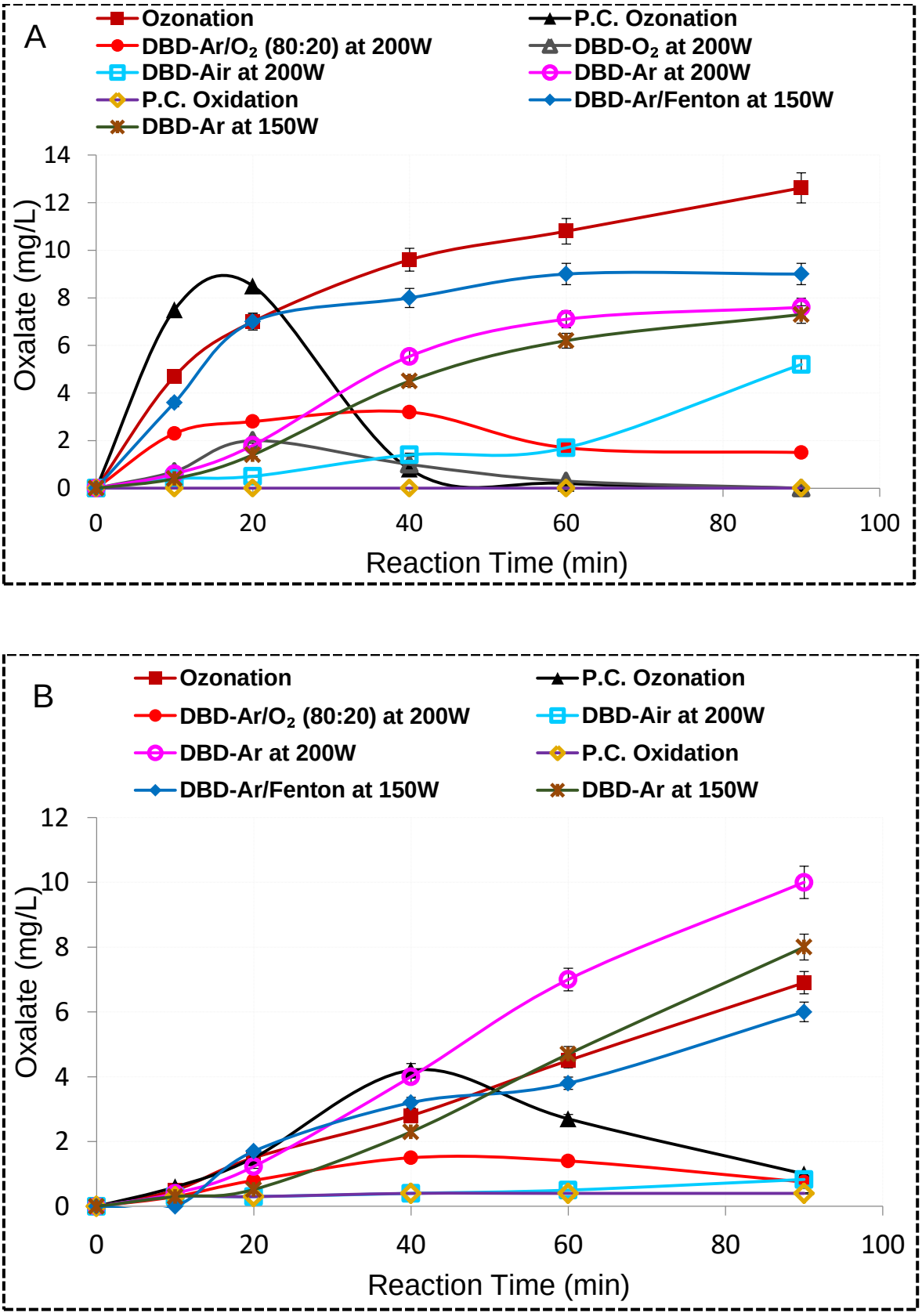

Figure 3.23 Variation of oxalate intermediate by-product concentrations during the degradation of 50 mg/L : (**A**) DCF, (**B**) IBP.

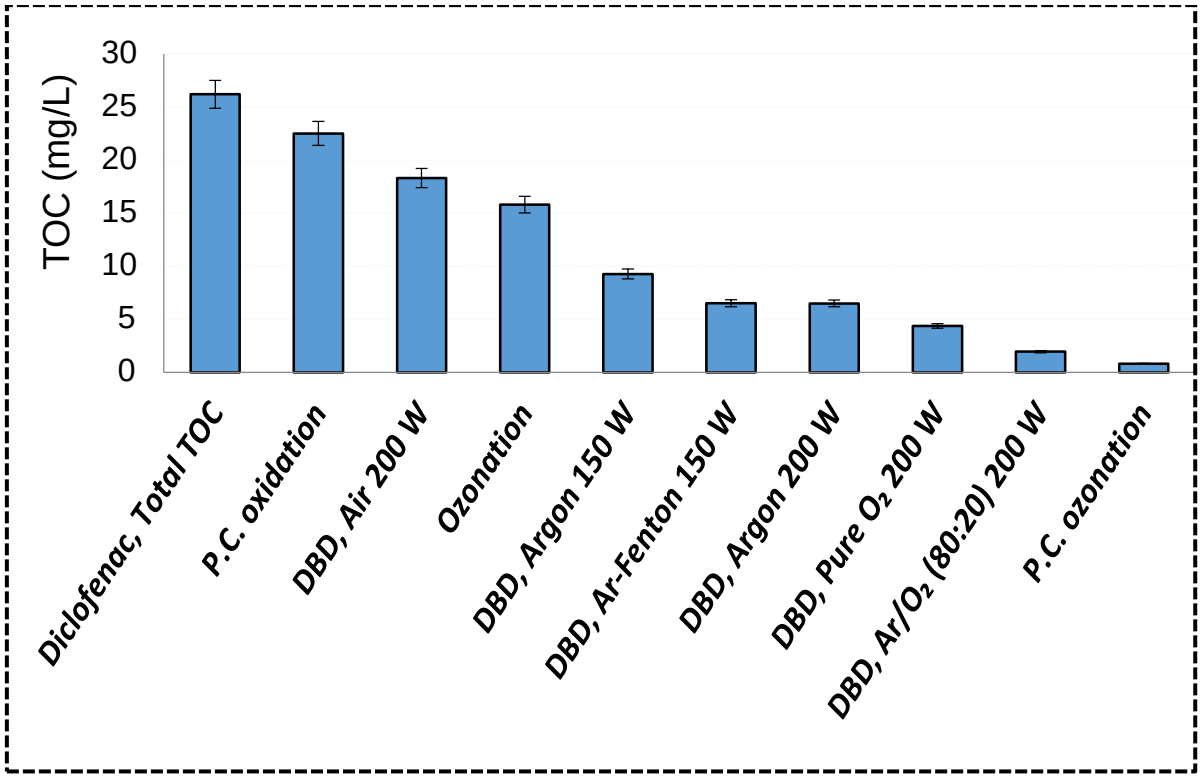

Figure 3.24 TOC removal after 90 min treatment of DCF (C_o= 50 mg/L, initial TOC 26.2 mg/L).

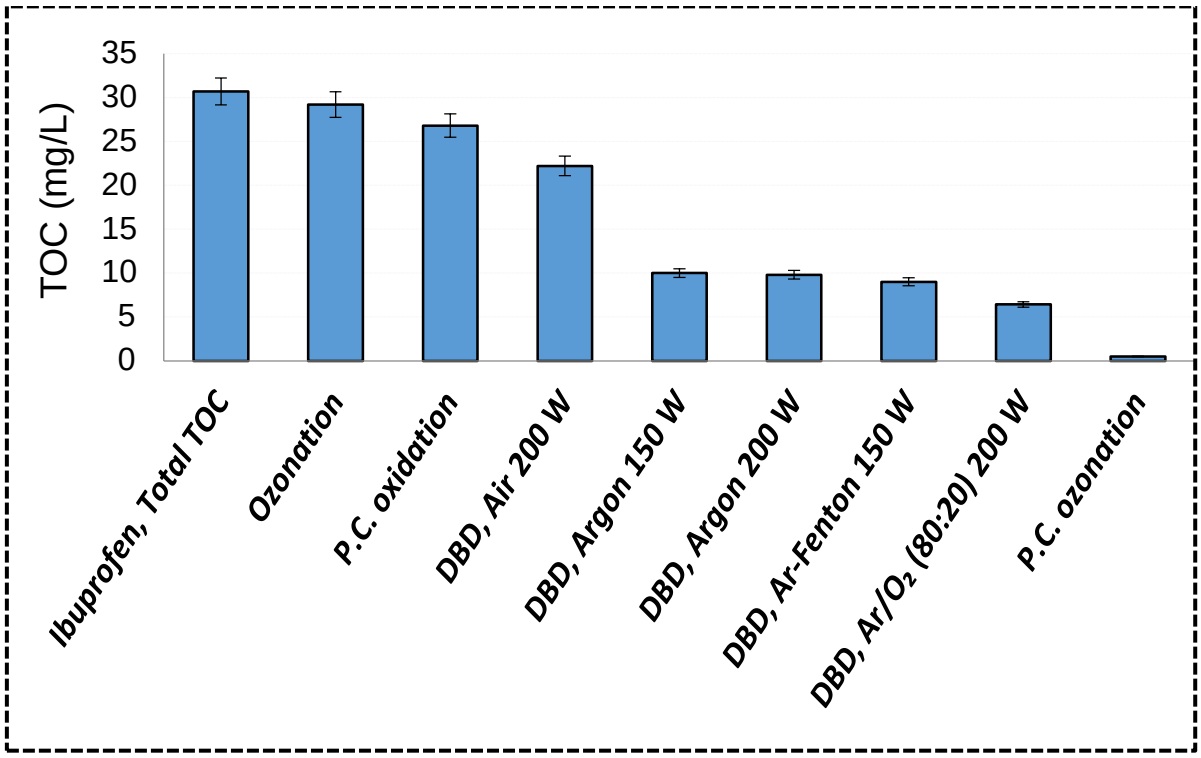

Figure 3.25 TOC removal after 90 min treatment of IBP (C_o= 50 mg/L, initial TOC 30.7 mg/L).

3.9.2 Proposed degradation pathways of DCF and IBP by photocatalysis

In order to identify degradation products during DCF and IBP treatment, samples have been collected at various time intervals and analyzed by gas chromatography mass spectrometry GC/MS. Also the identified low chain acid by-products obtained by ion chromatography which were used to propose the mechanism of degradation pathway for both pharmaceuticals.

3.9.2.1 Degradation products of DCF

The intermediate products of DCF produced by photocatalysis are identified by GC/MS which are presented in (table 3.2). In case of DBD plasma under argon atmosphere treatment, only 2,6-dichloroanile as an intermediate products is identified by GC/MS. This is due to the fast degradation of DCF by this method (see 3.5). The short chain acids as formate, acetate, oxalate, maleate, malonate and succinate are identified by ion-chromatography.

Figure 3.26 illustrates the possible degradation pathway of DCF by photocatalysis treatment. The proposed degradation pathway is based on the results presented in table 3.2. Low chain acids and possible expected products are identified by ion chromatography.

Table 3.2 Degradation products observed for DCF during photocatalysis identified by GC/MS.

Compound	m/z	Rt (min)
(1) Diclofenac	295.1	12.929
(2) [2-(2,6-Dichlorophenylamino)-phenyl]-hydroxy-acetic acid	311	11.334
(3) Dihydroxylation diclofenac	327.1	13.664
(4) 2-(2,6-Dichlorophenylamino)-benzaldehyde	265.1	11.294
(5) 2-(2-Chlorophenylamino)-benzaldehyde	231.1	10.777
(6) 1-(2,6-Dichlorophenyl)-1,3-dihydro-2H-endol-2-one	277.1	11.868
(7) 2-[2-(2-chloro-6-hydroxy anilino)phenyl]acetic acid	277.1	11.868
(8) 1-(2,6-Dichlorophenyl)-3-hydroxyindolin-2-one	293.1	13.392
(9) 1-(2,6-Dichlorophenyl)-5-hydroxyindolin-2-one	293.1	13.964
(10) 1-(2,6-Dichlorophenyl)-7-hydroxyindolin-2-one	293.1	14.467
(11) 1-(2,6-Dichloro-4-hydroxyphenyl)indolin-2-one	293.1	13.39
(12) 1-(2,6-Dichlorophenyl)-1H-benzo [1,2]oxazine-3-4H-one	293.1	13.964
(13) N-(2,6-Dichlorophenyl)-2-formylbenzamide	293.1	14.467
(14) 2,6-Dichloroaniline	161	5.068
(15) 2,6-Dichlorobenzonitrile	171	5.314
(16) 2,6-Dichlorophenol	162	4.768

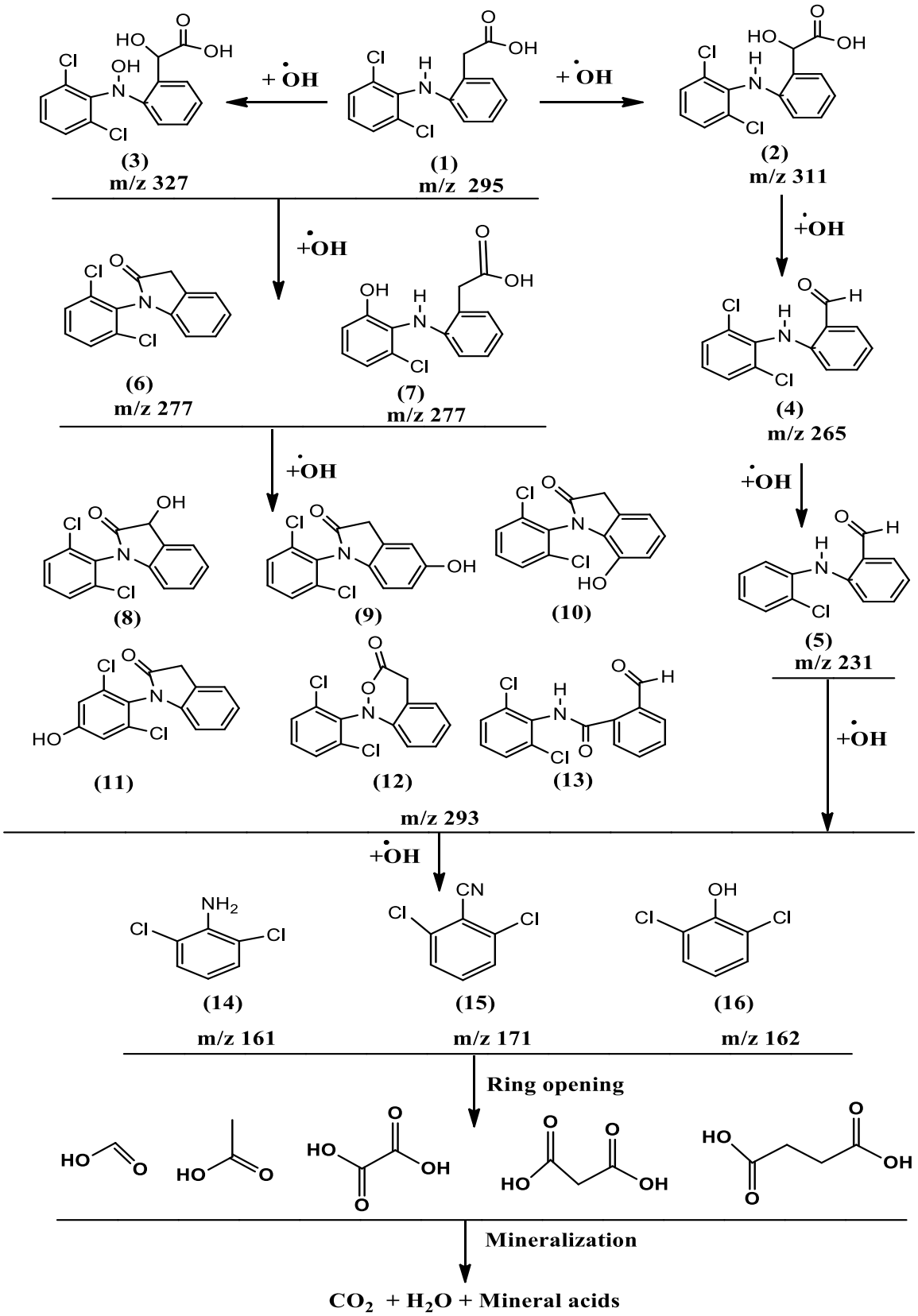

Figure 3.26 Proposed degradation pathways of DCF by photocatalysis.

3.9.2.2 Degradation products of IBP

In order to identify the reaction intermediate and to understand the degradation pathway of IBP during photocatalytic treatments, samples have been collected at various treatment times and have been analyzed by means GC/MS. The results indicate that a number of by-products listed in table (3.3) have been identified during the photocatalytic degradation of IBP. During DBD/Ar plasma treatment, the GC/MS results showed only the identification of one intermediate products 4-(2-methylpropyl)acetophenone, probably due to the effective degradation of IBP by DBD plasma in argon atmosphere. Based on the results showed in table 3.3, a photocatalytic degradation of IBP where proposed (Fig. 3.27).

Table 3.3 Degradation products observed for IBP during photocatalysis identified by GC/MS.

Compound	m/z	Rt (min)
(1) Ibuprofen	206.1	8.65
(2) 2-Hydroxy-2-(4-(1-hydroxy-2-methylpropyl)phenyl)propanoic acid	235.1	7.140
(3) 4-Isobutylbenzoic acid	178	6.704
(4) 4-Isobutylbenzaldehyde	162	6.063
(5) 4-Isopropylbenzaldehyde	148	4.636
(6) 4-Ethylacetophenone	148	6.165
(7) 4-Isobutylacetophenone	176	6.690
(8) 4-(1-carboxyethyl)benzoic acid	190	8.140

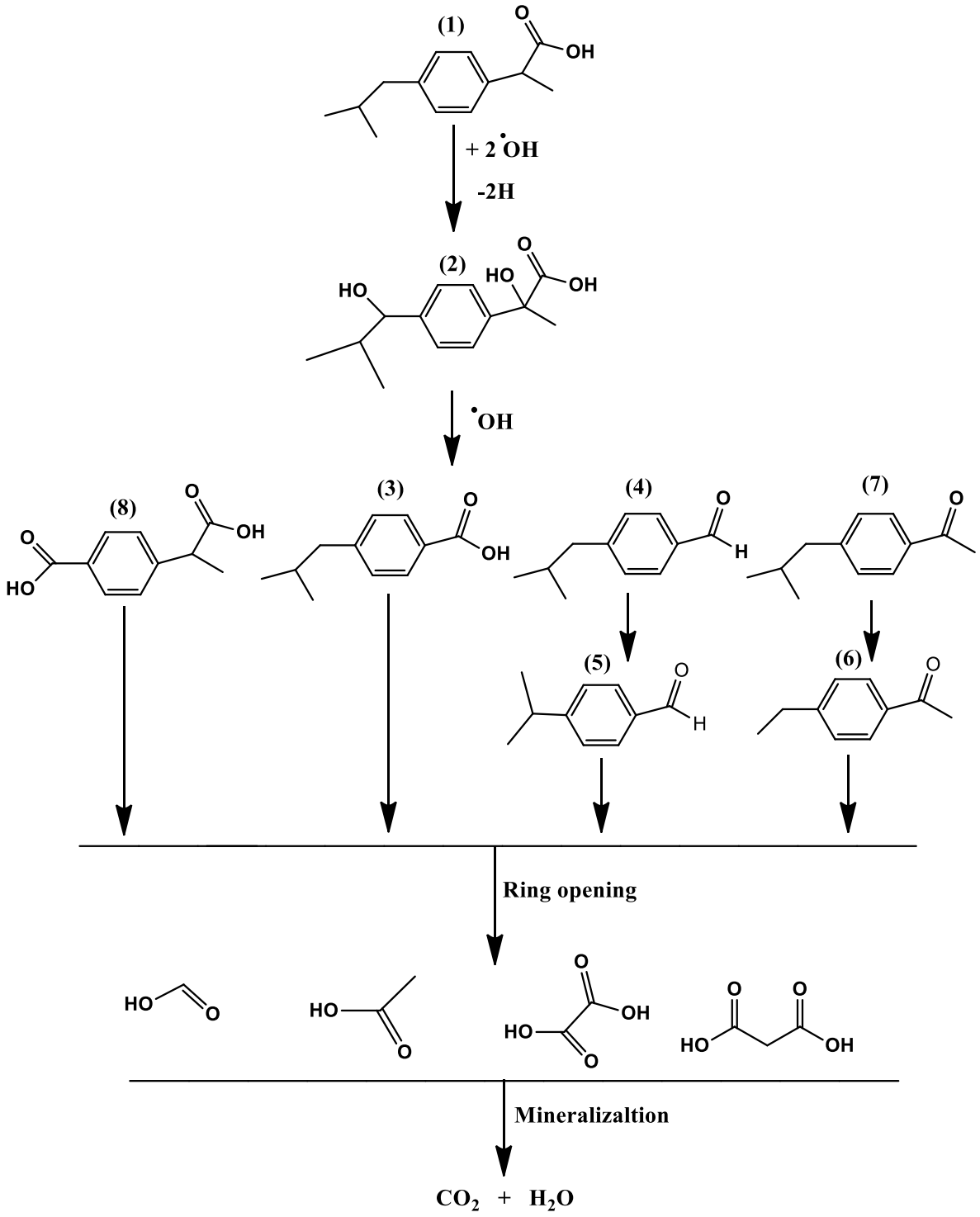

Figure 3.27 Proposed degradation pathways of IBP by photocatalysis.

3.9.3 Mineralization and by-products degradation of 2,4-D

Ion chromatography and HPLC analysis of the treated samples of 2,4-D by examined methods showed the simultaneous formation and degradation of some low chain acids namely; oxalic acid, glyoxylic acid, glycolic acid and 2,4-DCP as a main by-products during the degradation of 2,4-D. Figs. 3.28, 3.29, 3.30, and 3.31 show the comparative variation of the 2,4-DCP, oxalate, glycolate and glyoxylate concentrations during the degradation of 2,4-D respectively. It is observed that the concentration of produced by-products in most methods increased to peak value and then decreased over time, except oxalate ion which remains as by-products even after a complete degradation of 2,4-D by ozonation and DBD under argon atmosphere indicating the resistant of oxalic acid against these methods. Poor mineralization is the indication of remaining of some non-degradable intermediate by-products in the system which might be more toxic and carcinogenic than the initial pollutant [76]. The mineralization efficiency was measured by total organic carbon (TOC) analysis. Figs. 3.32 (A and B) presents abetment of TOC value by ozonation, P.C.ozoznation, P.C.oxidation and non-thermal DBD plasma under (argon, argon:oxygen, and air) processes with initial concentration of 100 mg/L of both pollutants. Ozonation in darkness is very effective for degradation of both pollutants. However, poor mineralization is observed. The TOC decay remains also low after P.C.oxidation and DBD under air. It could be seen from the results shown in Fig. 3.32 (A and B) that the combination of ozone with photocatalysis markedly enhances the TOC removal and complete mineralization is obtained after 60 min of treatment. The DBD/Ar subjected to additional Fenton oxidation and addition of oxygen to the gas atmosphere results is significant improvements in TOC reduction.

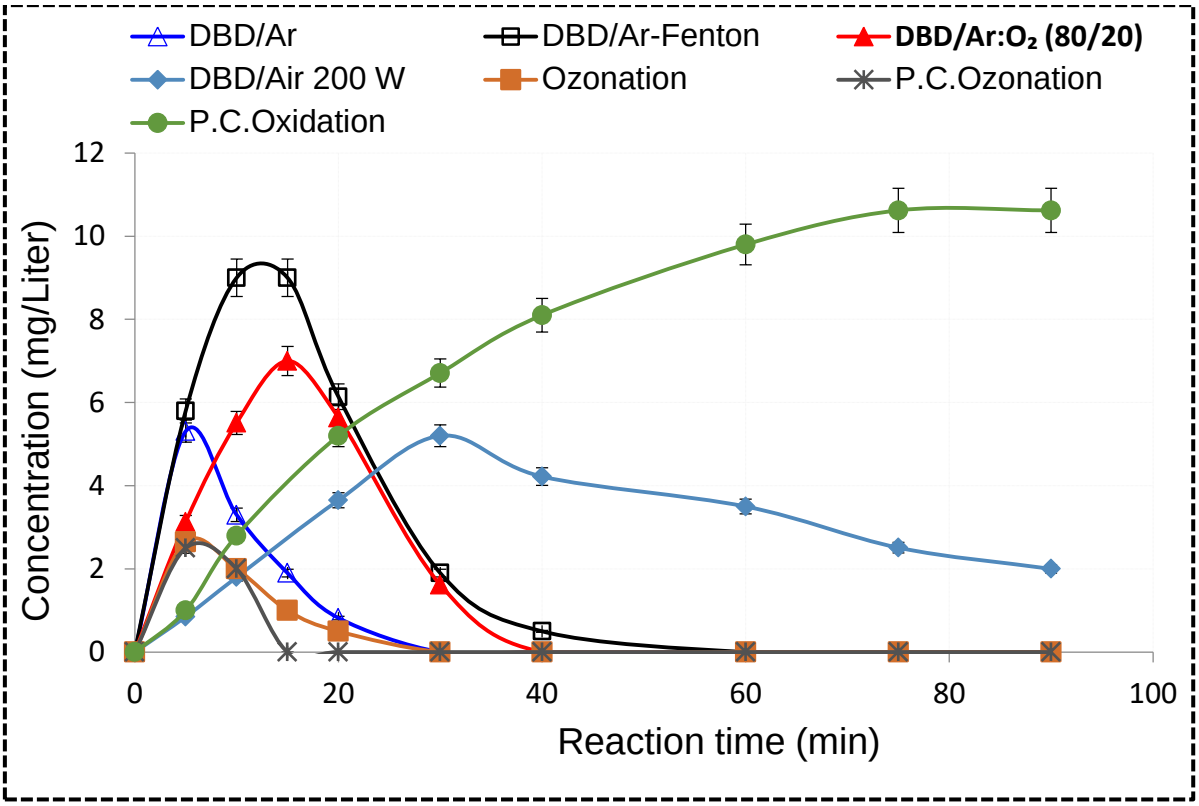

Figure 3.28 Variation of 2,4-DCP intermediate by-product concentrations during the degradation of 100 mg/L 2,4-D.

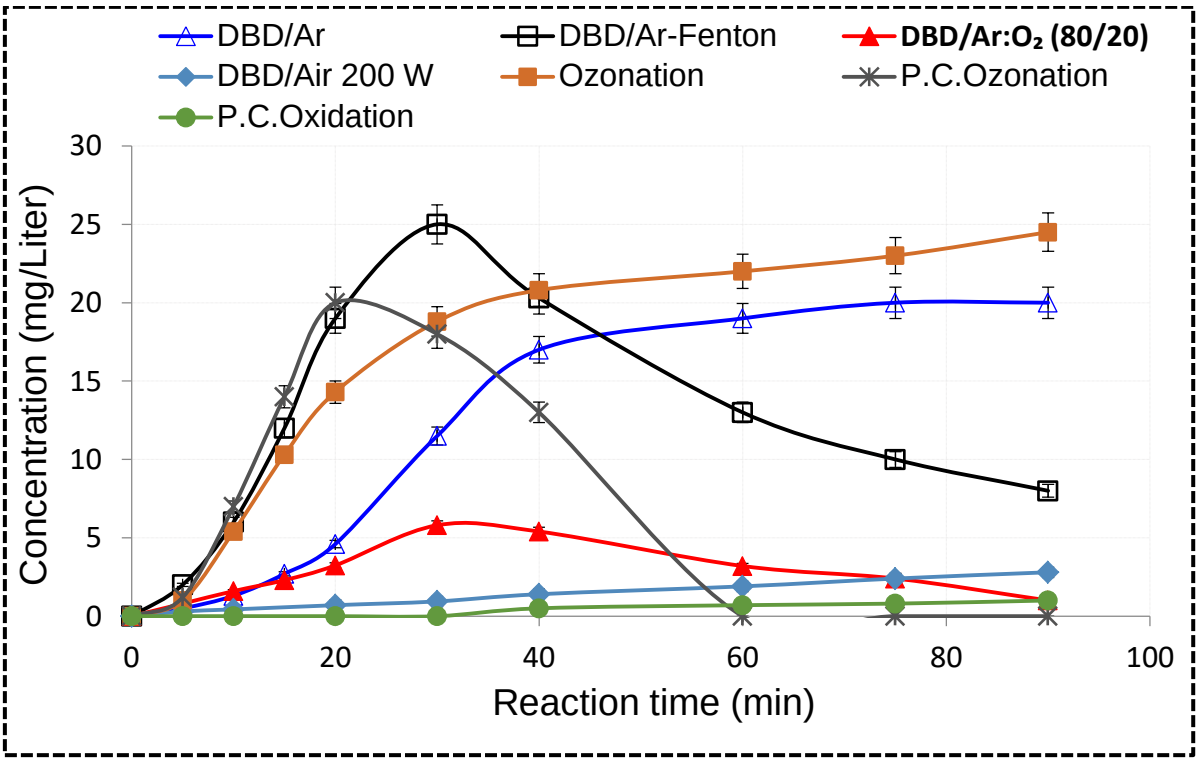

Figure 3.29 Variation of oxalate intermediate by-product concentrations during the degradation of 100 mg/L 2,4-D.

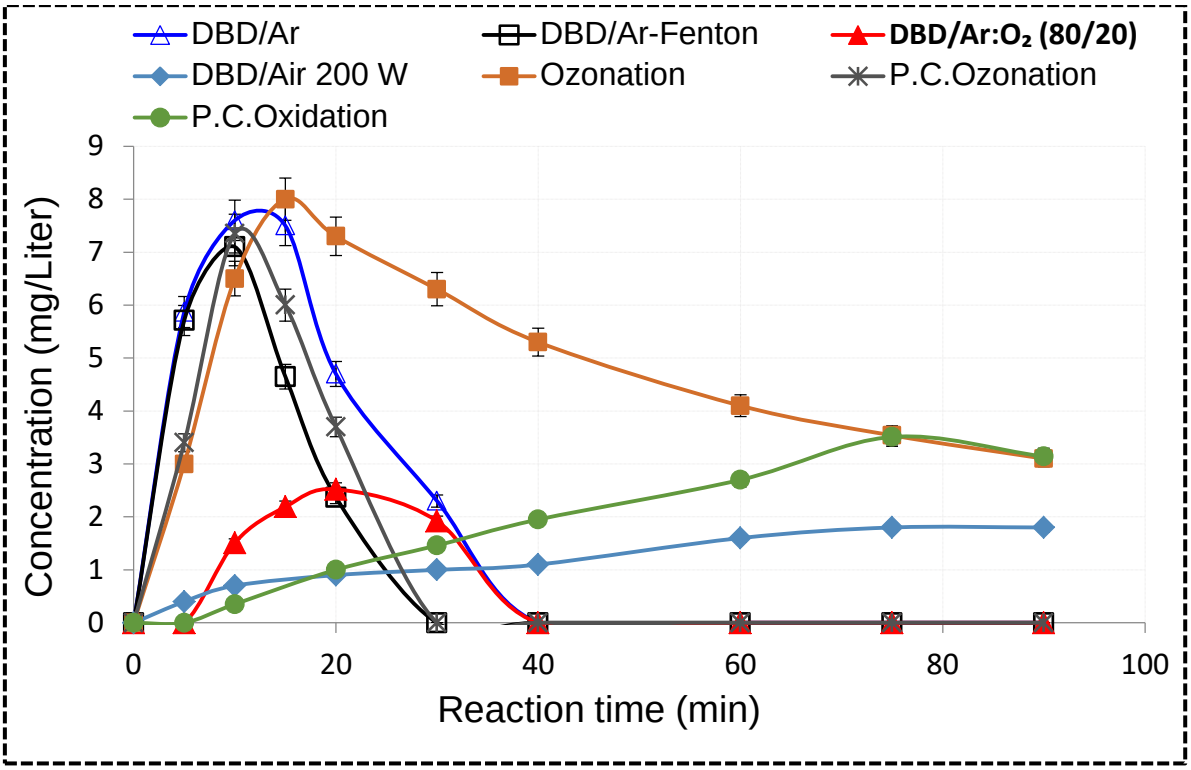

Figure 3.30 Variation of glycolate intermediate by-product concentrations during the degradation of 100 mg/L 2,4-D.

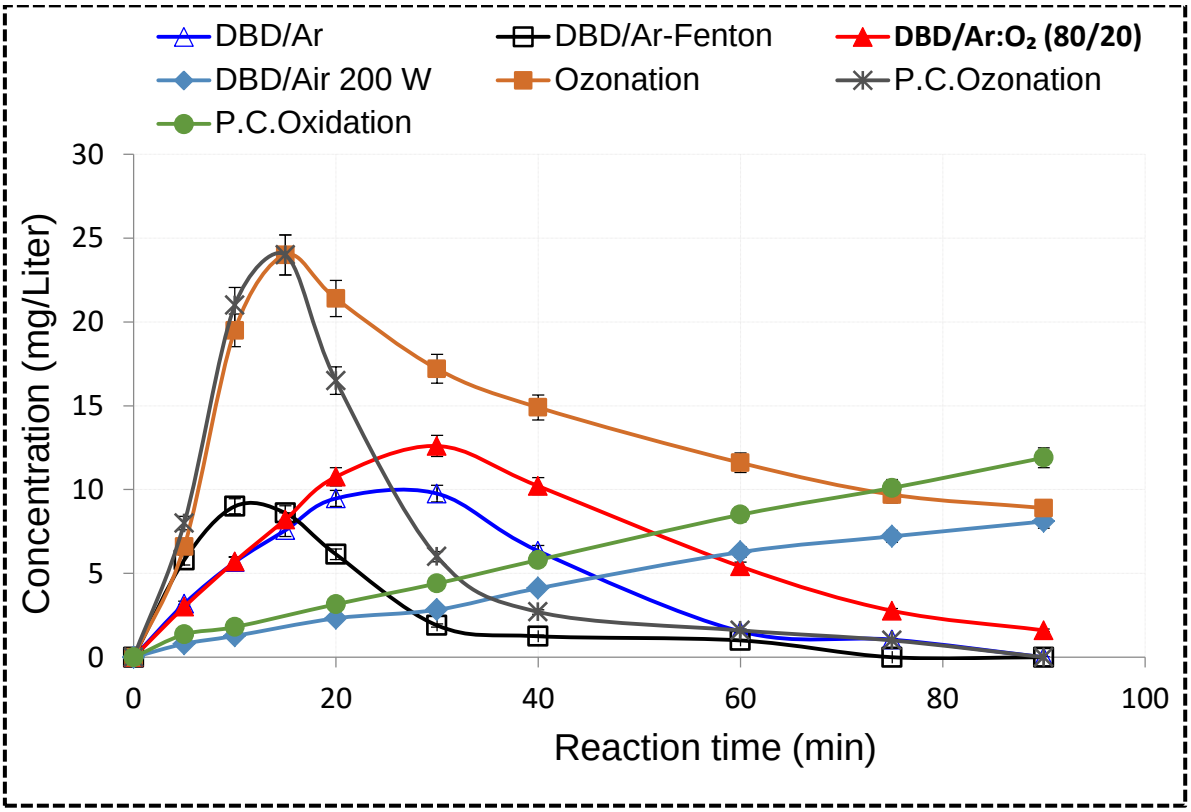

Figure 3.31 Variation of glyoxylate intermediate by-product concentrations during the degradation of 100 mg/L 2,4-D.

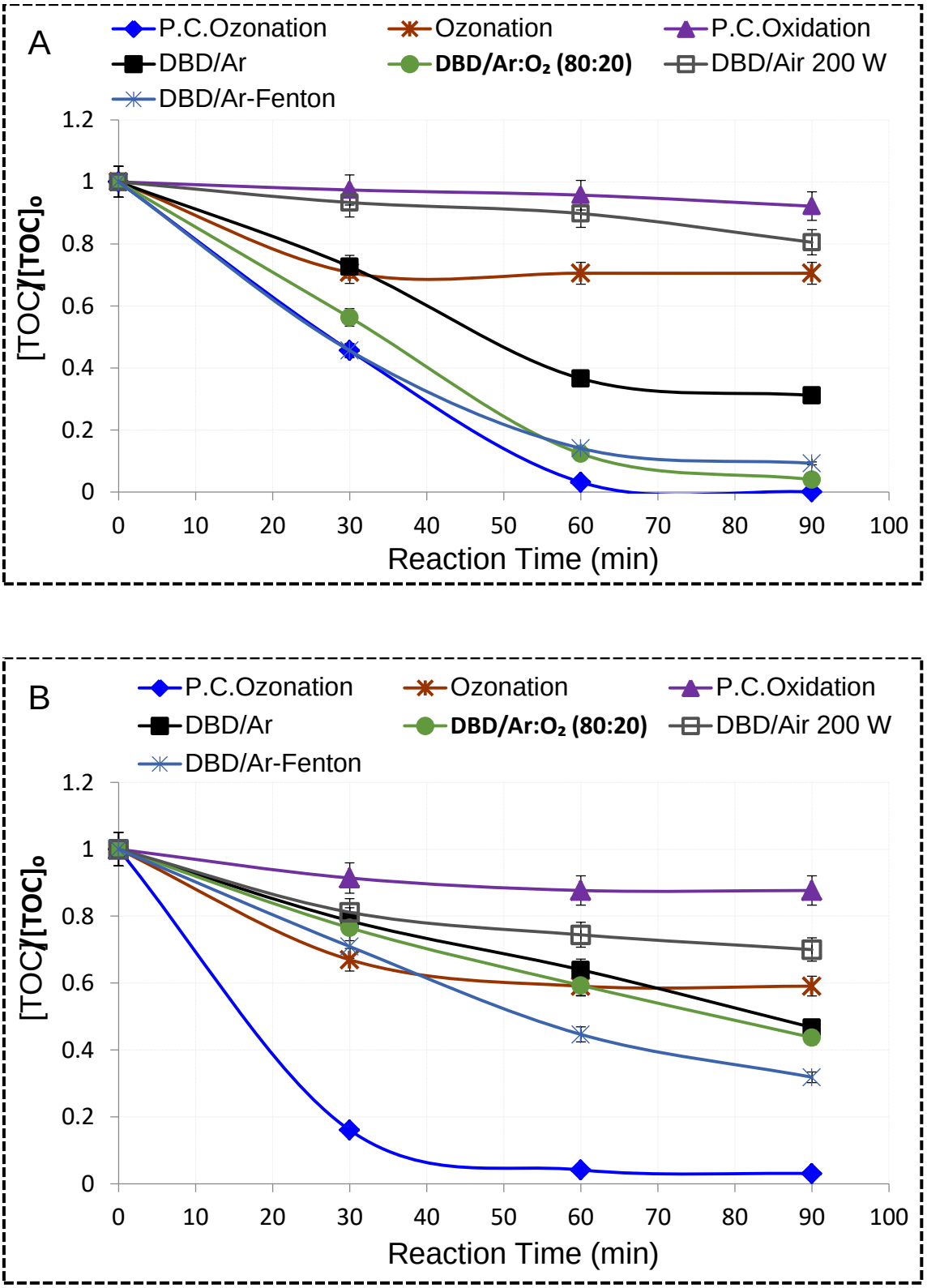

Figure 3.32 Relative TOC concentration profiles in ozonation and other applied AOPs: (A) 2,4-D (initial TOC = 42.1 mg/L) and (B) 2,4-DCP (initial TOC = 43 mg/L).

3.9.4 Mineralization and by-products degradation of MB

Degree of mineralization is an important key for the successful wastewater treatment system by AOPs. Poor mineralization is the indication of remaining of some refractory by-products in the system. Therefore, besides the decolorization of dye pollutants, it is also necessary to follow the degradation and mineralization of splitting by-products. To this end, ionic by-products of MB decomposition such as acetate, oxalate, and sulfate are identified and measured by ion chromatography. Figure 3.33, 3.34, and 3.35 indicate the formation of these anions during the degradation of MB by different AOPs. It is observed that a significant amount of acetate and oxalate as degradation by-products remain in the solution even after 90 min of treatment. Particularly in the case of ozonation and Fenton processes in the absence of UV light, considerable amounts of acetate and oxalate are accumulated in the treated solutions without sufficient mineralization. The combination of the UVA light with the ozonation and Fenton processes accelerates the decomposition of acetate and oxalate by the so-called photocatalytic ozonation and photo-Fenton processes. This is due to the excessive production of non-selective and highly reactive hydroxyl radicals.

In the Fenton method, it is not possible to measure the exact amount of sulfate produced during the degradation process due to the presence of ferrous sulfate which is used as the source of Fe^{2+}. As estimation for the complete decomposition of MB, it has been noticed that when the concentration of sulfate anion in the solution reaches to an amount which is equivalent to the summary of sulfate in MB and ferrous sulfate all sulfur containing organic molecules are decomposed. This is only observed in the case of ozonation and photocatalytic ozonation processes, while using other AOPs a part of the sulfur containing molecules remained untreated (Fig. 3.35).

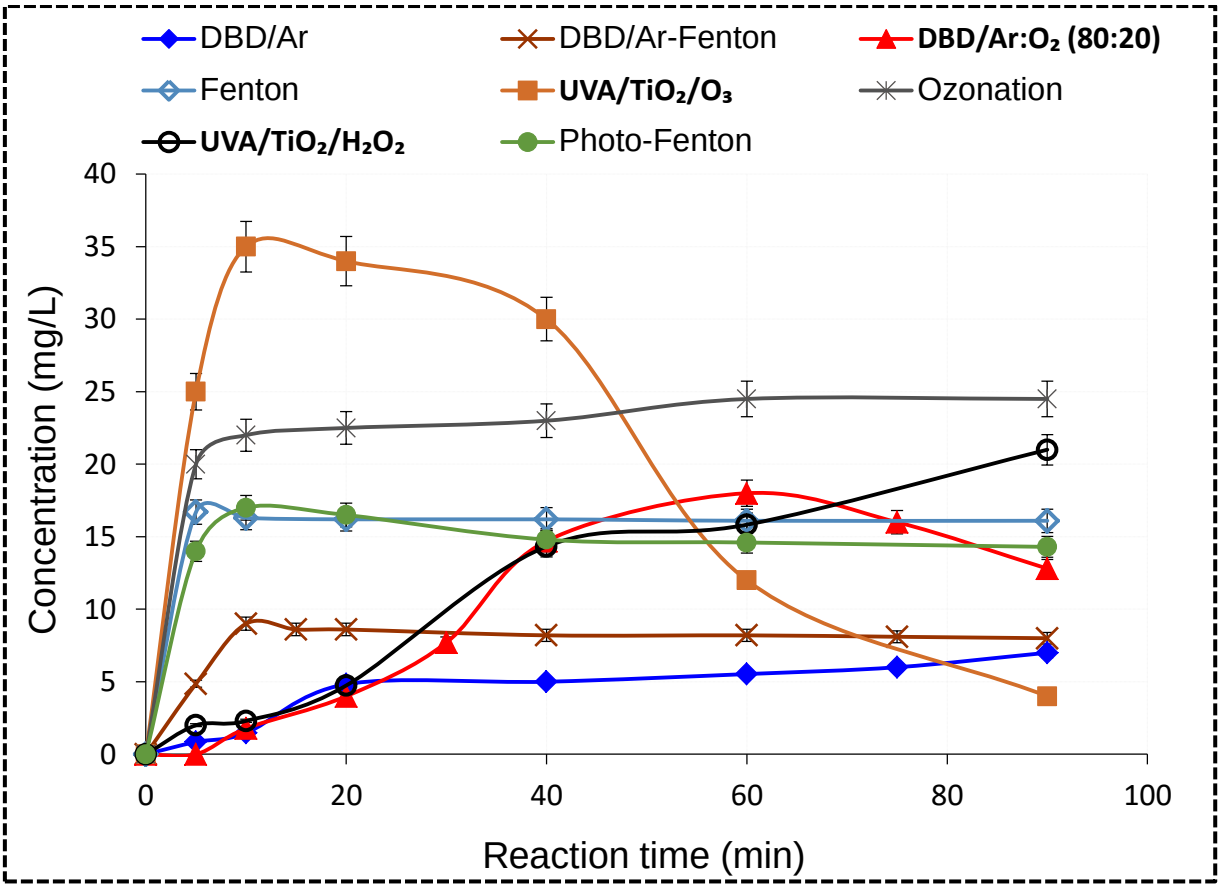

Figure 3.33 Variation of acetate intermediate by-product concentrations during the degradation of 50 mg/L MB.

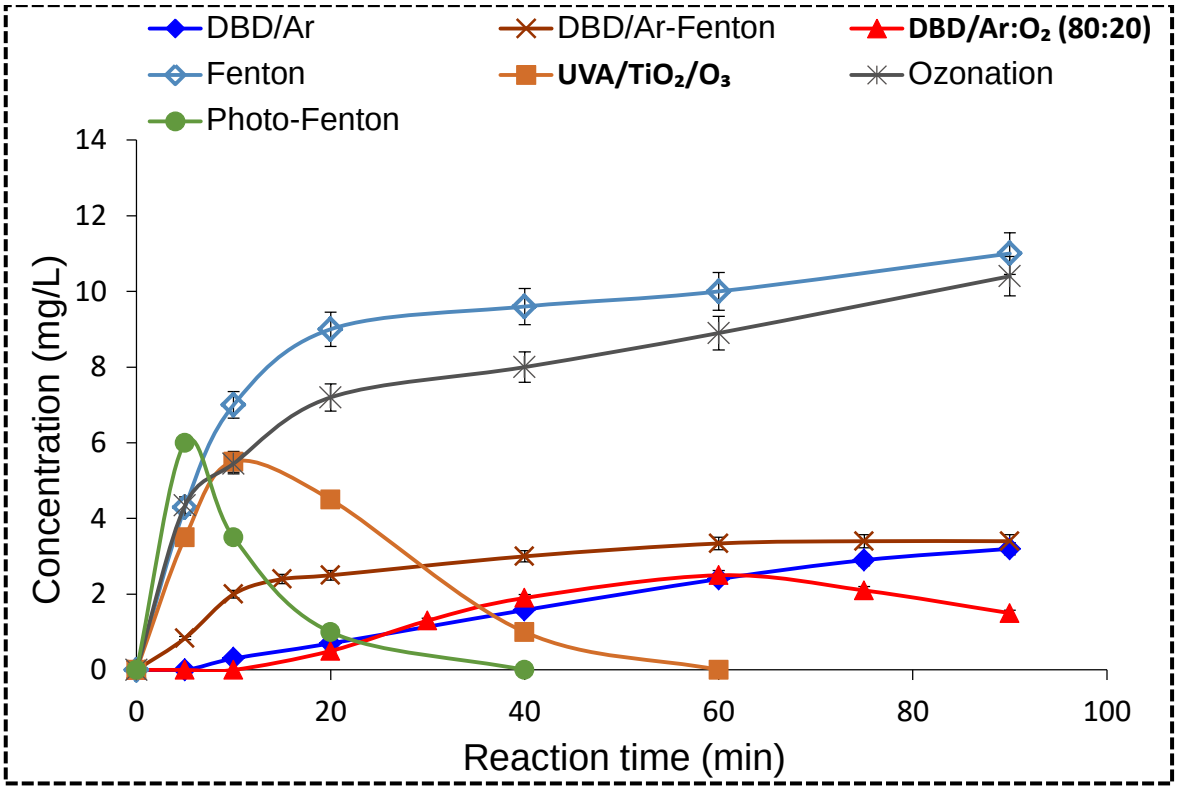

Figure 3.34 Variation of oxalate intermediate by-product concentrations during the degradation of 50 mg/L MB.

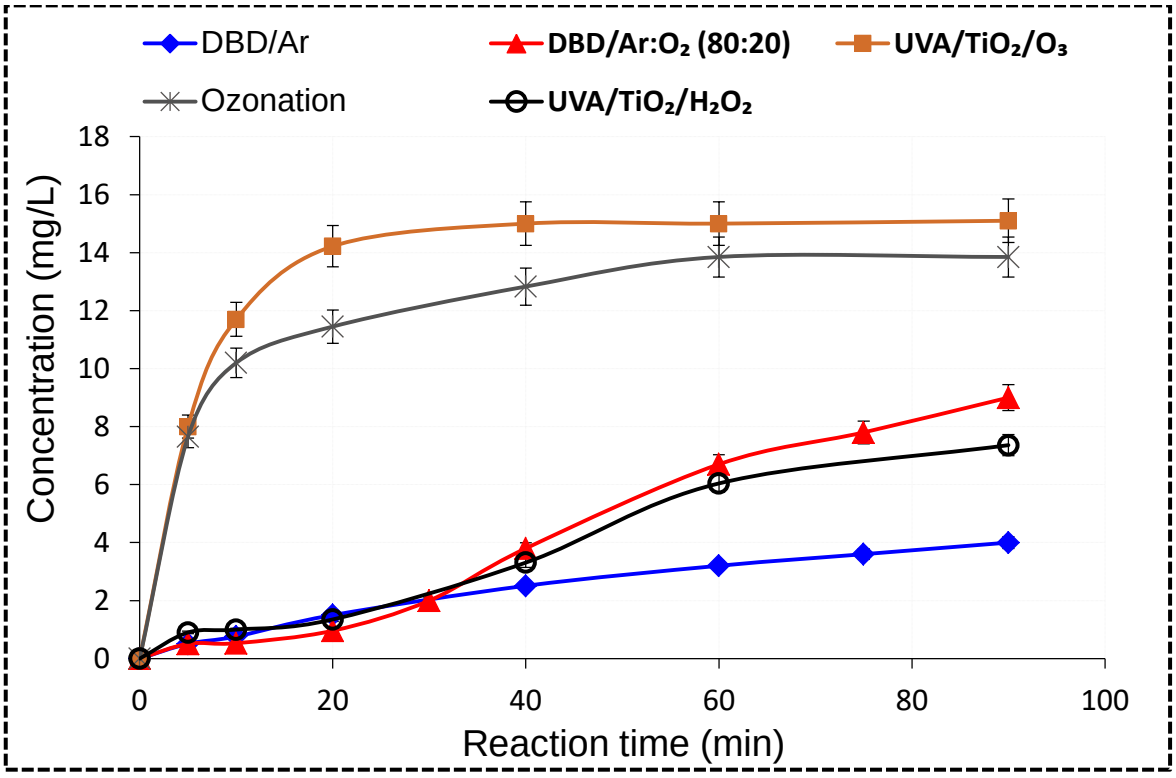

Figure 3.35 Variation of sulfate intermediate by-product concentrations during the degradation of 50 mg/L MB.

Abatement of the dissolved TOC can be used as an indicator for the mineralization efficiency of the treatment method. Figure 3.36 compares the efficiency of different treatment methods in the removal of TOC from a 50 mg/L MB solution after treatment by different AOPs for 60 and 90 min.

As mentioned before, the decolorization of MB by the ozonation is very fast and possesses the highest energy yield compared to other AOPs. However, it has low mineralization efficiency even after 90 min treatment (Fig. 3.36). This may be due to the relatively selective reaction of ozone molecule, in low pHs, with organic pollutants via the nucleophilic position in the aromatic ring of chromophoric molecules such as azo dyes. Therefore, this can leads to the formation of ozone resistant by-products like aldehydes, ketones and aliphatic carboxylic acids [172, 184]. Consequently, the combination of ozone with the UVA light and increasing the *pH* of the solution leads to a dramatic increase in the mineralization efficiency (Fig. 3.36). The combination of ozonation with the UVA light in the presence of TiO_2 photocatalyst can enhance the degradation efficiency of organic contaminants due to the generation of powerful non-selective $^{\bullet}OH$ radicals either by the photolysis of ozone molecules or via the photocatalysis. In the photocatalytic ozonation, ozone molecules can react with the photo-generated electrons on the surface of TiO_2 and generate $^{\bullet}OH$ radicals. In the ozonation at an alkaline *pH* (*pH* > 9), ozone decomposition by hydroxide ions accelerates the formation of $^{\bullet}OH$ radicals that they enhance the degradation of pollutants [185, 186].

The same observation has been made when H_2O_2 involved methods were illuminated by the UVA light (Fig. 3.36). The maximum mineralization (TOC removal) of MB by 88 percent is obtained using the DBD plasma under the argon atmosphere and in the presence of homogeneous Fe^{2+} catalyst which is due to the occurrence of an additional Fenton reaction. This is followed by 86

percent TOC removal after 90 min of performing the photocatalytic ozonation.

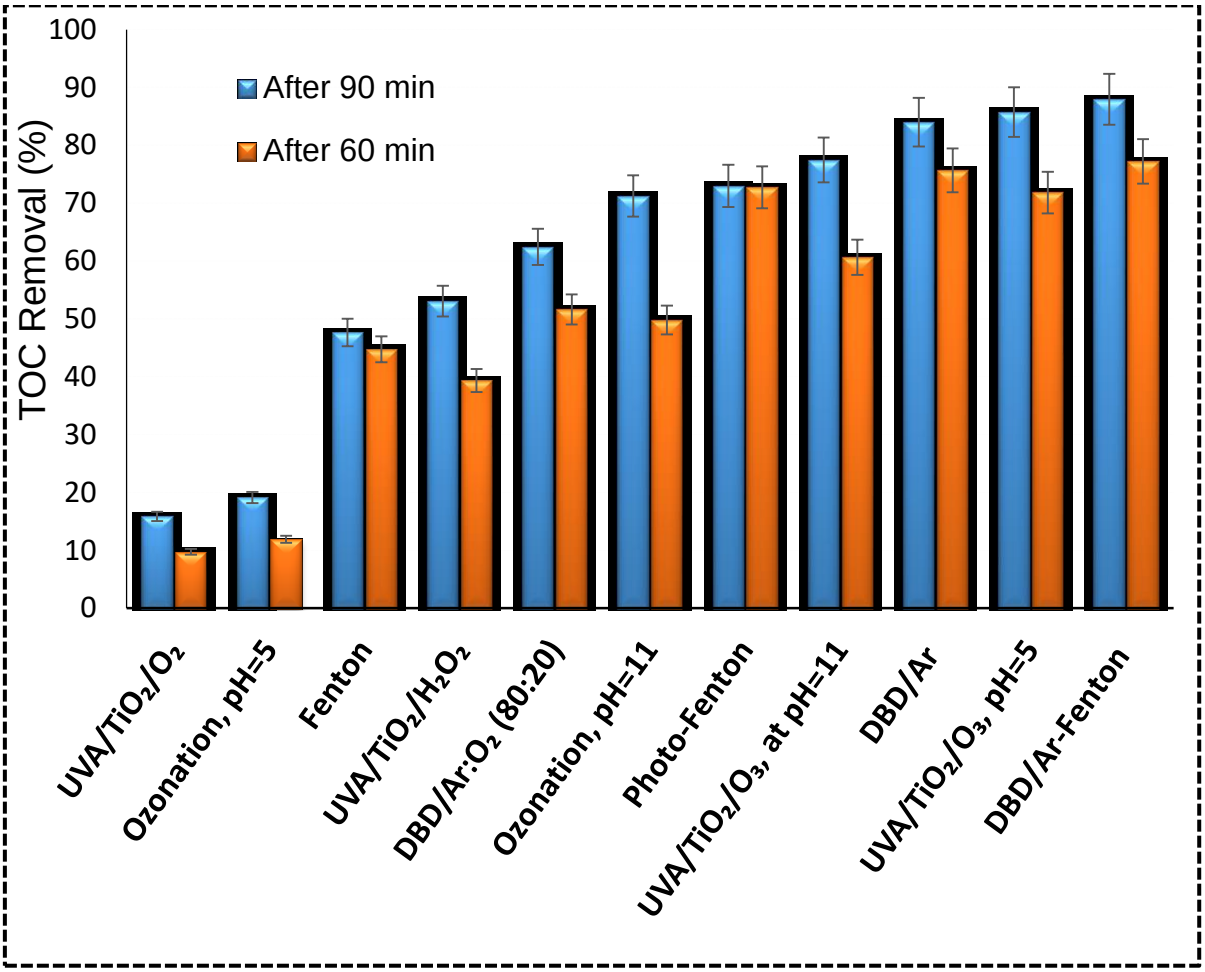

Figure 3. 36 TOC removal (%) from a MB solution (C_o= 50 mg/L MB, initial TOC = 27.7 mg/L) by ozonation and other applied AOPs.

3.10 Real wastewater treatment by DBD plasma in argon atmosphere

Table 3.4 shows how the DBD plasma under Ar atmosphere can remove various organic pollutants successfully. For this purpose two real wastewater samples have been taken. Sample (1) without biological treatment and sample (2) after biological treatment. After 30 min treatment, all organic pollutants were decomposed. However, poor mineralization has been observed probably due to the formation of low chain acids such as acetate and oxalate.

Table 3.4 Results of real wastewater treatment by DBD plasma (in µg/L); < BG = less than the quantification limit of the method

Pollutants	Sample 1 before treatment	Sample 1 after treatment	Sample 2 before treatment	Sample 2 after treatment
TOC (mg/L)	15.5	11.8	17.5	15.8
Total chlorobenzene	681	< BG	107.6	< BG
Monochlorobenzene	450	< 0.4	3.6	< 0.4
1,2-dichlorobenzene	66	< 0.4	54	< 0.4
1,3-dichlorobenzene	25	< 0.4	22	< 0.4
1,4-dichlorobenzene	140	< 0.4	28	< 0.4
Total chloroaniline	564	< BG	217	< BG
2-chloroaniline	73	< 0.4	70	< 0.4
2,3-dichloroaniline	25	< 0.4	19	< 0.4
2,4-dichloroaniline + 2,5-dichloroaniline	72	< 0.4	65	< 0.4
3-chloroaniline + 4-chloroaniline	270	< 0.4	1	< 0.4
3,4-dichloroaniline	92	< 0.4	28	< 0.4
3,5-dichloroaniline	32	< 0.4	34	< 0.4
Total dimethylaniline	490	< BG	198	< BG
2,4-dimethylaniline + 2,6-dimethylaniline	170	< 0.2	72	< 0.2
2,5-dimethylaniline + 3,5-dimethylaniline	220	< 0.2	88	< 0.2
2,3-dimethylaniline + 3,4-dimethylaniline	100	< 0.2	38	< 0.2
Total non-chlorinated aniline	214	< BG	< BG	< BG
Aniline	150	< 0.2	< 0.2	< 0.2
o-toluidine + p-toluidine + m-toluidine	64	< 0.2	< 0.2	< 0.2

Conclusions

The energy yields and the efficiencies of ozonation and various AOPs in the degradation and mineralization of aqueous solutions of different organic pollutants including DCF and IBP pharmaceuticals, 2,4-D phenoxy herbicide and its degradation by-product 2,4-DCP, and MB dye have been investigated and compared using a planar falling film reactor.

Due to the application of a common reactor design in all experiments, a direct comparison of the efficiencies of the examined treatment methods was possible. From the obtained results, it is found that the direct ozonation of pollutants is a very effective technique for the decomposition of all the studied organics. However, only a partial degradation of organic molecules with a poor mineralization is obtained and several ozone-resistant by-products are remained untreated. Removal of IBP and 2,4-D by the direct ozonation are slower than DCF and 2,4-DCP, respectively. The combination of ozonation with the photocatalysis considerably enhanced the degree of mineralization. Consequently, nearly complete TOC removal from 2,4-D and 2,4-DCP solutions is obtained after 60 min of the combination treatment, while the TOC removal for DCF, IBP and MB solutions after 90 min treatment is 97, 98 and 86 percent, respectively. Degradation of organics by the non-thermal DBD plasma depends on the composition of gas atmosphere and the input energy. The degradations of all the studied organic pollutants by the P.C. oxidation and DBD plasma under the air atmosphere are only moderate. The plasma assisted decomposition of DCF in argon atmosphere is not as efficient as in IBP. An addition of oxygen to the gas atmosphere in the DBD plasma process for the removal of DCF improves both the energy yield (5.1 g/kW h) and the mineralization efficiency. For IBP, the addition of oxygen to argon indicated a negative effect on the efficiency of degradation. However, the addition of ferrous ion to the solution improves the degradation and mineralization efficiencies under the argon atmosphere due to the occurrence

of additional Fenton oxidation. Depending on the target pollutant appropriate treatment method should be applied: For simple decomposition of the starting compounds, ozonation would be the method of choice, but for deeper removal also of the by-products and an extensive mineralization the photocatalytic ozonation or plasma assisted destruction in argon (or Ar/O_2) possibly in combination with Fenton oxidation is preferable. From the results, it can be concluded that the non-thermal plasma provides comparable degradation degrees with those achieved by the photocatalytic ozonation.

Appendix

The results of GC/MS for identification of intermediate by-products during the degradation of DCF and IBP are shown in the appendix on the attached CD.

Publications

1. Hama Aziz, K.H., Miessner, H., Mueller, S., Kalass, D., Moeller, D., Khorshid, I., Rashid, M.A.M., "Degradation of pharmaceutical diclofenac and ibuprofen in aqueous solution, a direct comparison of ozonation, photocatalysis, and non-thermal plasma" *Chemical Engineering Journal* 313: 1033-1041, (2017). **Impact factor: 6.216**

2. Hama Aziz, K.H., Miessner, H., Mueller, S., Mahyar, A., Kalass, D., Moeller, D., Khorshid, I., Rashid, M.A.M., "Comparative study on 2, 4-dichlorophenoxyacetic acid and 2, 4-dichlorophenol removal from aqueous solutions via ozonation, photocatalysis and non-thermal plasma using a planar falling film reactor" *Journal of Hazardous Materials* 343: 107-115, (2018). **Impact factor: 6.065**

3. Hama Aziz, K.H., Mahyar, A., Miessner, H., Mueller, S., Kalass, D., Moeller, D., Khorshid, I., Rashid, M.A.M., "Application of a planar falling film reactor for decomposition and mineralization of methylene blue in the aqueous media via ozonation, Fenton, photocatalysis and non-thermal plasma: Acomparative study" *Process Safety and Environmental Protection* 113: 319-329, (2018). **Impact factor: 2.905**

4. Attendance in the International Workshop on Plasmas for Energy and Environmental Applications (IWPEEA-2016) by giving an oral presentation entitled "**Degradation of pharmaceutical residues in aqueous solution by non-thermal plasma (dielectric barrier discharge) using a planar falling film reactor"** which was held in Liverpool, UK, from 21st to 24th August 2016.

Suggestions for future works

1. Study the mechanism and kinetics of degradation of these pollutants by various advanced oxidation processes.
2. Application of other types of non-thermal plasma such as corona discharge for the treatment of these pollutants and comparing with DBD performance.
3. Investigation on the possibility of using DBD plasma for the degradation of pollutants which are resistant against other treatment methods such as perfluorosurfactants.
4. Study the effects of different parameters such as the nature and thickness of dielectric, composition and shape of electrodes as well as the flow rate of gas atmosphere circulation in DBD plasma.
5. Attempt to combine the photocatalytic ozonation system with photovoltaic modules and utilization of solar energy as photon source for activation of photocatalyst surface and power generation for electrical equipment (ozone generator, pump and monitoring systems).
6. Attempt to improve the TOC removal by combination different advanced oxidation processes such as ozonation with non-thermal plasma.

References

[1] Maldaner, L. and I.C. Jardim, "Determination of some organic contaminants in water samples by solid-phase extraction and liquid chromatography–tandem mass spectrometry", *Talanta* 100: 38-44, (2012).

[2] Souza, F.S., da Silva, V.V., Rosin, C.K., Hainzenreder, L., Arenzon, A., Féris, L.A., "Comparison of different advanced oxidation processes for the removal of amoxicillin in aqueous solution", *Environmental Technology*: 1-9, (2017).

[3] Khan, S. and A. Malik, *Environmental and Health Effects of Textile Industry Wastewater*, in *Environmental Deterioration and Human Health: Natural and anthropogenic determinants*, Springer Netherlands: Dordrecht. p. 55-71, (2014).

[4] Petrie, B., R. Barden, and B. Kasprzyk-Hordern, "A review on emerging contaminants in wastewaters and the environment: current knowledge, understudied areas and recommendations for future monitoring" *Water Research* 72: 3-27, (2015).

[5] Foster, J.E., "Plasma-based water purification: Challenges and prospects for the future" *Physics of Plasmas* 24(5): 055501, (2017).

[6] Ferrari, B.t., Paxeus, N., Giudice, R.L., Pollio, A., Garric, J., "Ecotoxicological impact of pharmaceuticals found in treated wastewaters: study of carbamazepine, clofibric acid, and diclofenac" *Ecotoxicology and Environmental Safety* 55(3): 359-370, (2003).

[7] Vacchi, F.I., Von der Ohe, P.C., de Albuquerque, A.F., de Souza Vendemiatti, J.A., Azevedo, C.C.J., Honório, J.G., da Silva, B.F., Zanoni, M.V.B., Henry, T.B., Nogueira, A.J., "Occurrence and risk assessment of an azo dye–The case of Disperse Red 1" *Chemosphere* 156: 95-100, (2016).

[8] Sabik, H., R. Jeannot, and B. Rondeau, "Multiresidue methods using solid-phase extraction techniques for monitoring priority pesticides, including triazines and degradation products, in ground and surface waters" *Journal of Chromatography A* 885(1–2): 217-236, (2000).

[9] Fusco, G., Gallo, F., Tortolini, C., Bollella, P., Ietto, F., De Mico, A., D'Annibale, A., Antiochia, R., Favero, G., Mazzei, F., "AuNPs-functionalized PANABA-MWCNTs nanocomposite-based impedimetric immunosensor for 2, 4-dichlorophenoxy acetic acid detection" *Biosensors and Bioelectronics* 93: 52-56, (2017).

[10] Laville, N., Aıt-Aıssa, S., Gomez, E., Casellas, C., Porcher, J., "Effects of human pharmaceuticals on cytotoxicity, EROD activity and ROS production in fish hepatocytes" *Toxicology* 196(1): 41-55, (2004).

[11] Moutaouakkil, A. and M. Blaghen, "Decolorization of the anthraquinone dye Cibacron Blue 3G-A with immobilized Coprinus cinereus in fluidized bed bioreactor" *Applied biochemistry and microbiology* 47(1): 59-65, (2011).

[12] Kolpin, D.W., J.E. Barbash, and R.J. Gilliom, "Occurrence of pesticides in shallow groundwater of the United States: Initial results from the National Water-Quality Assessment Program" *Environmental Science & Technology* 32(5): 558-566, (1998).

[13] Kosjek, T., E. Heath, and A. Krbavčič, "Determination of non-steroidal anti-inflammatory drug (NSAIDs) residues in water samples" *Environment International* 31(5): 679-685, (2005).

[14] Cleuvers, M., "Mixture toxicity of the anti-inflammatory drugs diclofenac, ibuprofen, naproxen, and acetylsalicylic acid" *Ecotoxicology and environmental safety* 59(3): 309-315, (2004).

[15] Rashed, M.N., "Adsorption technique for the removal of organic pollutants from water and wastewater" *Organic pollutants-monitoring, risk and treatment.* InTech, (2013).

[16] Ali, I., M. Asim, and T.A. Khan, "Low cost adsorbents for the removal of organic pollutants from wastewater" *Journal of environmental management* 113: 170-183, (2012).

[17] Zhou, Y., L. Zhang, and Z. Cheng, "Removal of organic pollutants from aqueous solution using agricultural wastes: a review" *Journal of Molecular Liquids* 212: 739-762, (2015).

[18] Hijosa-Valsero, M., Molina, R., Schikora, H., Müller, M., Bayona, J.M., "Removal of priority pollutants from water by means of dielectric barrier discharge atmospheric plasma" *Journal of hazardous materials* 262: 664-673, (2013).

[19] Giri, R.R., Ozaki, H., Ishida, T., Takanami, R., Taniguchi, S., "Synergy of ozonation and photocatalysis to mineralize low concentration 2, 4-dichlorophenoxyacetic acid in aqueous solution" *Chemosphere* 66(9): 1610-1617, (2007).

[20] Andreozzi, R., Caprio, V., Insola, A., Marotta, R., "Advanced oxidation processes (AOP) for water purification and recovery" *Catalysis today* 53(1): 51-59, (1999).

[21] Martins, A.F., "Advanced oxidation processes applied to effluent streams from an agrochemical industry" *Pure and applied chemistry* 70(12): 2271-2279, (1998).

[22] Deng, Y. and R. Zhao, "Advanced oxidation processes (AOPs) in wastewater treatment" *Current Pollution Reports* 1(3): 167-176, (2015).

[23] Hufschmidt, D., Bahnemann, D., Testa, J.J., Emilio, C.A., Litter, M.I., "Enhancement of the photocatalytic activity of various TiO_2 materials by platinisation" *Journal of Photochemistry and Photobiology A: Chemistry* 148(1): 223-231, (2002).

[24] Pelaez, M., Nolan, N.T., Pillai, S.C., Seery, M.K., Falaras, P., Kontos, A.G., Dunlop, P.S., Hamilton, J.W., Byrne, J.A., O'shea, K., "A review on the visible light active titanium dioxide photocatalysts for environmental applications" *Applied Catalysis B: Environmental* 125: 331-349, (2012).

[25] Górska, P., Zaleska, A., Kowalska, E., Klimczuk, T., Sobczak, J.W., Skwarek, E., Janusz, W., Hupka, J., "TiO_2 photoactivity in vis and UV light: the influence of calcination temperature and surface properties" *Applied Catalysis B: Environmental* 84(3): 440-447, (2008).

[26] Ohtani, B., Prieto-Mahaney, O., Li, D., Abe, R., "What is Degussa (Evonik) P25? Crystalline composition analysis, reconstruction from isolated pure particles and photocatalytic activity test" *Journal of Photochemistry and Photobiology A: Chemistry* 216(2): 179-182, (2010).

[27] Carp, O., C.L. Huisman, and A. Reller, "Photoinduced reactivity of titanium dioxide" *Progress in solid state chemistry* 32(1): 33-177, (2004).

[28] Lettmann, C., Hildenbrand, K., Kisch, H., Macyk, W., Maier, W.F., "Visible light photodegradation of 4-chlorophenol with a coke-containing titanium dioxide photocatalyst" *Applied Catalysis B: Environmental* 32(4): 215-227, (2001).

[29] Daghrir, R., P. Drogui, and D. Robert, "Modified TiO_2 for environmental photocatalytic applications: a review" *Industrial & Engineering Chemistry Research* 52(10): 3581-3599, (2013).

[30] Fujishima, A., T.N. Rao, and D.A. Tryk, "Titanium dioxide photocatalysis" *Journal of Photochemistry and Photobiology C: Photochemistry Reviews* 1(1): 1-21, (2000).

[31] Addamo, M., Augugliaro, V., García-López, E., Loddo, V., Marcì, G., Palmisano, L., "Oxidation of oxalate ion in aqueous suspensions of TiO_2 by photocatalysis and ozonation" *Catalysis Today* 107: 612-618, (2005).

[32] Zhao, J. and X. Yang, "Photocatalytic oxidation for indoor air purification: a literature review" *Building and Environment* 38(5): 645-654, (2003).

[33] Konstantinou, I.K. and T.A. Albanis, "TiO_2-assisted photocatalytic degradation of azo dyes in aqueous solution: kinetic and mechanistic investigations: a review" *Applied Catalysis B: Environmental* 49(1): 1-14, (2004).

[34] Pirilä, M., Saouabe, M., Ojala, S., Rathnayake, B., Drault, F., Valtanen, A., Huuhtanen, M., Brahmi, R., Keiski, R.L., "Photocatalytic degradation of organic pollutants in wastewater" *Topics in Catalysis* 58(14-17): 1085-1099, (2015) .

[35] Gassim, F.A.-Z.G., A.N. Alkhateeb, and F.H. Hussein, "Photocatalytic oxidation of benzyl alcohol using pure and sensitized anatase" *Desalination* 209(1-3): 342-349, (2007).

[36] Beltrán, F.J., Ozone reaction kinetics for water and wastewater systems, Lewis publisher, CRC Press, (2003).

[37] Summerfelt, S.T. and J.N. Hochheimer, "Review of ozone processes and applications as an oxidizing agent in aquaculture" *The Progressive Fish-Culturist* 59(2): 94-105, (1997).

[38] Pera-Titus, M., García-Molina, V., Baños, M.A., Giménez, J., Esplugas, S., "Degradation of chlorophenols by means of advanced oxidation processes: a general review" *Applied Catalysis B: Environmental* 47(4): 219-256, (2004).

[39] Černigoj, U., U.L. Štangar, and P. Trebše, "Degradation of neonicotinoid insecticides by different advanced oxidation processes and studying the effect of ozone on TiO_2 photocatalysis" *Applied Catalysis B: Environmental* 75(3): 229-238, (2007).

[40] Jiang, B., Zheng, J., Qiu, S., Wu, M., Zhang, Q., Yan, Z., Xue, Q., "Review on electrical discharge plasma technology for wastewater remediation" *Chemical Engineering Journal* 236: 348-368, (2014).

[41] Chu, P.K. and Lu, X.P., Low temperature plasma technology: methods and applications, Taylor and Francis Group, CRC Press, (2013).

[42] Wagner, H.-E., Brandenburg, R., Kozlov, K., Sonnenfeld, A., Michel, P., Behnke, J., "The barrier discharge: basic properties and applications to surface treatment" *Vacuum* 71(3): 417-436, (2003).

[43] Hijosa-Valsero, M., Molina, R., Montràs, A., Müller, M., Bayona, J.M., "Decontamination of waterborne chemical pollutants by using atmospheric pressure nonthermal plasma: a review" *Environmental Technology Reviews* 3(1): 71-91, (2014).

[44] Malik, M.A., "Water Purification by Plasmas: Which Reactors are Most Energy Efficient?" *Plasma Chemistry and Plasma Processing* 30(1): 21-31, (2010).

[45] Magureanu, M., Piroi, D., Mandache, N.B., David, V., Medvedovici, A., Parvulescu, V.I., "Degradation of pharmaceutical compound pentoxifylline in water by non-thermal plasma treatment" *water research* 44(11): 3445-3453, (2010).

[46] Magureanu, M., Dobrin, D., Mandache, N.B., Bradu, C., Medvedovici, A., Parvulescu, V.I., "The mechanism of plasma destruction of enalapril and related metabolites in water" *Plasma Processes and Polymers* 10(5): 459-468, (2013).

[47] Reddy, P.M.K., S. Mahammadunnisa, and C. Subrahmanyam, "Catalytic non-thermal plasma reactor for mineralization of endosulfan in aqueous medium: A green approach for the treatment of pesticide contaminated water" *Chemical Engineering Journal* 238: 157-163, (2014).

[48] Dojčinović, B.P., Roglić, G.M., Obradović, B.M., Kuraica, M.M., Kostić, M.M., Nešić, J., Manojlović, D.D., "Decolorization of reactive textile dyes using water falling film dielectric barrier discharge" *Journal of hazardous materials* 192(2): 763-771, (2011).

[49] Barbosa, M.O., Moreira, N.F., Ribeiro, A.R., Pereira, M.F., Silva, A.M., "Occurrence and removal of organic micropollutants: an overview of the watch list of EU Decision 2015/495" *Water research* 94: 257-279, (2016).

[50] Schwaiger, J., Ferling, H., Mallow, U., Wintermayr, H., Negele, R., "Toxic effects of the non-steroidal anti-inflammatory drug diclofenac: Part I: histopathological alterations and bioaccumulation in rainbow trout" *Aquatic Toxicology* 68(2): 141-150, (2004).

[51] Ikehata, K., N. Jodeiri Naghashkar, and M. Gamal El-Din, "Degradation of aqueous pharmaceuticals by ozonation and advanced oxidation processes: a review" *Ozone: Science and Engineering* 28(6): 353-414, (2006).

[52] Klavarioti, M., D. Mantzavinos, and D. Kassinos, "Removal of residual pharmaceuticals from aqueous systems by advanced oxidation processes" *Environment international* 35(2): 402-417, (2009).

[53] Khalaf, S., Shoqeir, J.H., Lelario, F., Scrano, L., Karaman, R., Bufo, S.A., "Removal of Diclofenace Sodium from Aqueous Environments Using Heterogeneous Photocatalysis Treatment" *Imperial Journal of Interdisciplinary Research* 3(9), (2017).

[54] Kanakaraju, D., Motti, C.A., Glass, B.D., Oelgemöller, M., "Photolysis and TiO_2-catalysed degradation of diclofenac in surface and drinking water using circulating batch photoreactors" *Environmental Chemistry* 11(1): 51-62, (2014).

[55] Sun, W., Chu, H., Dong, B., Cao, D., Zheng, S., "The degradation of naproxen and diclofenac by a nano-TiO_2/diatomite photocatalytic reactor" *Int. J. Electrochem. Sci.* 9: 4566-4573, (2014).

[56] Sarasidis, V.C., Plakas, K.V., Patsios, S.I., Karabelas, A.J., "Investigation of diclofenac degradation in a continuous photo-catalytic membrane reactor Influence of operating parameters" *Chemical Engineering Journal* 239: 299-311, (2014).

[57] Rizzo, L., Meric, S., Kassinos, D., Guida, M., Russo, F., Belgiorno, V., "Degradation of diclofenac by TiO_2 photocatalysis: UV absorbance kinetics and process evaluation through a set of toxicity bioassays" *Water Research* 43(4): 979-988, (2009).

[58] Calza, P., Sakkas, V., Medana, C., Baiocchi, C., Dimou, A., Pelizzetti, E., Albanis, T., "Photocatalytic degradation study of diclofenac over aqueous TiO 2 suspensions" *Applied Catalysis B: Environmental* 67(3): 197-205, (2006) .

[59] Sein, M.M., Zedda, M., Tuerk, J., Schmidt, T.C., Golloch, A., Sonntag, C.v., "Oxidation of diclofenac with ozone in aqueous solution" *Environmental science & technology* 42(17): 6656-6662, (2008).

[60] Naddeo, V., Belgiorno, V., Kassinos, D., Mantzavinos, D., Meric, S., "Ultrasonic degradation, mineralization and detoxification of diclofenac in water: optimization of operating parameters" *Ultrasonics sonochemistry* 17(1): 179-185, (2010).

[61] Hartmann, J., Bartels, P., Mau, U., Witter, M., Tümpling, W., Hofmann, J., Nietzschmann, E., "Degradation of the drug diclofenac in water by sonolysis in presence of catalysts" *Chemosphere* 70(3): 453-461, (2008).

[62] Naddeo, V., Belgiorno, V., Ricco, D., Kassinos, D., "Degradation of diclofenac during sonolysis, ozonation and their simultaneous application" *Ultrasonics sonochemistry* 16(6): 790-794, (2009).

[63] García-Araya, J.F., F.J. Beltrán, and A. Aguinaco, "Diclofenac removal from water by ozone and photolytic TiO_2 catalysed processes" *Journal of chemical technology and biotechnology* 85(6): 798-804, (2010).

[64] Aguinaco, A., Beltrán, F.J., García-Araya, J.F., Oropesa, A., "Photocatalytic ozonation to remove the pharmaceutical diclofenac from water: influence of variables" *Chemical Engineering Journal* 189: 275-282, (2012).

[65] Vogna, D., Marotta, R., Napolitano, A., Andreozzi, R., d'Ischia, M., "Advanced oxidation of the pharmaceutical drug diclofenac with UV/H_2O_2 and ozone" *Water Research* 38(2): 414-422, (2004).

[66] Manu, B., "Degradation kinetics of diclofenac in water by Fenton's oxidation" *Journal of Sustainable Energy & Environment* 3(4), (2012).

[67] Hofmann, J., Freier, U., Wecks, M., Hohmann, S., "Degradation of diclofenac in water by heterogeneous catalytic oxidation with H_2O_2" *Applied Catalysis B: Environmental* 70(1): 447-451, (2007).

[68] Pérez-Estrada, L.A., Malato, S., Gernjak, W., Agüera, A., Thurman, E.M., Ferrer, I., Fernández-Alba, A.R., "Photo-Fenton degradation of diclofenac: identification of main intermediates and degradation pathway" *Environmental Science & Technology* 39(21): 8300-8306, (2005).

[69] Banaschik, R., Jablonowski, H., Bednarski, P.J., Kolb, J.F., "Degradation and intermediates of diclofenac as instructive example for decomposition of recalcitrant pharmaceuticals by hydroxyl radicals generated with pulsed corona plasma in water" *Journal of hazardous materials* 342: 651-660, (2018).

[70] Dobrin, D., Bradu, C., Magureanu, M., Mandache, N., Parvulescu, V., "Degradation of diclofenac in water using a pulsed corona discharge" *Chemical engineering journal* 234: 389-396, (2013).

[71] Rong, S., Sun, Y., Zhao, Z., Wang, H., "Dielectric barrier discharge induced degradation of diclofenac in aqueous solution" *Water Science and Technology* 69(1): 76-83, (2014).

[72] Iovino, P., Chianese, S., Canzano, S., Prisciandaro, M., Musmarra, D., "Degradation of ibuprofen in aqueous solution with UV light: the effect of reactor volume and pH" *Water, Air, & Soil Pollution* 227(6): 194, (2016).

[73] Choina, J., Kosslick, H., Fischer, C., Flechsig, G.-U., Frunza, L., Schulz, A., "Photocatalytic decomposition of pharmaceutical ibuprofen pollutions in water over titania catalyst" *Applied Catalysis B: Environmental* 129: 589-598, (2013).

[74] Jallouli, N., Pastrana-Martínez, L.M., Ribeiro, A.R., Moreira, N.F., Faria, J.L., Hentati, O., Silva, A.M., Ksibi, M., "Heterogeneous photocatalytic degradation of ibuprofen in ultrapure water, municipal and pharmaceutical industry wastewaters using a TiO_2/UV-LED system" *Chemical Engineering Journal* 334: 976-984, (2018).

[75] Adityosulindro, S., Barthe, L., González-Labrada, K., Haza, U.J.J., Delmas, H., Julcour, C., "Sonolysis and sono-Fenton oxidation for removal of ibuprofen in (waste) water" *Ultrasonics Sonochemistry*, (2017).

[76] Madhavan, J., F. Grieser, and M. Ashokkumar, "Combined advanced oxidation processes for the synergistic degradation of ibuprofen in aqueous environments" *Journal of Hazardous Materials* 178(1): 202-208, (2010).

[77] Méndez-Arriaga, F., Torres-Palma, R., Pétrier, C., Esplugas, S., Gimenez, J., Pulgarin, C., "Ultrasonic treatment of water contaminated with ibuprofen" *Water research* 42(16): 4243-4248, (2008).

[78] Quero-Pastor, M., Garrido-Perez, M., Acevedo, A., Quiroga, J., "Ozonation of ibuprofen: a degradation and toxicity study" *Science of the Total Environment* 466: 957-964, (2014).

[79] Rey, A., Garcia-Munoz, P., Hernández-Alonso, M., Mena, E., García-Rodríguez, S., Beltrán, F., "WO_3–TiO_2 based catalysts for the simulated solar radiation assisted photocatalytic ozonation of emerging contaminants in a municipal wastewater treatment plant effluent" *Applied Catalysis B: Environmental* 154: 274-284, (2014).

[80] Scheers, T., Appels, L., Dirkx, B., Jacoby, L., Van Vaeck, L., Van der Bruggen, B., Luyten, J., Degrève, J., Van Impe, J., Dewil, R., "Evaluation of peroxide based advanced oxidation processes (AOPs) for the degradation of ibuprofen in water" *Desalination and Water Treatment* 50(1-3): 189-197, (2012).

[81] Mendez-Arriaga, F., S. Esplugas, and J. Gimenez, "Degradation of the emerging contaminant ibuprofen in water by photo-Fenton" *Water research* 44(2): 589-595, (2010).

[82] Zheng, B., Li, C., Zhang, J., Zheng, Z., "Dielectric barrier discharge induced the degradation of the emerging contaminant ibuprofen in aqueous solutions" *Desalination and Water Treatment* 52(22-24): 4469-4475, (2014).

[83] Marković, M., Jović, M., Stanković, D., Kovačević, V., Roglić, G., Gojgić-Cvijović, G., Manojlović, D., "Application of non-thermal plasma reactor and Fenton reaction for degradation of ibuprofen" *Science of The Total Environment* 505: 1148-1155, (2015).

[84] Banaschik, R., Lukes, P., Jablonowski, H., Hammer, M.U., Weltmann, K.-D., Kolb, J.F., "Potential of pulsed corona discharges generated in water for the degradation of persistent pharmaceutical residues" *Water research* 84: 127-135, (2015).

[85] Zeng, J., Yang, B., Wang, X., Li, Z., Zhang, X., Lei, L., "Degradation of pharmaceutical contaminant ibuprofen in aqueous solution by cylindrical wetted-wall corona discharge" *Chemical Engineering Journal* 267: 282-288, (2015).

[86] Oturan, N., Sirés, I., Oturan, M.A., Brillas, E., "Degradation of pesticides in aqueous medium by electro-Fenton and related methods. A review" *J. Environ. Eng. Manage* 19(5): 235-255, (2009).

[87] Zazou, H., Oturan, N., Zhang, H., Hamdani, M., Oturan, M.A., "Comparative study of electrochemical oxidation of herbicide 2,4,5-T: kinetics, parametric optimization and mineralization pathway" *Sustainable Environment Research* 27(1): 15-23, (2017).

[88] Chiron, S., Fernandez-Alba, A., Rodriguez, A., Garcia-Calvo, E., "Pesticide chemical oxidation: state-of-the-art" *Water Research* 34(2): 366-377, (2000).

[89] Boivin, A., Amellal, S., Schiavon, M., Van Genuchten, M.T., "2, 4-Dichlorophenoxyacetic acid (2,4-D) sorption and degradation dynamics in three agricultural soils" *Environmental Pollution* 138(1): 92-99, (2005).

[90] Kuśmierek, K., L. Dąbek, and A. Świątkowski, "A comparative study on oxidative degradation of 2,4-dichlorophenol and 2,4-dichlorophenoxyacetic acid by ammonium persulfate" *Desalination and Water Treatment* 57(3): 1098-1106, (2016).

[91] Kuśmierek, K., M. Szala, and A. Świątkowski, "Adsorption of 2,4-dichlorophenol and 2,4-dichlorophenoxyacetic acid from aqueous solutions on carbonaceous materials obtained by combustion synthesis" *Journal of the Taiwan Institute of Chemical Engineers* 63: 371-378, (2016).

[92] Jung, B.K., Z. Hasan, and S.H. Jhung, "Adsorptive removal of 2, 4-dichlorophenoxyacetic acid (2,4-D) from water with a metal–organic framework" *Chemical engineering journal* 234: 99-105, (2013).

[93] Luna, A.J., Nascimento, C.A., Foletto, E.L., Moraes, J.E., Chiavone-Filho, O., "Photo-Fenton degradation of phenol, 2,4-dichlorophenoxyacetic acid and 2,4-dichlorophenol mixture in saline solution using a falling-film solar reactor" *Environmental technology* 35(3): 364-371, (2014).

[94] Bukowska, B., "Effects of 2,4-D and its metabolite 2,4-dichlorophenol on antioxidant enzymes and level of glutathione in human erythrocytes" *Comparative Biochemistry and Physiology Part C: Toxicology & Pharmacology* 135(4): 435-441, (2003).

[95] Piera, E., Calpe, J.C., Brillas, E., Domènech, X., Peral, J., "2,4-Dichlorophenoxyacetic acid degradation by catalyzed ozonation: TiO_2/UVA/O_3 and Fe(II)/UVA/O_3 systems" *Applied Catalysis B: Environmental* 27(3): 169-177, (2000).

[96] Giri, R., Ozaki, H., Takanami, R., Taniguchi, S., "Heterogeneous photocatalytic ozonation of 2,4-D in dilute aqueous solution with TiO_2 fiber" *Water Science and Technology* 58(1): 207-216, (2008).

[97] Giri, R., Ozaki, H., Taniguchi, S., Takanami, R., "Photocatalytic ozonation of 2, 4-dichlorophenoxyacetic acid in water with a new TiO_2 fiber" *International Journal of Environmental Science & Technology* 5(1): 17-26, (2008).

[98] YU, Y.-h., M. Jun, and Y.-j. HOU, "Degradation of 2,4-dichlorophenoxyacetic acid in water by ozone-hydrogen peroxide process" *Journal of Environmental Sciences* 18(6): 1043-1049, (2006).

[99] Rezaei, R. and M. Mohseni, "Impact of pH on the kinetics of photocatalytic oxidation of 2,4-dichlorophenoxy acetic acid in a fluidized bed photocatalytic reactor" *Applied Catalysis B: Environmental* 205: 302-309, (2017).

[100] Qiu, P., Yao, J., Chen, H., Jiang, F., Xie, X., "Enhanced visible-light photocatalytic decomposition of 2,4-dichlorophenoxyacetic acid over ZnIn2S4/gC3N4 photocatalyst" *Journal of hazardous materials* 317: 158-168, (2016).

[101] Lemus, M.A., López, T., Recillas, S., Frias, D., Montes, M., Delgado, J., Centeno, M., Odriozola, J., "Photocatalytic degradation of 2,4-dichlorophenoxyacetic acid using nanocrystalline cryptomelane composite catalysts" *Journal of Molecular Catalysis A: Chemical* 281(1): 107-112, (2008).

[102] Li, J., Guan, W., Yan, X., Wu, Z., Shi, W., "Photocatalytic Ozonation of 2, 4-Dichlorophenoxyacetic Acid using $LaFeO_3$ Photocatalyst Under Visible Light Irradiation" *Catalysis Letters*: 1-7, (2017).

[103] Chen, H., Zhang, Z., Yang, Z., Yang, Q., Li, B., Bai, Z., "Heterogeneous fenton-like catalytic degradation of 2,4-dichlorophenoxyacetic acid in water with FeS" *Chemical Engineering Journal* 273: 481-489, (2015).

[104] Chu, W., Kwan, C., Chan, K., Chong, C., "An unconventional approach to studying the reaction kinetics of the Fenton's oxidation of 2,4-dichlorophenoxyacetic acid" *Chemosphere* 57(9): 1165-1171, (2004).

[105] Conte, L.O., A.V. Schenone, and O.M. Alfano, "Photo-Fenton degradation of the herbicide 2,4-D in aqueous medium at pH conditions close to neutrality" *Journal of environmental management* 170: 60-69, (2016).

[106] García, O., Isarain-Chávez, E., Garcia-Segura, S., Brillas, E., Peralta-Hernández, J.M., "Degradation of 2,4-dichlorophenoxyacetic acid by electro-oxidation and electro-Fenton/BDD processes using a pre-pilot plant" *Electrocatalysis* 4(4): 224-234, (2013).

[107] Bradu, C., M. Magureanu, and V. Parvulescu, "Degradation of the chlorophenoxyacetic herbicide 2,4-D by plasma-ozonation system" *Journal of Hazardous Materials* 336: 52-56, (2017).

[108] Singh, R.K., L. Philip, and S. Ramanujam, "Removal of 2,4-dichlorophenoxyacetic acid in aqueous solution by pulsed corona discharge treatment: Effect of different water constituents, degradation pathway and toxicity assay" *Chemosphere* 184: 207-214, (2017).

[109] Trapido, M., Hirvonen, A., Veressinina, Y., Hentunen, J., Munter, R., "Ozonation, ozone/UV and UV/H_2O_2 degradation of chlorophenols" *Ozone: Science & Engineering* 19(1):75-96, (1997).

[110] Barik, A.J. and P.R. Gogate, "Degradation of 2,4-dichlorophenol using combined approach based on ultrasound, ozone and catalyst" *Ultrasonics sonochemistry* 36: 517-526, (2017).

[111] Liu, L., Chen, F., Yang, F., Chen, Y., Crittenden, J., "Photocatalytic degradation of 2,4-dichlorophenol using nanoscale Fe/TiO_2" *Chemical Engineering Journal* 181: 189-195, (2012).

[112] Lukes, P., Clupek, M., Babicky, V., Sunka, P., Winterova, G., Janda, V., "Non-thermal plasma induced decomposition of 2-chlorophenol in water" *Acta Physica Slovaca* 53(6): 423-428, (2003).

[113] Hao, X.L. and M.H. Zhou, "Non-thermal plasma-induced photocatalytic degradation of 4-chlorophenol in water" *Journal of hazardous materials* 141(3): 475-482, (2007).

[114] Marković, M.D., Dojčinović, B.P., Obradović, B.M., Nešić, J., Natić, M.M., Tosti, T.B., Kuraica, M.M., Manojlović, D.D., "Degradation and detoxification of the 4-chlorophenol by non-thermal plasma-influence of homogeneous catalysts" *Separation and Purification Technology* 154: 246-254, (2015).

[115] Li, R., Gao, Y., Jin, X., Chen, Z., Megharaj, M., Naidu, R., "Fenton-like oxidation of 2,4-DCP in aqueous solution using iron-based nanoparticles as the heterogeneous catalyst" *Journal of colloid and interface science* 438: 87-93, (2015).

[116] Al Momani, F., C. Sans, and S. Esplugas, "A comparative study of the advanced oxidation of 2,4-dichlorophenol" *Journal of Hazardous Materials* 107(3): 123-129, (2004).

[117] Chequer, F.M.D., de Oliveira, G.A.R., Ferraz, E.R.A., Cardoso, J.C., Zanoni, M.V.B., de Oliveira, D.P., "Textile dyes: dyeing process and environmental impact, in Eco-friendly textile dyeing and finishing" InTech, (2013).

[118] Lam, S.-M., Sin, J.-C., Abdullah, A.Z., Mohamed, A.R., "Degradation of wastewaters containing organic dyes photocatalysed by zinc oxide: a review" *Desalination and Water Treatment* 41(1-3): 131-169, (2012).

[119] Wang, S., Boyjoo, Y., Choueib, A., Zhu, Z., "Removal of dyes from aqueous solution using fly ash and red mud" *Water research* 39(1): 129-138, (2005).

[120] Jiang, B., Zheng, J., Lu, X., Liu, Q., Wu, M., Yan, Z., Qiu, S., Xue, Q., Wei, Z., Xiao, H., "Degradation of organic dye by pulsed discharge non-*thermal plasma technology assisted with modified activated carbon fibers" Chemical engineering journal* 215: 969-978, (2013).

[121] Badr, Y., M.A. El-Wahed, and M. Mahmoud, "Photocatalytic degradation of methyl red dye by silica nanoparticles" *Journal of hazardous materials* 154(1): 245-253, (2008).

[122] Martínez-Huitle, C.A. and E. Brillas, "Decontamination of wastewaters containing synthetic organic dyes by electrochemical methods: a general review" *Applied Catalysis B: Environmental* 87(3): 105-145, (2009).

[123] Khandegar, V. and A.K. Saroha, "Electrocoagulation for the treatment of textile industry effluent–a review" *Journal of environmental management* 128: 949-963, (2013).

[124] Forgacs, E., T. Cserhati, and G. Oros, "Removal of synthetic dyes from wastewaters: a review" *Environment international* 30(7): 953-971, (2004).

[125] Dos Santos, A.B., F.J. Cervantes, and J.B. van Lier, "Review paper on current technologies for decolourisation of textile wastewaters: perspectives for anaerobic biotechnology" *Bioresource technology* 98(12): 2369-2385, (2007).

[126] Brillas, E. and C.A. Martínez-Huitle, "Decontamination of wastewaters containing synthetic organic dyes by electrochemical methods. An updated review" *Applied Catalysis B: Environmental* 166: 603-643, (2015).

[127] Naim, M.M. and Y.M. El Abd, "Removal and recovery of dyestuffs from dyeing wastewaters" *Separation and Purification Methods* 31(1): 171-228, (2002).

[128] Solís, M., Solís, A., Pérez, H.I., Manjarrez, N., Flores, M., "Microbial decolouration of azo dyes: a review" *Process Biochemistry* 47(12): 1723-1748, (2012).

[129] Robinson, T., McMullan, G., Marchant, R., Nigam, P., "Remediation of dyes in textile effluent: a critical review on current treatment technologies with a proposed alternative" *Bioresource technology* 77(3): 247-255, (2001).

[130] Kasiri, M.B., N. Modirshahla, and H. Mansouri, "Decolorization of organic dye solution by ozonation; Optimization with response surface methodology" *International Journal of Industrial Chemistry* 4(1): 3, (2013) .

[131] Lin, S.H. and C.M. Lin, "Treatment of textile waste effluents by ozonation and chemical coagulation" *Water research* 27(12): 1743-1748, (1993).

[132] Hassaan, M.A., A. El Nemr, and F.F. Madkour, "Testing the advanced oxidation processes on the degradation of Direct Blue 86 dye in wastewater" *The Egyptian Journal of Aquatic Research* 43(1): 11-19, (2017).

[133] El-Ashtoukhy, E.-S. and Y. Fouad, "Liquid–liquid extraction of methylene blue dye from aqueous solutions using sodium dodecylbenzenesulfonate as an extractant" *Alexandria Engineering Journal* 54(1): 77-81, (2015).

[134] Kannan, N. and M.M. Sundaram, "Kinetics and mechanism of removal of methylene blue by adsorption on various carbons-a comparative study" *Dyes and pigments* 51(1): 25-40, (2001).

[135] Hameed, B., A.M. Din, and A. Ahmad, "Adsorption of methylene blue onto bamboo-based activated carbon: kinetics and equilibrium studies" *Journal of hazardous materials* 141(3): 819-825, (2007).

[136] Wu, J. and S.R. Upreti, "Continuous ozonation of methylene blue in water" *Journal of Water Process Engineering* 8: 142-150, (2015).

[137] Turhan, K., Durukan, I., Ozturkcan, S.A., Turgut, Z., "Decolorization of textile basic dye in aqueous solution by ozone" *Dyes and Pigments* 92(3): 897-901, (2012).

[138] Vaishnave, P., Ameta, G., Kumar, A., Sharma, S., Ameta, S.C., "Sono-photo-Fenton and photo-Fenton degradation of methylene blue: A comparative study" *Journal of the Indian Chemical Society* 88(3): 397-403, (2011).

[139] Li, M., Qiang, Z., Pulgarin, C., Kiwi, J., "Accelerated methylene blue (MB) degradation by Fenton reagent exposed to UV or VUV/UV light in an innovative micro photo-reactor" *Applied Catalysis B: Environmental* 187: 83-89, (2016).

[140] Kim, J.R. and E. Kan, "Heterogeneous photo-Fenton oxidation of methylene blue using CdS-carbon nanotube/TiO_2 under visible light" *Journal of Industrial and Engineering Chemistry* 21: 644-652, (2015).

[141] Houas, A., Lachheb, H., Ksibi, M., Elaloui, E., Guillard, C., Herrmann, J.-M., "Photocatalytic degradation pathway of methylene blue in water" *Applied Catalysis B: Environmental* 31(2): 145-157, (2001).

[142] Dariani, R., Esmaeili, A., Mortezaali, A., Dehghanpour, S., "Photocatalytic reaction and degradation of methylene blue on TiO_2 nano-sized particles" *Optik-International Journal for Light and Electron Optics* 127(18): 7143-7154, (2016).

[143] Mansour, A.M., E.M. El Bakry, and N.T. Abdel-Ghani, "Photocatalytic degradation of methylene blue with copper (II) oxide synthesized by thermal decomposition of Flubendazole complexes" *Journal of Photochemistry and Photobiology A: Chemistry* 327: 21-24, (2016).

[144] Phaltane, S.A., Vanalakar, S., Bhat, T., Patil, P., Sartale, S., Kadam, L., "Photocatalytic degradation of methylene blue by hydrothermally synthesized CZTS nanoparticles" *Journal of Materials Science: Materials in Electronics* 28(11): 8186-8191, (2017).

[145] Trandafilović, L., Jovanović, D., Zhang, X., Ptasińska, S., Dramićanin, M., "Enhanced photocatalytic degradation of methylene blue and methyl orange by ZnO: Eu nanoparticles" *Applied Catalysis B: Environmental* 203: 740-752, (2017).

[146] Magureanu, M., Piroi, D., Mandache, N.B., Parvulescu, V., "Decomposition of methylene blue in water using a dielectric barrier discharge: optimization of the operating parameters" *Journal of applied physics* 104(10): 103306, (2008).

[147] Magureanu, M., Bradu, C., Piroi, D., Mandache, N.B., Parvulescu, V., "Pulsed corona discharge for degradation of methylene blue in water" *Plasma Chemistry and Plasma Processing* 33(1): 51-64, (2013).

[148] Reddy, P.M.K., Raju, B.R., Karuppiah, J., Reddy, E.L., Subrahmanyam, C., "Degradation and mineralization of methylene blue by dielectric barrier discharge non-thermal plasma reactor" *Chemical Engineering Journal* 217: 41-47, (2013).

[149] Chandana, L., P.M.K. Reddy, and C. Subrahmanyam, "Atmospheric pressure non-thermal plasma jet for the degradation of methylene blue in aqueous medium" *Chemical Engineering Journal* 282: 116-122, (2015).

[150] Liu, X., Zhang, H., Qin, D., Yang, Y., Kang, Y., Zou, F., Wu, Z., "Radical-Initiated Decoloration of Methylene Blue in a Gas–Liquid Multiphase System Via DC Corona Plasma" *Plasma Chemistry and Plasma Processing* 35(2): 321-337, (2015).

[151] Wang, B., Dong, B., Xu, M., Chi, C., Wang, C., "Degradation of methylene blue using double-chamber dielectric barrier discharge reactor under different carrier gases" *Chemical Engineering Science* 168: 90-100, (2017).

[152] García, M.C., Mora, M., Esquivel, D., Foster, J.E., Rodero, A., Jiménez-Sanchidrián, C., Romero-Salguero, F.J., "Microwave atmospheric pressure plasma jets for wastewater treatment: Degradation of methylene blue as a model dye" *Chemosphere* 180: 239-246, (2017).

[153] Chin, P. and D.F. Ollis, "Decolorization of organic dyes on Pilkington Activ™ photocatalytic glass" *Catalysis Today* 123(1): 177-188, (2007).

[154] Mills, A., Lepre, A., Elliott, N., Bhopal, S., Parkin, I.P., O'Neill, S.A., "Characterisation of the photocatalyst Pilkington Activ™: a reference film photocatalyst?" *Journal of Photochemistry and Photobiology A: Chemistry* 160(3): 213-224, (2003).

[155] Sellers, R.M., "Spectrophotometric determination of hydrogen peroxide using potassium titanium (IV) oxalate" *Analyst* 105(1255): 950-954, (1980).

[156] Brandhuber, P. and G.V. Korshin, "Methods for the Detection of Residual Concentations of Hydrogen Peroxide in Advanced Oxidation Processes" *WateReuse Foundation*, (2009).

[157] Mehrjouei, M., S. Müller, and D. Möller, "Design and characterization of a multi-phase annular falling-film reactor for water treatment using advanced oxidation processes" *Journal of environmental management* 120: 68-74, (2013).

[158] Gottschalk, C., J.A. Libra, and A. Saupe, Ozonation of water and waste water: A practical guide to understanding ozone and its applications, *John Wiley & Sons*, (2009).

[159] Hoigné, J. and H. Bader, "Rate constants of reactions of ozone with organic and inorganic compounds in water—II: dissociating organic compounds" *Water research* 17(2): 185-194, (1983).

[160] Tanaka, K., K. Abe, and T. Hisanaga, "Photocatalytic water treatment on immobilized TiO_2 combined with ozonation" *Journal of Photochemistry and Photobiology A: Chemistry* 101(1): 85-87, (1996).

[161] Lukes, P., B.R. Locke, and J.L. Brisset, "Aqueous-Phase Chemistry of Electrical Discharge Plasma in Water and in Gas–Liquid Environments" *Plasma Chemistry and Catalysis in Gases and Liquids*: 243-308, (2012).

[162] Kovačević, V.V., Dojčinović, B.P., Jović, M., Roglić, G.M., Obradović, B.M., Kuraica, M.M., "Measurement of reactive species generated by dielectric barrier discharge in direct contact with water in different atmospheres" *Journal of Physics D: Applied Physics* 50(15): 155205, (2017).

[163] Locke, B.R. and K.-Y. Shih, "Review of the methods to form hydrogen peroxide in electrical discharge plasma with liquid water" *Plasma Sources Science and Technology* 20(3): 034006, (2011).

[164] Benetoli, L.O.d.B., Cadorin, B.M., Postiglione, C.d.S., Souza, I.G.d., Debacher, N.A., "Effect of temperature on methylene blue decolorization in aqueous medium in electrical discharge plasma reactor" *Journal of the Brazilian Chemical Society* 22(9): 1669-1678, (2011).

[165] Kirkpatrick, M.J. and B.R. Locke, "Hydrogen, oxygen, and hydrogen peroxide formation in aqueous phase pulsed corona electrical discharge" *Industrial & engineering chemistry research* 44(12): 4243-4248, (2005).

[166] Wandell, R.J. and B.R. Locke, "Hydrogen peroxide generation in low power pulsed water spray plasma reactors" *Industrial & Engineering Chemistry Research* 53(2): 609-618, (2014).

[167] Malik, M.A., A. Ghaffar, and S.A. Malik, "Water purification by electrical discharges" *Plasma Sources Science and Technology* 10(1): 82, (2001).

[168] Bian, W., M. Zhou, and L. Lei, "Formations of active species and by-products in water by pulsed high-voltage discharge" *Plasma Chemistry and Plasma Processing* 27(3): 337-348, (2007).

[169] Staehelin, J. and J. Hoigne, "Decomposition of ozone in water: rate of initiation by hydroxide ions and hydrogen peroxide" *Environmental Science & Technology* 16(10): 676-681, (1982).

[170] Kornev, I., Osokin, G., Galanov, A., Yavorovskiy, N., Preis, S., "Formation of nitrite-and nitrate-ions in aqueous solutions treated with pulsed electric discharges" *Ozone: Science & Engineering* 35(1): 22-30, (2013).

[171] Singh, H. and M. Muneer, "Photodegradation of a herbicide derivative, 2, 4-dichlorophenoxy acetic acid in aqueous suspensions of titanium dioxide" *Research on chemical intermediates* 30(4-5): 317-329, (2004).

[172] Nawrocki, J. and B. Kasprzyk-Hordern, "The efficiency and mechanisms of catalytic ozonation" *Applied Catalysis B: Environmental* 99(1): 27-42, (2010).

[173] Huber, M.M., Canonica, S., Park, G.-Y., Von Gunten, U., "Oxidation of pharmaceuticals during ozonation and advanced oxidation processes" *Environmental science & technology* 37(5): 1016-1024, (2003).

[174] Peller, J. and P.V. Kamat, "Radiolytic transformations of chlorinated phenols and chlorinated phenoxyacetic acids" T*he Journal of Physical Chemistry A* 109(42): 9528-9535, (2005).

[175] Moreira, N.F., Orge, C.A., Ribeiro, A.R., Faria, J.L., Nunes, O.C., Pereira, M.F.R., Silva, A.M., "Fast mineralization and detoxification of amoxicillin and diclofenac by photocatalytic ozonation and application to an urban wastewater" *Water research* 87: 87-96, (2015).

[176] Mehrjouei, M., S. Müller, and D. Möller, "Catalytic and photocatalytic ozonation of tert-butyl alcohol in water by means of falling film reactor: Kinetic and cost–effectiveness study" *Chemical Engineering Journal* 248: 184-190, (2014).

[177] Sreeja, P. and K. Sosamony, "A Comparative Study of Homogeneous and Heterogeneous Photo-fenton Process for Textile Wastewater Treatment" *Procedia Technology* 24: 217-223, (2016).

[178] Cornish, B.J., L.A. Lawton, and P.K. Robertson, "Hydrogen peroxide enhanced photocatalytic oxidation of microcystin-LR using titanium dioxide" *Applied Catalysis B: Environmental* 25(1): 59-67, (2000).

[179] Zhang, J., Zheng, Z., Zhang, Y., Feng, J., Li, J., "Low-temperature plasma-induced degradation of aqueous 2, 4-dinitrophenol" *Journal of hazardous materials* 154(1): 506-512, (2008).

[180] Singh, R.K., L. Philip, and S. Ramanujam, "Removal of 2,4-dichlorophenoxyacetic acid in aqueous solution by pulsed corona discharge treatment: Effect of different water constituents, degradation pathway and toxicity assay" *Chemosphere* 184: 207-214, (2017).

[181] Bradu, C., M. Magureanu, and V.I. Parvulescu, "Degradation of the chlorophenoxyacetic herbicide 2,4-D by plasma-ozonation system" *Journal of Hazardous Materials* 336: 52-56, (2017).

[182] Ikoma, S., K. Satoh, and H. Itoh, "Decomposition of Methylene Blue in an Aqueous Solution Using a Pulsed-Discharge Plasma at Atmospheric Pressure" *Electrical Engineering in Japan* 179(3): 1-9, (2012).

[183] Sweeney, E.A., J.K. Chipman, and S.J. Forsythe, "Evidence for direct-acting oxidative genotoxicity by reduction products of azo dyes" *Environmental health perspectives* 102(6): 119, (1994).

[184] Zhang, S., Wang, D., Zhang, S., Zhang, X., Fan, P., "Ozonation and carbon-assisted ozonation of methylene blue as model compound: effect of solution pH" *Procedia Environmental Sciences* 18: 493-502, (2013).

[185] Piera, E., Calpe, J.C., Brillas, E., Domènech, X., Peral, J., "2,4-Dichlorophenoxyacetic acid degradation by catalyzed ozonation: TiO_2/UVA/O_3 and Fe(II)/UVA/O_3 systems" *Applied Catalysis B: Environmental* 27(3): 169-177, (2000).

[186] Xiao, J., Y. Xie, and H. Cao, "Organic pollutants removal in wastewater by heterogeneous photocatalytic ozonation" *Chemosphere* 121: 1-17, (2015).

الخلاصة

تم بحث و مقارنة كفاءة و فعالية التعامل بالاوزون (Ozonation) وغيرها من عمليات الاكسدة المتطورة (AOPs) المعتمدة على التحفيز الضوئى (Photocatalysis) والبلازما غير الحرارية الناتجة بواسطة تفريغ العزل الكهربائى الحاجزى (DBD) فى اجواء غازية مختلفة, و ان التفكك و التمعدن (Mineralization) للمحاليل المائية للملوثات العضوية و بضمنها العقاقير غير الستيرويدية المضادة للالتهابات (NSAIDs) ديكلوفيناك (DCF) و ايبوبروفين (IBP), كلوروفينوكسى مبيدات الاعشاب الثنائى كلوروفينوكسى حامض الخليك (2,4-D), الثنائى كلوروفينول (2,4-DCP) و الميثيلين الازرق (MB). ان ازالة MB اعقبها ايضا فينتون و فوتوفينتون و الاكسدة الضوئية الحافزة بوجود بيروكسيد الهايدروجين. و من اجل المقارنة المباشرة لكفائة الطرق المذكورة تم استخدام مفاعل الفلم الساقط المستوى ذو تصميم مشابه او قابل للمقارنة.ان النتائج التى تم الحصول عليها من خلال هذا البحث تبين ان تفكك جميع الملوثات العضوية التى تم دراستها بواسطة الاكسدة الضوئية الحافزة و طريقة بلازما (DBD) فى الهواء كانت معتدلة فقط, بينما التفكك الحاصل بواسطة الاوزون فى الظلام كان فعالا جدا وتمتلك اعلى طاقة انتاجية فى حال 50% من التحويل (G_{50}) جميع الملوثات. و مع ذلك, لوحظ ان تمعدن المواد العضوية المدروسة كانت ضعيفة. و يعود ذلك الى تكوين نواتج عرضية مستقرةتجاه الاوزون. و خاصة السلاسل القصيرة من الاحماض الكاربوكسيلية. و قد تم متابعة و مناقشة مصير هذه النواتج الثانوية من خلال التفكك باستخدام طرق مختلفة.

تركيبة من الاوزون و التحفيز الضوئى بين تأثيرا مشتركا على تفكك IBP و 2,4-D و ان سرعة التمعدن لكافة الملوثات قد عززت. و مع ذالك, ان الطاقة الناتجة عند G_{50} قد انخفضت و ذلك بسبب الحاجة الى قوة اضافية لل UVA ضوء. و قد لوحظ تعزيز كبير فى ازالة اللون للمثيلين الازرق بعد اضافة H_2O_2 الى طريقة الاكسدة الضوئية الحافزة و تم تحقيق ازالة اللون بشكل كامل بعدة ساعة واحدة من التعامل.

كفاءة التفكك و تكوين الاصناف الفعالة مثل الاوزون و البيروكسيد الهايدروجين من قبل DBD بلازما تعتمد بشكل كبير على طبيعة الغاز المستخدم و كمية الطاقة الكهربائية المستخدمة. ان تأثير الغازات المختلفة و قوة الطاقة المستخدمة فى تكوين بيروكسيد الهايدروجين و الاوزون و ايضا على كفاءة التفكك الملوثات بطرق المستخدمة قد تم التحقق منها.

ان اضافة Fe^{+2} الى المحلول يحسن إزالة الملوثات بطريقة DBD فى جو من الارجون و هذا يعود الى حدوث تفاعل الفينتون.

كفاءة التمعدن لجميع طرق الاكسدة المستخدمة والتى تعاقبت بقياس إزالة الكاربون العضوى الكلى (TOC). حيث تم الحصول على أعلى إزالة (TOC) بواسطة التحفيز الضوئى الاوزونى و DBD بلازما اما بتوحيدها مع الاكسدة بفنتون او فى جو من (Ar/O_2) .

تطبيق مفاعل جديد للفلم المستوى الساقط لتفكيك و تعدين بعض الادوية و الملوثات العضوية فى المحاليل المائية بواسطة الاوزون, التحفيز الضوئى و البلازما غير الحرارية

أطروحة

مقدمة الى مجلس كلية العلوم

فى جامعة السليمانية كجزء من متطلبات

نيل شهادة دكتورا في علوم

الكيمياء

(كيمياء البيئة)

من قبل

كوسار حكمت حمة عزيز

ماجستير كيمياء (٢٠١١), جامعة السليمانية

باشراف

د. ابراهيم خورشيد احمد

أستاذ

د. ديتلف مولر

أستاذ

د. محمد امين محمد رشيد

أستاذ مساعد

١٤٣٩هـ, رجب

٢٠١٨م, ازار

پوختە

کاریگەری و توانای هەریەکە لە ئۆزۆنکردن و ڕێگا جیاوازەکانی کردارە ئۆکسانە پێشکەوتووەکان (AOPs) لە سەر بنچینەی تیشکە کاراکردن (Photocatalysis) و پلازمای نا گەرمی دروست بوو بە هۆی خاڵیبونەوەی بەربەستی نەگەیەنەر (DBD) لە چەند گازێکی جیاوازدا بۆ هەڵوەشان و بە مینراڵکردنی ماددە ئەندامی یە پیسکەرەکان لە گیراوە ئاویەکانیاندا لە نێوانیاندا وەك نمونە دەرمانە ناستیرۆیدە دژە هەوکەرەکان (NSADs) دیکلوفیناك (DCF) و ئیبوپروفین (IBP), دەرمانە دژە گیا زیانبەخشەکان دوانە کلۆریدی فینۆکسی ترشی سرکیك (2,4-D), دوانە کلۆریدی فینۆل (2,4-DCP) و بۆیەی مەتیلینی شین لێکۆڵینەوەی لەسەر کرا و بەراورد کرا. لەگەڵ ئەوەشدا لابردنی مەتیلینی شین بەهۆی ڕێگاکانی فینتۆن و فۆتۆ-فینتۆن و هەروەها ئۆکسانی تیشکە کاراکردن بە بونی هایدرۆجین پیرۆکساید (H_2O_2) تاقی کراوەتەوە و بەراورد کراوە. بۆ ئەوەی بتوانرێت توانای تەکنیکەکان بە شێوەیەکی ڕاستەخۆ بەراورد بکرێن کارتیاکەری فیلمی ڕوو تەختی کەوتوو لە سەر هەمان دیزاین بەکار هێنرا.

ئەنجامەکان کە لەم کارە زانستیەدا بەدەست هاتوون ئەوەیان دەرخست کە هەڵوەشانی هەموو ماددە ئەندامی یە پیسکەرەکان بە ئۆکسان بەهۆی تیشکە کاراکردن و پلازما (DBD) لە هەوادا تەنها لە ئاستێکی مام ناوەندایە. بەڵام هەڵوەشان بە ئۆزۆن لە تاریکیدا (ئۆزۆنکردنی ڕاستەوخۆ) زۆر کاریگەر بوو و زۆرترین دەرئەنجامە ووزە (Energy yield) بە دەست هات لە کاتی لە سەدا پەنجای هەڵوەشان (G_{50}) بۆ هەموو ماددە ئەندامی یە پیسکەرەکان. پێویستە تێبینی ئەوە بکرێت کە بە مینەراڵکردنی ماددە ئەندامی یەکان زۆر کەم بوو. هۆکەی دەگەڕێتەوە بۆ دروستبونی ماددە لاوەکیە جێگیرەکان لە بەرامبەر ئۆزۆن بەتایبەت زنجیرە کورتەکانی ترشە کابۆکسیلەکان. چارەنوسی ئەم بەرهەمە لاوەکیانە لە ئەنجامی کرداری لێکهەڵوەشان بە ڕێگا چارەسەرە جیاوازەکان لێی کۆڵرایەوە و باسکرا.

پێکەوەبەستنی ئۆزۆن کردن لە گەڵ تیشکە کاراکردن کایگەر بوو لە کرداری لێکهەڵوەشانی IBP و 2,4-D وە توانای خێرا مینراڵکردنی هەموو پیسکەرەکان زیادیکرد. بەڵام دەرەنجامە ووزەی (G_{50}) بۆ هەڵوەشانی ماددە پیسکەرەکان کەمی کرد ئەوەش بە هۆی بەکارهێنانی ووزەی زیاتر بۆ سەرچاوەی تیشکی

UVA. توانای لابردنی ڕەنگی مەتیلینی شین بە شێوەیەکی بەرچاو زیادی کرد بە زیادکردنی H_2O_2 بۆ سیستەمی ئۆکسان بە تیشکە کاراکردن و لابردنی تەواوەتی ڕەنگ بە دەست هات دوای یەك کاتژمێر لە کارلێك. توانای لێك هەڵوەشان وە بەرهەم هێنانی ماددەی کارا وەك ئۆزۆن و H_2O_2 بە هۆی پلازمای DBD بەشێوەیەکی بەرچاو بەندە لەسەر پێکهاتەی گازی ناوەندەکە و بری کارەبای بەکارهاتوو. کاریگەری جۆری گازەکانی ناوەندەکە و بڕی کارەبای بەکارهاتوو لە سەر دروستبونی H_2O_2 و ئۆزۆن وە هەروەها لەسەر توانای هەڵوەشان بۆ ئەم ڕێگایانە لێی کۆڵرایەوە. زیادکردنی Fe^{+2} بۆ گیراوەکە دەبێتە هۆی باشکردنی کرداری لابردنی پیسکەرەکان لە ڕێگای DBD پلازمادا لە ناوەندی گازی ئارگۆندا بەهۆی ڕووداتی کارلێکی فینتۆن. توانای مینرالکردن بۆ هەریەکە لە ڕێگاکانی ئۆکسان لێی کۆڵراوەتەوە بە هۆی پێوانەکردنی کۆی کاربۆن لە مادە ئەندامیەکان (TOC). بەرزترین لابردنی TOC بەدەست هات لە هەریەکە لە ڕێگاکانی تیشکە کاراکردنی ئۆزۆن کردن و پلازما لە کاتی پێکەوەبەستنی لەگەڵ کارلێکی فینتۆن یان لە کاتی بەکارهێنانی تێکەڵە گازی ئۆکسجین و ئارگۆن.

بەکارهێنانی کارتیاکەری فیلمی رووتەختی کەوتووی تازە بۆ هەڵوەشان و بە مینرالکردنی هەندێك لە دەرمانەکان و ماددە ئەندامیە پیسکەرەکان لە گیراوە ئاویەکاندا بە هۆی ڕێگاکانی ئۆزۆنکردن , تیشکە کاراکردن و پلازمای نا گەرمی

تێزێکە

پێشکەش کراوە بە ئەنجومەنی کۆلێجی

زانست لە زانکۆی سلێمانی وەك بەشێك لە پێداویستیەکانی

بەدەست هێنانی بروانامەی دکتۆرا

لە زانستی کیمیا

(کیمیای ژینگە)

لەلایەن

کۆسار حکمت حمە عزیز

ماستەر لە کیمیای شیکاری (٢٠١١), زانکۆی سلێمانی

بەسەرپەرشتی

د. ابراهیم خورشید — پرۆفیسۆر

د. دێتلف مولەر — پرۆفیسۆر

د.محمد امین محمد رشید

پرۆفیسۆری یاریدەدەر

٢٧١٨ ك, نەورۆز — ٢٠١٨ ز, ئازار